Appendix B
Effects of Water Project Operations on Delta Hydrodynamics

January 2017

TABLE OF CONTENTS

Page

B.1 INTRODUCTION AND BACKGROUND B-1

B.2 WATER FLOW AND VELOCITY MONITORING B-4

B.3 HYDRODYNAMIC SIMULATION MODELS B-5

B.3.1 Model Description, Calibration and Validation B-6
B.3.1.1 Three-Dimensional Models B-6
B.3.1.2 Vertically Averaged Two-Dimensional Models B-7
B.3.1.3 One-Dimensional Models B-8
B.3.1.4 Model Calibration and Validation B-8
B.3.1.5 Comparison of Modeled to Measured Water Flow and Velocity B-9
B.3.2 Comparison of One-Dimensional and Two-Dimensional Model Results B-17

B.4 TEMPORARY, OPERABLE, AND NON-PHYSICAL BARRIERS B-21

B.4.1 Temporary Barriers B-21
B.4.2 Head of Old River Barrier B-22
B.4.3 Delta Cross Channel B-22
B.4.4 Georgiana Slough Non-physical Barrier B-24
B.4.5 Clifton Court Forebay Gate Operations B-29

B.5 HYDRODYNAMIC EFFECTS OF EXPORT OPERATIONS B-29

B.5.1 Methods B-29
B.5.2 Conceptual model B-30
B.5.3 Export Effects on Flow B-31
B.5.3.1 San Joaquin River Mainstem B-40
B.5.3.2 Old River B-45
B.5.3.3 Middle River B-46
B.5.3.4 Georgianna Slough B-46
B.5.3.5 Conclusions B-47
B.5.3.6 Gaps in Information B-48
B.5.4 Export Effects on Velocities B-49
B.5.4.1 San Joaquin River Mainstem B-55
B.5.4.2 Old River B-57
B.5.4.3 Middle River B-61
B.5.4.4 Conclusions B-61
B.5.4.5 Gaps in Information B-62

B.6 REFERENCES B-62

LIST OF FIGURES

Figure B.1-1. Major Annual Inflows to and Diversions from the Sacramento-San Joaquin Delta B-2
Figure B.1-2. Modeled Maximum Flows at Four Locations in the Sacramento-San Joaquin Delta using DSM2 at Low Inflows of 12,000 cfs, High Exports of 10,000 cfs, and Head of Old River Out B-3
Figure B.2-1. Surface Water Stations in the Sacramento-San Joaquin Delta in the DWR CDEC Data Repository B-4
Figure B.2-2. Surface Water Monitoring Stations in the Sacramento-San Joaquin Delta in the USGS NWIS B-5
Figure B.3-1. Model Dimensionality B-6
Figure B.3-2. Fifteen-minute Flow Data over 24 Hours at Turner Cut Represented by Both DSM2 Model Results and Measured Data B-9
Figure B.3-3. Location of Monitoring Stations used for Comparing Historical DSM2 Simulations with Field-measured Data and for Evaluating DSM2 Model Comparisons B-10
Figure B.3-4. Comparison of Field Measurements and DSM2 Simulation Results for 15-minute and Tidally Filtered 15-minute Flow Immediately Upstream and Downstream of the CCF Intake B-11
Figure B.3-5. Comparison of Field Measurements and DSM2 Simulation Results for 15-minute and Tidally Filtered 15-minute Velocity Immediately Upstream and Downstream of the CCF Intake B-11
Figure B.3-6. Comparison of Field Measurements and DSM2 Simulation Results for 15-minute and Tidally Filtered Daily Average Flow at the Old River and West Canal Intakes B-12
Figure B.3-7. Comparison of Field Measurements and DSM2 Simulation Results for 15-minute and Tidally Filtered Daily Average Velocity at the Old River and West Canal Intakes B-13
Figure B.3-8. Comparison of Field Measurements and DSM2 Simulation Results for 15-minute and Tidally Filtered Daily Average Flow at the Old River at Highway 4 and Turner Cut B-14
Figure B.3-9. Comparison of Field Measurements and DSM2 Simulation Results for 15-minute and Tidally Filtered Daily Average Velocity at the Old River at Highway 4 and Turner Cut B-15
Figure B.3-10. Comparison of Field Measurements and DSM2 Simulation Results for 15-minute and Tidally Filtered Daily Average Flow at Turner Cut for Water Years 2011 and 2012 ..... B-16
Figure B.4-1. Fine-scale Velocity Vectors in the Sacramento River at the Delta Cross Channel over a 9-hour Period B-23
Figure B.4-2. Streamtraces in the Sacramento River at the Delta Cross Channel During a Rising Tide B-25

Figure B.4-3. ADCP Deployment Locations in the Sacramento River at Georgiana Slough for the 2011 (upper) and 2012 (lower) Non-physical Barrier Study B-26
Figure B.4-4. Drifter Release Locations (yellow dots) During Ebb Tides and Modeled Particle Paths and Critical Streamline Under Downstream Conditions B-27
Figure B.4-5. Drifter Release Locations (yellow dots) During Flood Tides and Modeled Particle Paths and Critical Streamline Under Upstream Conditions B-28
Figure B.4-6. Drifter Release Locations (yellow dots) During a Converging Stage and Modeled Particle Paths and Critical Streakline Under Converging Conditions B-28
Figure B.5-1. DSM2 Modeled Daily Average, Maximum, and Minimum Flow in Each DSM2 Channel Reach for Each of Six Model Scenarios in Each of Three Routes in the South Delta With the HORB In..... B-32
Figure B.5-2. DSM2 Modeled Daily Average, Maximum, and Minimum Flow in Each DSM2 Channel Reach for Each of Six Model Scenarios in Each of Three Routes in the South Delta With the HORB Out..... B-33
Figure B.5-7. Effect of Export Rate and Delta Inflow on Percent of Flow and Export Difference in the Lower San Joaquin River B-38
Figure B.5-8. DSM2 Modeled Daily Average Flow at Each DSM2 Channel Reach in the South Delta at Three Export Rates and Three Delta Inflow Rates. The Export Rates Were 2,000, 6,000 and 10,000 cfs, and the Delta Inflow Rates Were 12,000, 21,000, and 38,000 cfs..... B-40
Figure B.5-9. DSM2 Modeled Instantaneous 15-minute Flow Versus Time Over 24 Hours at the Junction of the San Joaquin River and Head of Old Rivers in Three DSM2 Channel Reaches for Nine Model Scenarios B-42
Figure B.5-10. DSM2 Modeled Instantaneous 15-minute Flow Versus Time Over 24 Hours at the Junction of San Joaquin River and Turner Cut in Three DSM2 Channel Reaches for Nine Model Scenarios..... B-43
Figure B.5-11. DSM2 Modeled Instantaneous 15-minute Flow Versus Time Over 24 Hours at the Junction of San Joaquin River and Columbia Cut in Five DSM2 Channel Reaches for Nine Model Scenarios..... B-44
Figure B.5-12. Flow at Georgiana Slough Junction Channels Over 24 Hours..... B-47
Figure B.5-13. DSM2 Modeled Instantaneous 15-minute Interval Velocity Versus Time Over One Tidal Cycle (~25 Hours) in DSM2 Channel Reaches in Three Routes of the South Delta..... B-50
Figure B.5-14. DSM2 modeled average daily velocity and instantaneous maximum velocity associated in each channel reach, in each of two routes in the south Delta. The two model scenarios were, left panels - low exports at low and high inflows, and right panels - high inflows at low and high exports. We limited the export scenarios to low exports and the inflow scenario to high inflows because high exports are not permitted at low inflows. In each graph, the upper set of lines represents the maximum velocities for the scenario, and middle set on lines represents the daily average velocities for the scenario and the lower set of lines represents the minimum velocities for the scenario. The

minimum and maximum velocities are associated with the flood and ebb tides, respectively.....B-51
Note: The three routes are San Joaquin mainstem, Old River and Middle River. The x axis is the serial DSM2 model channel number. B-51
Figure B.5-15. Effect of Export Rate and Delta Inflow on Percent of Flow and Export Difference in the Lower San Joaquin River B-52
Figure B.5-16. DSM2 Modeled Instantaneous Minimum and Maximum Velocity Associated With the Ebb and Flood Tide Phases, Respectively, in Each Channel for Each of Three Model Scenarios, in Each of Three Routes in the South Delta B-53
Figure B.5-17. Difference Between DSM2 Modeled Scenarios of Instantaneous Minimum and Maximum Velocity Associated With the Ebb and Flood Tide Phases, Respectively, in Each Channel for Each of Three Model Scenarios, in Each of Three Routes in the South Delta.....B-54
Figure B.5-18. DMS2 Modeled Instantaneous 15-minute Velocity Versus Time Over a Complete Tidal Cycle (~25 Hours) in Three Channels at the Junction of the San Joaquin River Mainstem and the Head of Old River.....B-58
Figure B.5-19. DMS2 Modeled Instantaneous 15-minute Velocity Versus Time Over a Complete Tidal Cycle (~25 Hours) in Three Channels at the Junction of the San Joaquin River Mainstem and Turner Cut B-59
Figure B.5-20. DMS2 Modeled Instantaneous 15-minute Velocity Versus Time Over a Complete Tidal Cycle (~25 Hours) in Three Channels at the Junction of the San Joaquin River Mainstem and the Mouth of Old River B-60

LIST OF TABLES

Table B.1-1. Major Sacramento-San Joaquin River Delta Inflows and Diversions, 1990-2014 (DWR 2014a).....B-2
Table B.3-1. Regression Slope and Coefficients for a Comparison Between Empirical Flow and Velocity Data and Corresponding Modeled Results for Four Stations in the South Delta.....B-15
Table B.3-2. Summary of Flow Error Metrics and Model Skill.....B-19
Table B.3-3. Summary of Velocity Error Metrics and Model Skill B-20
Table B.5-1. Hydrodynamics Drivers, Linkages, and Outcomes [DLOs] Components for Analysis (DLOs not included in the analysis are shown in red italic text).....B-31
Table B.5-2. Summary of Hydrodynamic Simulation Model Results for Flows and Changes in Flow at Various Locations Within the South Delta With and Without the Head of Old River Barrier B-39
Table B.5-3. Summary of Hydrodynamic Simulation Model Results for Changes in Water Velocities at Specific Locations Within the South Delta Without the Head of Old River Barrier for the Three Scenarios: 1) Low Inflow/Low Export; 2) High Inflow/Low Export; and 3) High Inflow/High Export B-56

B.1 INTRODUCTION AND BACKGROUND

This appendix is an assessment of the effect of water project operations on hydrodynamics in the South Delta, at the Delta Cross Channel (DCC), and in the Georgiana Slough area in the North Delta. The assessment is based on empirical data from monitoring programs and hydrodynamic model results from historical and synthetic scenarios. Comparing a historical scenario to empirical data provides a means to evaluate the accuracy of the models. Synthetic scenarios also provide information on a range of possible conditions allowing individual variables to be evaluated independently. The water project variables assessed were State Water Project (SWP) and Central Valley Project (CVP) exports, river inflow to the Delta, diversions and barriers.

Hydrodynamic conditions in the Delta, including the distribution of flows through the Delta, are influenced by a variety of factors including freshwater inflows, tides, channel geometry and channel bed characteristics, configuration of channels, water diversions, and operation of barriers and tidal gates. Under periods of low inflow, most of the system is strongly tidal with reversing flows. As inflows increase, channels become riverine, where flows do not reverse.

As described in more detail below, exports can influence the direction of daily (or tidally) averaged flow in the South Delta, with high exports causing more negative daily average flows in Old and Middle rivers (OMR) (see Section B.5.3). Operation of the DCC affects the balance of flow between the western and eastern/southern sides of the Delta. Opening the DCC allows flow to transfer from the Sacramento River channel to the Mokelumne River and then on to the lower San Joaquin River and Interior Delta (DeGeorge 2013). The flow patterns in the South Delta tend to be more complex than the North Delta due to the influence of the Clifton Court radial gate operations and export pumps on OMR, the more complex interconnected channels, the presence of South Delta temporary barriers, and greater tidal excursion along the mainstem of the San Joaquin River. Flow splits at critical junctions may be affected by the conveyance characteristics of the connecting channels, tidal phasing, and installation and operation of barriers and gates (DWR 2011a, 2011b).

Table B.1-1 provides annual average inflows and diversions from the Delta from 1990 to 2014. The location and relative magnitude of the major inflows and diversions are shown graphically in Figure B.1-1.

Table B.1-1. Major Sacramento-San Joaquin River Delta Inflows and Diversions, 1990-2014 (DWR 2014a)

Inflow/Diversion	Annual Average (maf)	Annual Minimum (maf)	Annual Maximum (maf)
Sacramento River	16	6.5	29
San Joaquin River	2.8	.6	8.5
Eastside Tributaries	3.7	.9	11
Delta Outflow	16	3.9	43
In-Delta Average Diversions	1.7	1.7	1.7
Precipitation	.9	.5	1.4
SWP Exports	2.6	.9	7
CVP Exports	2.3	1.0	2.7

Note: maf = million acre feet

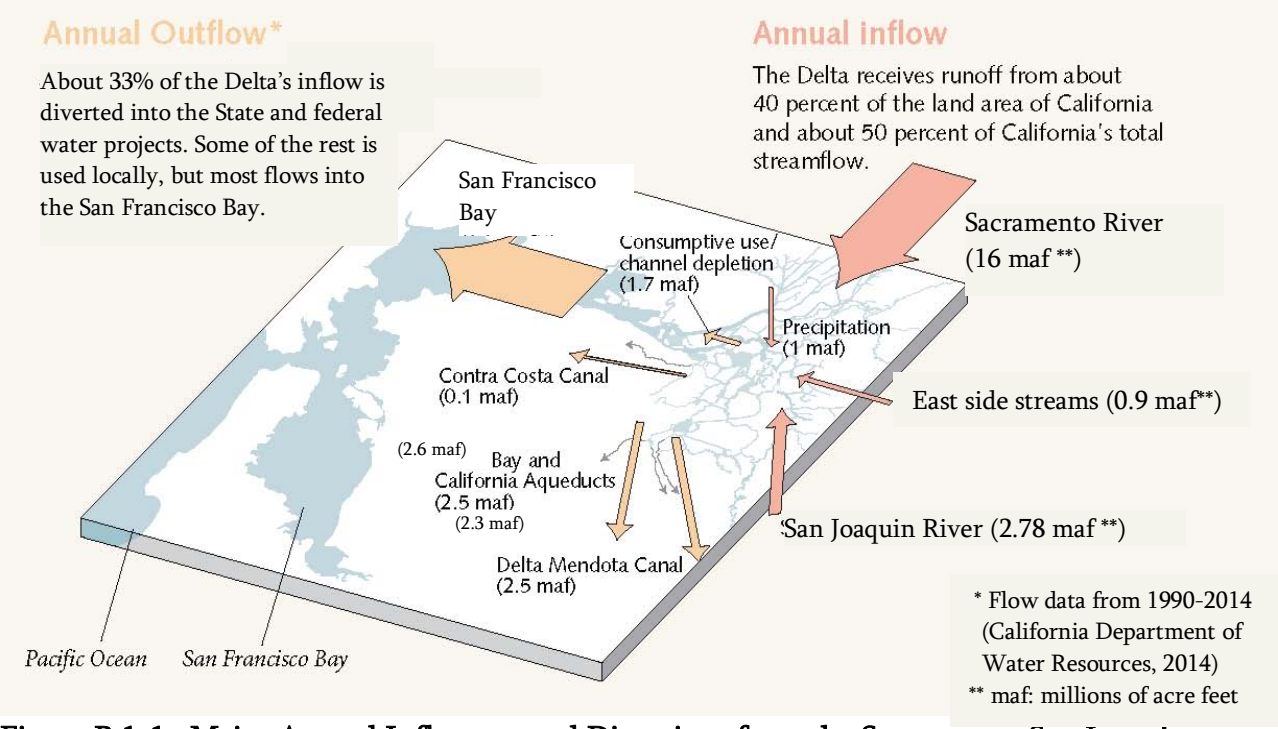

Figure B.1-1. Major Annual Inflows to and Diversions from the Sacramento-San Joaquin Delta

Source: Illustration from USGS (2000); data updated from Dayflow (DWR 2014a)

Tides are a significant factor affecting hydrodynamics in parts of the Delta, depending on inflow. DSM2 model scenarios from Kimmerer and Nobriga (2008) indicate that maximum and minimum flows range from +150,000 to -155,000 cubic feet per second (cfs) in the western Delta at Chipps Island; from +29,000 to -29,000 cfs in the lower San Joaquin River at the mouth of Middle River; and from +2,500 to -2,900 cfs in the San Joaquin River between Upper and Lower Roberts Island (Figure B.1-2) (Cavallo et al. 2013).

Under the same scenarios, maximum and minimum velocities ranged from + 1.9 to -1.8 feet per second (ft/sec) in the western Delta near Jersey Point; from +1.3 to -1.2 ft/sec in the lower San Joaquin River at the mouth of Middle River; and from +1.4 to -1.8 ft/sec between Middle and Lower Roberts Island.

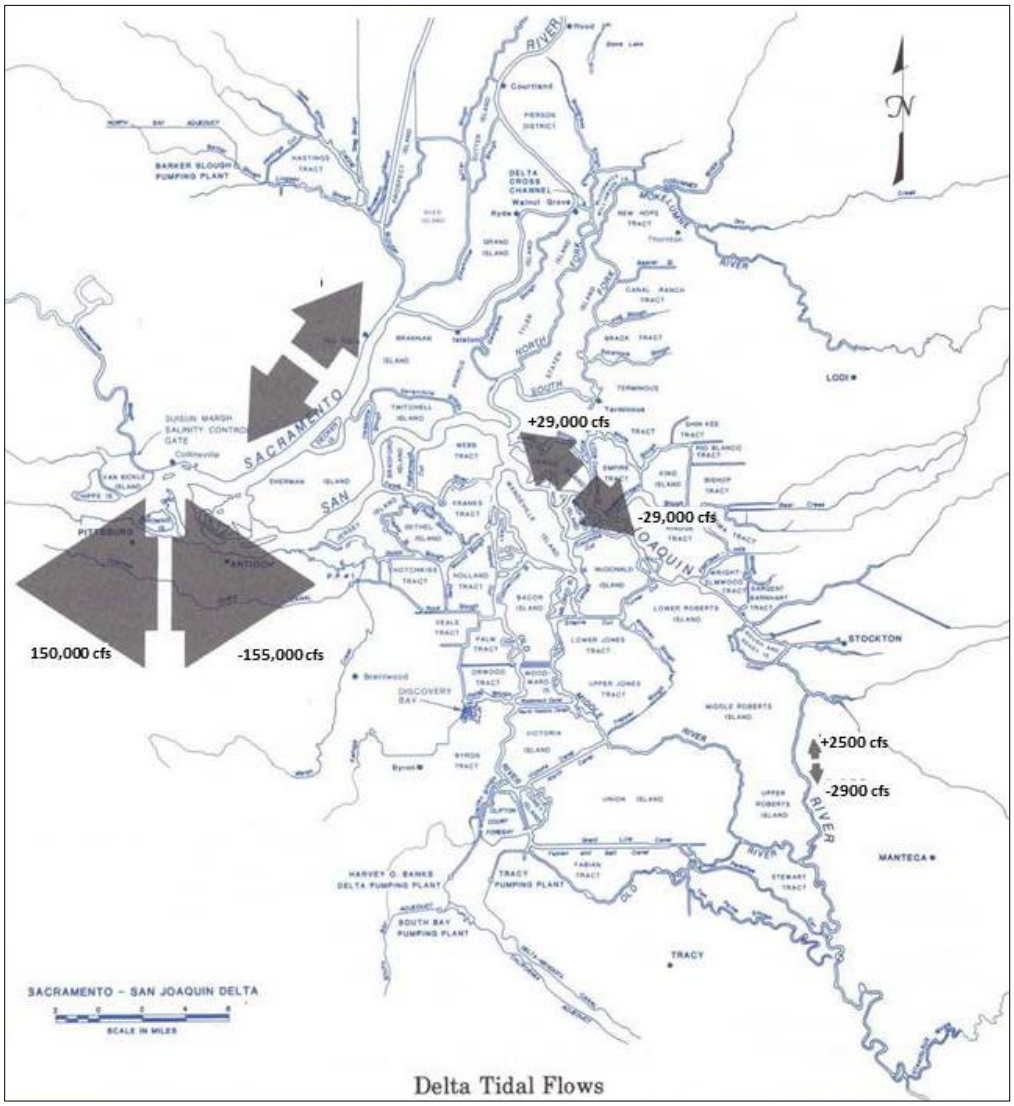

Figure B.1-2. Modeled Maximum Flows at Four Locations in the Sacramento-San Joaquin Delta using DSM2 at Low Inflows of 12,000 cfs, High Exports of 10,000 cfs, and Head of Old River Out

Note: Flows are dominated by large tidal oscillation in the western Delta, which diminishes as you move upstream. Source: Graphic from DWR (1995) Delta Atlas; model results from DSM2 scenarios from Kimmerer and Nobriga (2008).

The SWP and CVP pumping facilities in the South Delta divert Sacramento River and San Joaquin River water. Sacramento River water is diverted through the open DCC, which was built to combat saltwater intrusion in the Delta, dilute local pollution, and improve the

quality of irrigation supplies in the Central Valley. The Sacramento River water flows through the Interior Delta for agricultural use and export at the South Delta export facilities. Sacramento River water also regularly flows into Georgiana and Three Mile sloughs, and moves through OMR to reach the South Delta and the SWP and CVP export facilities.

B.2 WATER FLOW AND VELOCITY MONITORING

There is a large network of hydrologic monitoring stations in the Delta operated by the U.S. Geological Survey (USGS), California Department of Water Resources (DWR), and U.S. Bureau of Reclamation (USBR). Much of the data from these stations is telemetered to data repositories managed by DWR in the California Data Exchange Center (CDEC) (DWR 2014b). Most stations record flow in cubic feet per second, while some also record velocity and water quality parameters. The data on CDEC is sometimes preliminary and not quality assured or controlled. Stations record at a time frequency of at least one hour. Many stations record at a frequency of every 15 minutes. Figure B.2-1 shows the location of CDEC surface water stations in the Delta. The USGS also manages a data repository referred to as the National Water Information System (NWIS). In addition to flow and water quality parameters, the USGS records turbidity at some stations. Figure B.2-2 shows the location of NWIS surface water stations in the Delta.

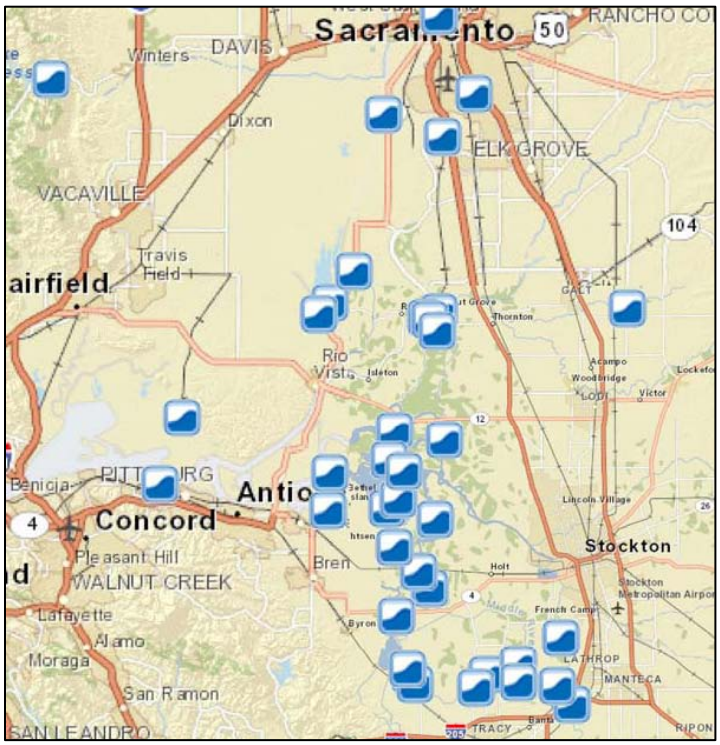

Figure B.2-1. Surface Water Stations in the Sacramento-San Joaquin Delta in the DWR CDEC Data Repository

Source: DWR (2014a)

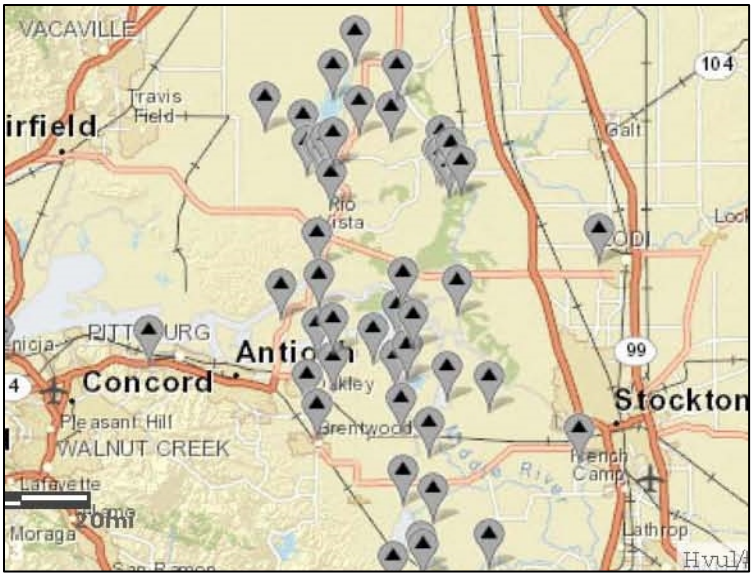

Figure B.2-2. Surface Water Monitoring Stations in the Sacramento-San Joaquin Delta in the USGS NWIS

Source: USGS (2014)

B.3 HYDRODYNAMIC SIMULATION MODELS

Hydrodynamic simulation models are useful for forecasting and planning. Forecast guidance means that predictions of flow and velocity (and temperature and salinity for instance) conditions in the future are available to water project operators and water users. For planning purposes, simulation models are useful to compare different scenarios and isolating and evaluating individual model variables.

There are several platforms commonly used for modeling hydrodynamics in the Delta. These include one-dimensional (1-D) models such as DSM2, two-dimensional (2-D) models such as RMA2, and three-dimensional (3-D) models such as UnTRIM. A more detailed description of available hydrodynamic models is provided in Appendix C. Hydrodynamic models are typically developed based on a spatial computational mesh, a bathymetric dataset, boundary conditions, initial conditions and several model parameters. The accuracy of the model application depends on the accuracy of these inputs, including site-specific parameters, and reduction of numerical error by choosing appropriate time step, grid size, and orientation for the solution. Various modeling approaches and types of model grids are shown in Figure B.3-1 and discussed by Moffat & Nichol Engineers (2003).

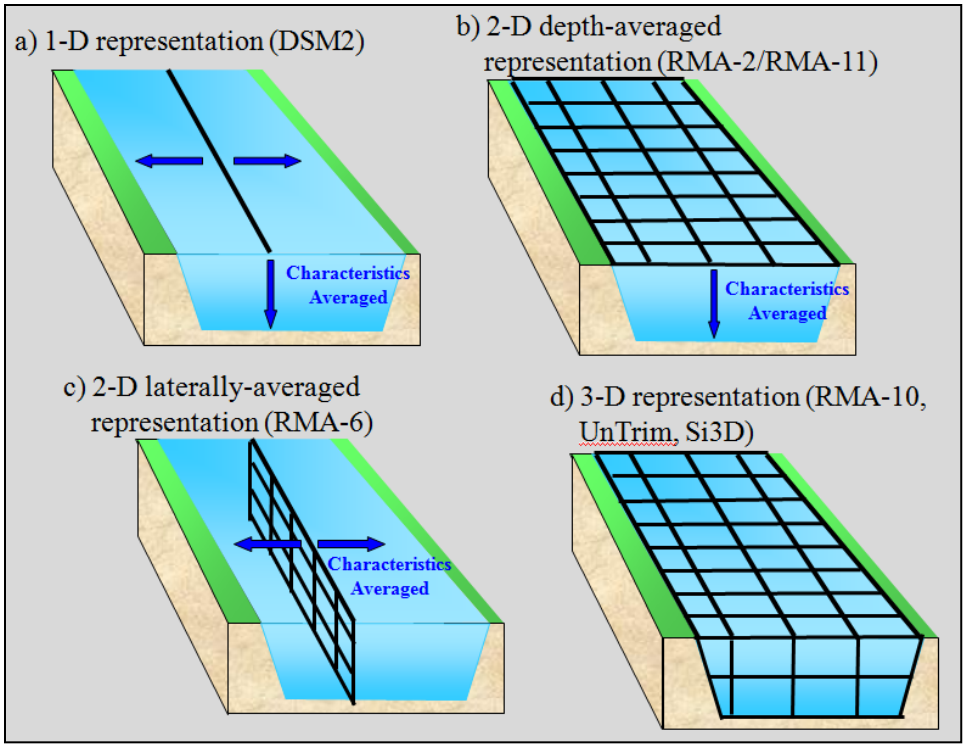

Figure B.3-1. Model Dimensionality

Note: Though not shown on the figure, the RMA2 model also supports a 1-D representation.
Source: Bombardelli et al. (2011)

All numerical modeling approaches have limitations. 3-D models generally provide more information about the spatial distribution of velocity, salinity, and other variables than lower dimensional models. Perhaps more critically, as described below, 3-D models are more mechanistic and, therefore, rely on fewer empirical parameters.

B.3.1 Model Description, Calibration and Validation

B.3.1.1 Three-Dimensional Models

3-D models estimate flow characteristics in three dimensions and through the tidal cycle, providing a detailed approximation of hydrodynamics. In actuality, flows in the Delta are turbulent, involving chaotic and unsteady velocities, changing on the time scale of seconds. Simulation of turbulent motion for a system the size of the Delta is not computationally feasible because it would require prohibitively small grid cells and time steps. Therefore, large-scale models average over the turbulent time scales to describe tidal motions. The limitations of 3-D models include:

- Spatial resolution/computational cost – the spatial resolution of the bathymetry of the model domain, and velocity, is typically limited by the large computational expense associated with high-resolution models. However, recently the resolution of bathymetry

has been decoupled from the resolution of the computational mesh allowing high-resolution bathymetry to be represented on a coarse computational mesh (Casulli and Stelling 2010).

- Site-specific parameters – at minimum, 3-D models require bottom friction coefficients to parameterize the resistance to flow at solid boundaries. These parameters are specified in model calibration either from standard reference manuals (e.g., Brater et al. 1996) or by tuning to improve calibration and may be specified globally or in map form[1].
- Turbulence closure – the effect of turbulent motions on the tidal time scale motions is estimated by a turbulence closure. While many turbulence closures are available (e.g., Umlauf and Burchard 2003), this is an ongoing area of research and, particularly in stratified settings, the effect of turbulence on tidal flows is not easy to estimate accurately and different turbulence closures may give significantly different results (Wang et al. 2011).
- Numerical errors – a numerical method approximates the governing equations to some level of accuracy. The predictions of the model can vary substantially among different numerical methods (e.g., Gross et al. 1999) and refinement of numerical methods is an ongoing area of research. Even numerical methods that are theoretically accurate often have unfavorable stability properties that require use of unrealistic diffusion coefficients or diffusive filters to maintain stability. Some models may have additional limitations, for example, not allowing wetting and drying of computational cells.

B.3.1.2 Vertically Averaged Two-Dimensional Models

Vertically averaged 2-D models average the 3-D (turbulent averaged) equations of motion over the vertical dimension and discretize the resulting equations. This typically provides an order of magnitude reduction in the total number of grid cells, and computational expense, associated with these models relative to 3-D models. The vertical distributions of velocity are not represented by 2-D models; therefore, they have a limited ability to represent density-driven and wind-driven flow. The effect of the unresolved vertical distributions of velocity on mixing and transport is parameterized by dispersion coefficients. These dispersion coefficients represent "three-dimensional processes" and are typically several orders of magnitude larger than eddy diffusivity (the effect of turbulence), indicating substantial reliance of 2-D models on these empirical parameters. The limitations of vertically averaged models are:

1 Map form: 1. A geographic map on which meteorological conditions or elements are represented by figures, symbols, or isopleths. 2. Data values that are projected relative to a precise latitude–longitude grid in any specified projection, such as Mercator or polar stereographic.

- No characterization of vertical variation in velocity or salinity.
- Heavy reliance on dispersion coefficients. These site-specific parameters vary spatially and should theoretically be varied with flow conditions and tidal conditions (Monismith et al. 2002). In practice, a constant set of dispersion coefficients, often in map form, are applied for all flow and tidal conditions. For this reason, 2-D models are likely to be less accurate than well-calibrated 3-D models for unusual flow and/or tidal conditions.

B.3.1.3 One-Dimensional Models

1-D models average the 3-D (turbulent averaged) equations of motion over the vertical and lateral directions and discretize the resulting equations. Therefore, salinity in regards to transport, is assumed to be fully mixed over the cross-section. 1-D models have minimal computational expense, relative to 3-D models, but also provide quite limited information about velocity and salinity distribution. The limitations of 1-D models include:

- No characterization of lateral variability in velocity or salinity.
- Heavy reliance on dispersion coefficients.

B.3.1.4 Model Calibration and Validation

Model calibration efforts are highly specific and depend on the project to which the model is being applied and the geographic focus and relevant time periods of model application. Well-calibrated 1- or 2-D models may perform better for many applications than poorly calibrated 3-D models.

Several potential problems have been identified in the literature relative to hydrodynamic model calibration and validation in the South Delta (MacWilliams et al. 2008). One is the representation of the Clifton Court Forebay (CCF) operation. Inflow at CCF radial gates is not measured continuously; it is estimated. There are two estimation methods used by DWR. The first method involves calculating the difference between expected storage and actual storage in CCF, with expected storage estimated from the export pump's rating. The second method involves using stage data measured inside and outside of the forebay gates and gate heights. The two methods provide similar results, but neither is an actual measurement of inflow within the channel into CCF.

Another factor affecting validation is the time phase difference between modeled results and measured data. During the 2012 Stipulation Study, modeled flow data were compared to measured data at Turner Cut (Delaney et al. 2014). The time was out of phase by about two hours, and the flow magnitude during the high-low tide was different by about 1,500 cfs (Figure B.3-2). At the time of the writing of the 2012 Stipulation Study, the source of the error (modeled or empirical) was unknown.

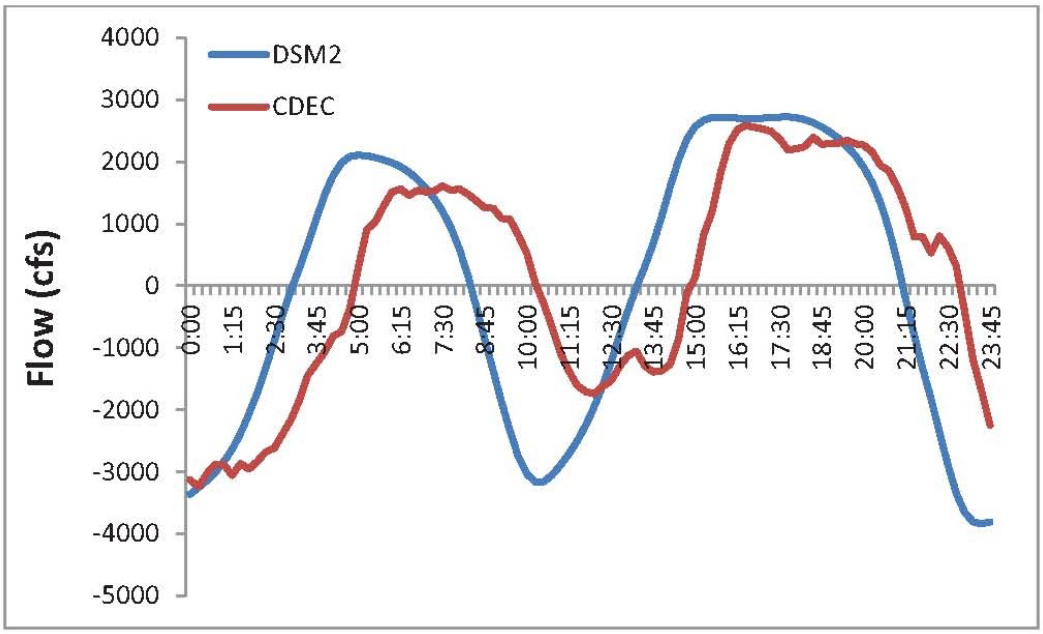

Figure B.3-2. Fifteen-minute Flow Data over 24 Hours at Turner Cut Represented by Both DSM2 Model Results and Measured Data

Source: Delaney et al. (2014)

Other factors identified as adversely affecting hydrodynamic model calibration and validation in the South Delta are inadequate bathymetry data in the South Delta, and inadequate Delta Consumptive Use data. Channel configuration has a major effect on the influence of inflow and exports on the magnitude, direction, and proportion of flow entering downstream channels through the interior, central, and South Delta. Current, high-resolution channel bathymetry is necessary to better determine the combined hydrologic effects of exports, tides, and river inflows on salmonid movement and survival through the Delta. Delta Consumptive Use becomes extremely important at low net Delta outflows. DWR has an ongoing program to develop better Delta Consumptive Use estimates called DETAW. There is also work ongoing at UC Davis on this topic (baydeltaoffice.water.ca.gov/modeling/deltamodeling/delta/reports/annrpt/2006/2006Ch7.pdf and www.cwemf.org/Activities/DETAWWorkshop/IDCPres.pdf).

B.3.1.5 Comparison of Modeled to Measured Water Flow and Velocity

To assess the accuracy of DSM2 hydrologic model simulations in the South Delta, we compared results from a historical hydrodynamic simulation to field-measured hydrologic data from four monitoring stations in the South Delta: the head of Turner Cut, Old River at Highway 4, Old River near the intake to Clifton Court, and West Canal near the intake to Clifton Court (Figure B.3-3).

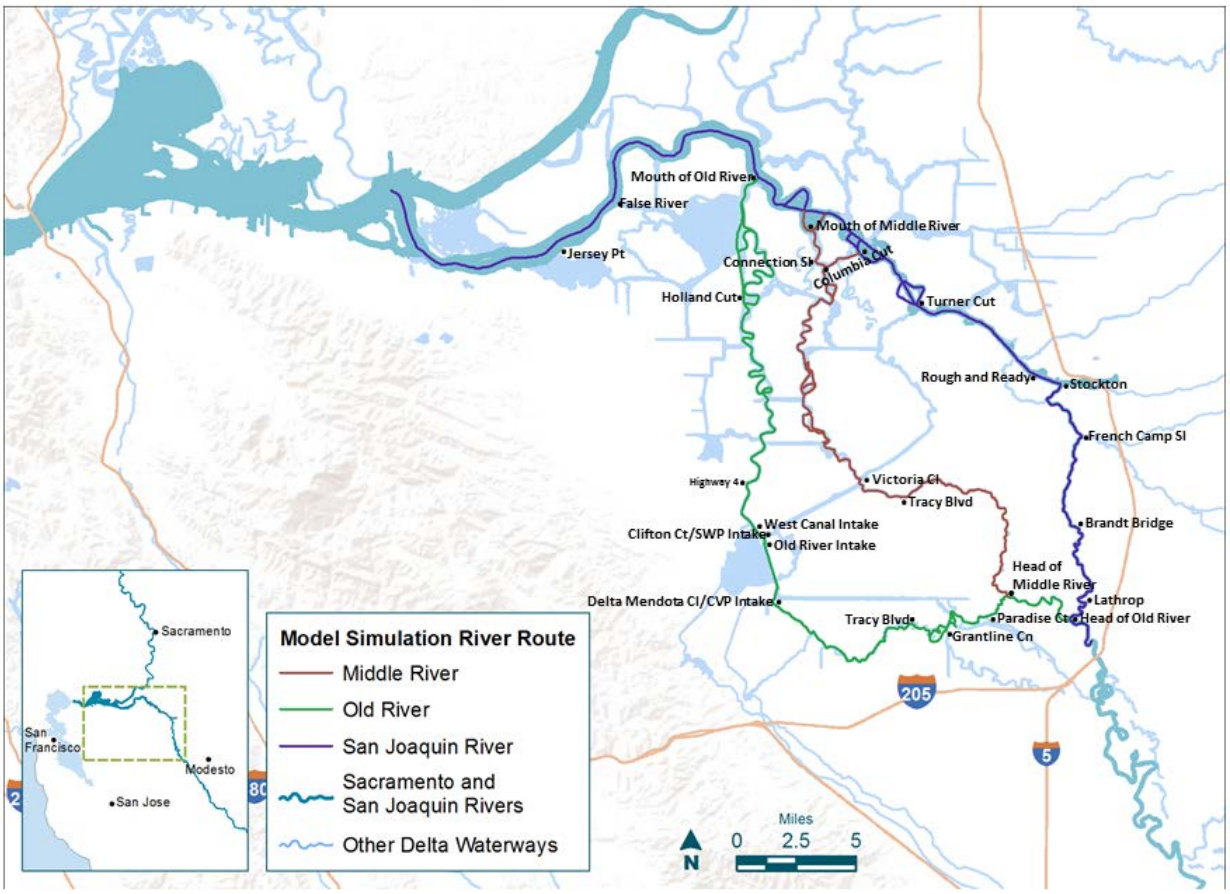

Figure B.3-3. Location of Monitoring Stations used for Comparing Historical DSM2 Simulations with Field-measured Data and for Evaluating DSM2 Model Comparisons

We compared historical measured 15-minute flow and velocity data over a one-month period, immediately upstream and downstream of the CCF intake to simulated model results for similar locations (Figure B.3-4 and Figure B.3-5). The model results and empirical data were obtained from RMA. The tidal phase shift (or lag) was removed for the comparison. The monitoring stations examined were West Canal Intake and Old River at Clifton Court Intake. The corresponding DSM2 channels were 132 and 82, respectively. The cyclic effect of tidal action on flows and velocities in South Delta channels are clear both in the observed field measurements and in the model simulations. In addition to showing the 15-minute time step, Figure B.3-4 and Figure B.3-5 show tidally filtered flows and velocities to remove the tidal effects from the data.

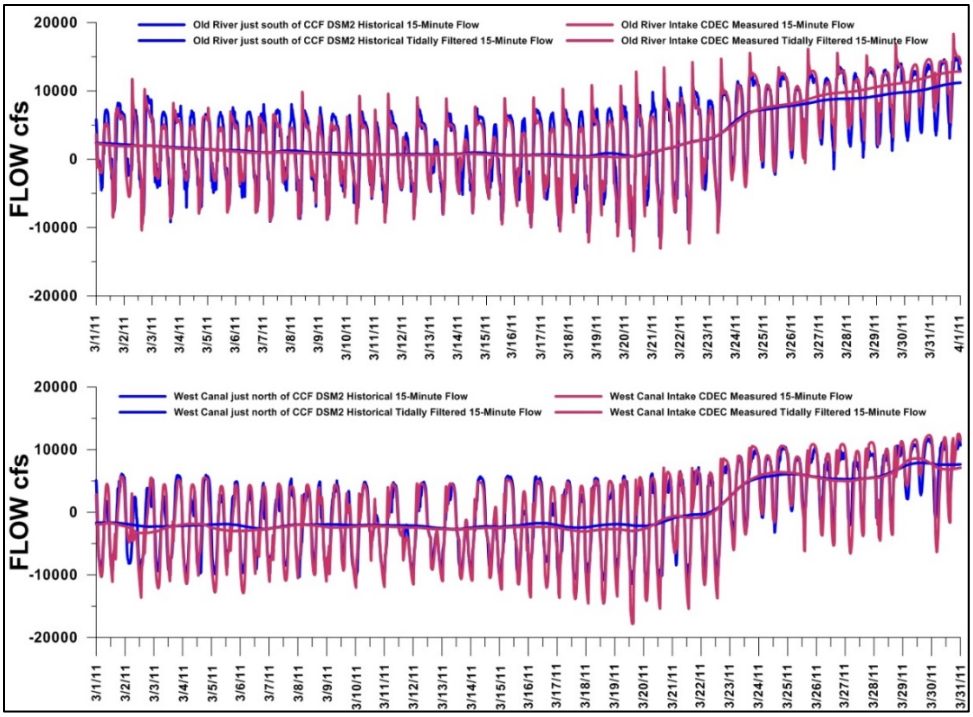

Figure B.3-4. Comparison of Field Measurements and DSM2 Simulation Results for 15-minute and Tidally Filtered 15-minute Flow Immediately Upstream and Downstream of the CCF Intake

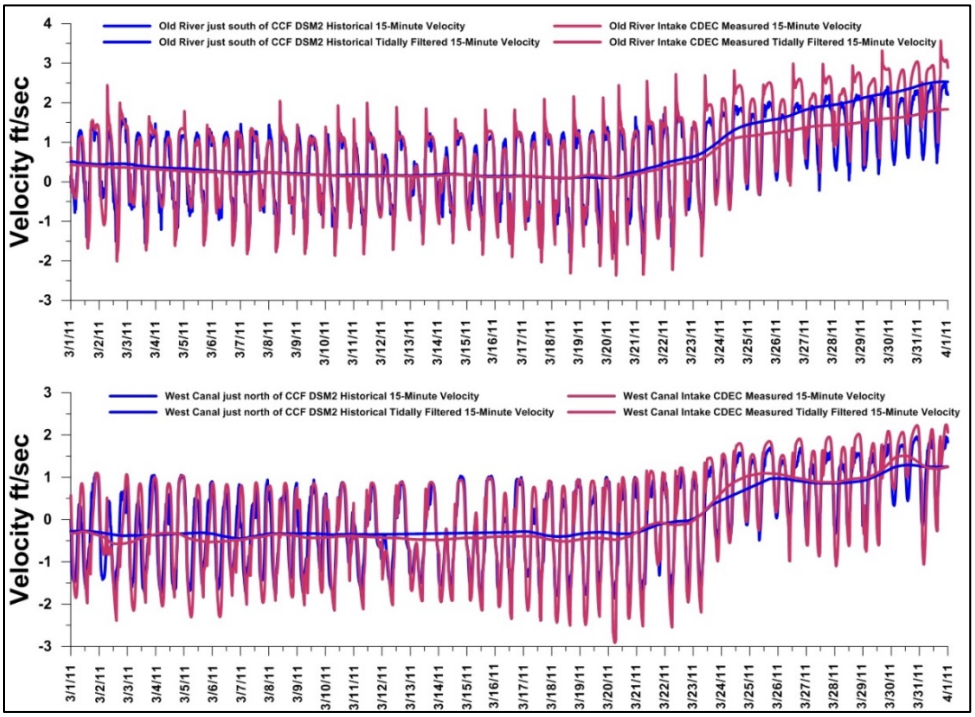

Figure B.3-5. Comparison of Field Measurements and DSM2 Simulation Results for 15-minute and Tidally Filtered 15-minute Velocity Immediately Upstream and Downstream of the CCF Intake

We also examined X:Y scatter plots of the measured and simulated flow and velocity data (Figure B.3-6 through Figure B.3-9). If the model predictions and field observations are in perfect agreement, a regression fit to the data would have a slope of 1.0 and a correlation coefficient (r^2) equal to 1.0. Regression coefficients for each of the South Delta locations included in the comparative analysis are summarized in Table B.3-1.

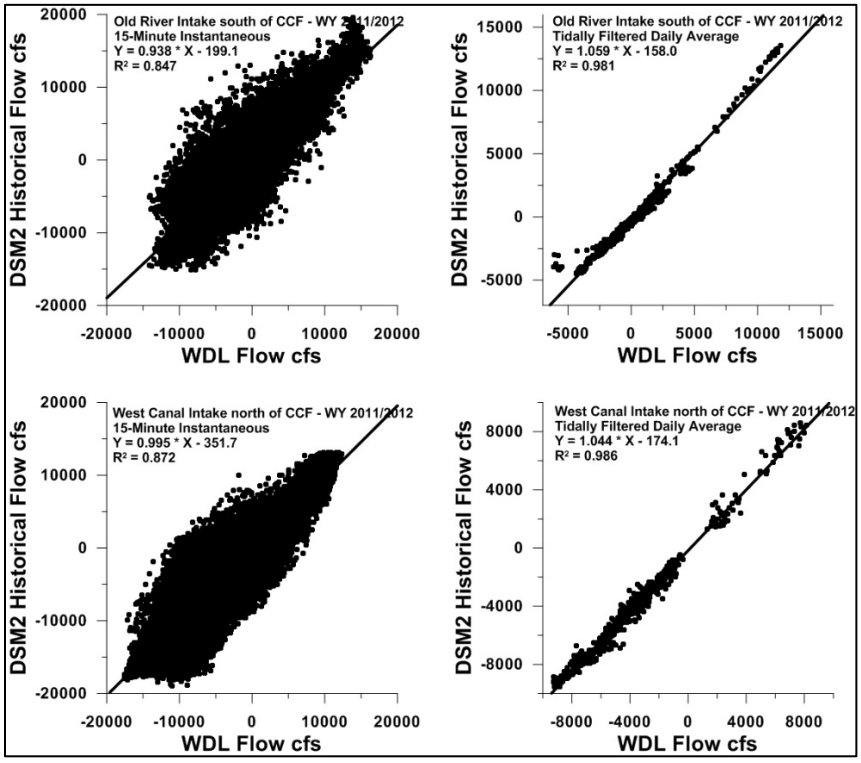

Figure B.3-6. Comparison of Field Measurements and DSM2 Simulation Results for 15-minute and Tidally Filtered Daily Average Flow at the Old River and West Canal Intakes

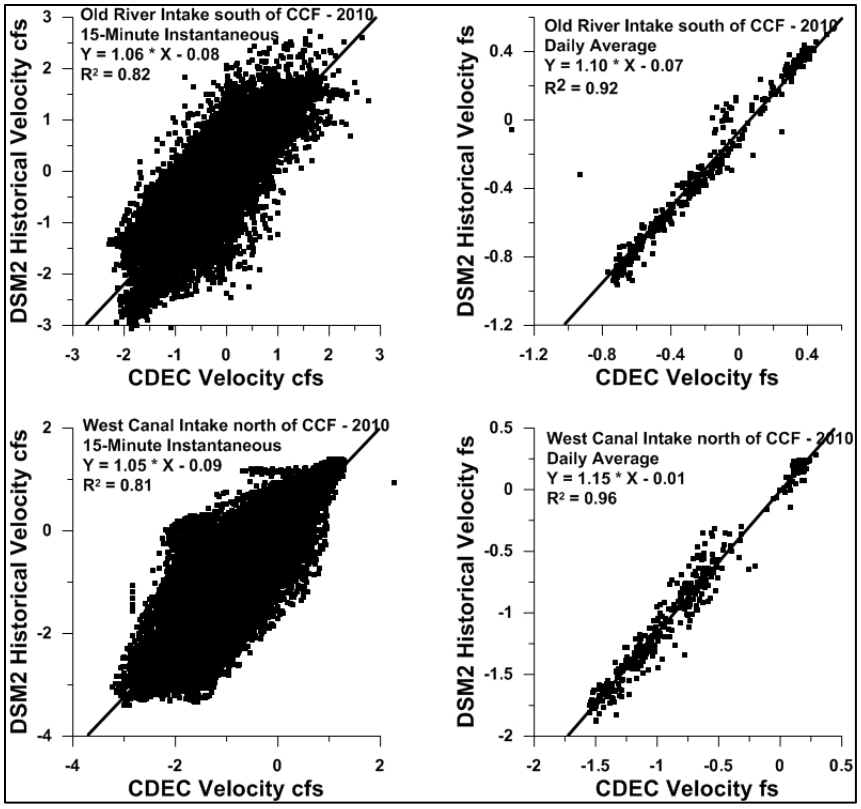

Figure B.3-7. Comparison of Field Measurements and DSM2 Simulation Results for 15-minute and Tidally Filtered Daily Average Velocity at the Old River and West Canal Intakes

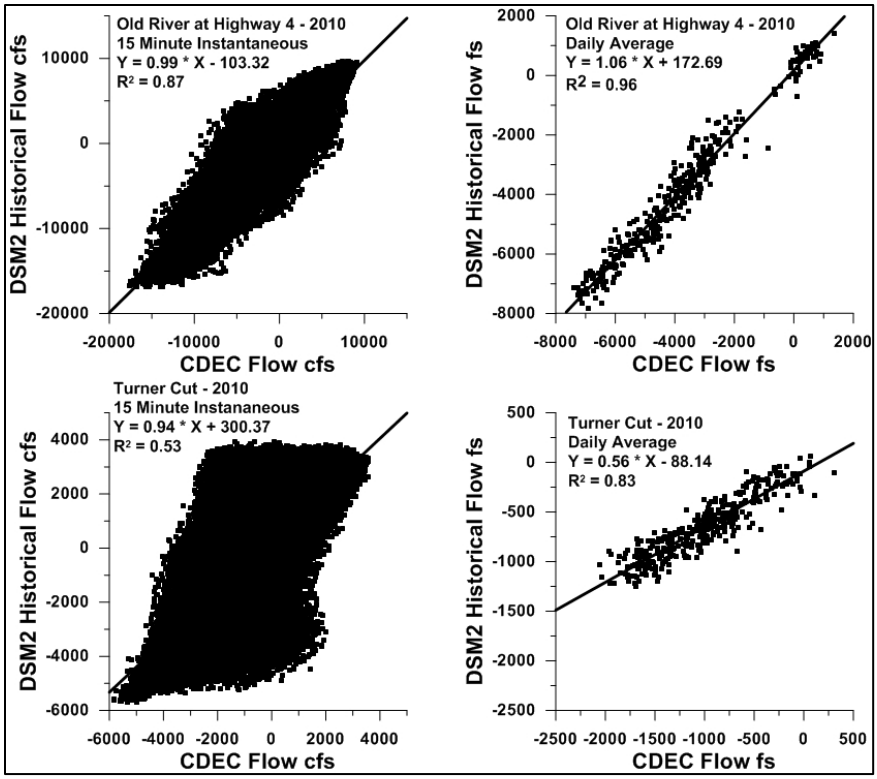

Figure B.3-8. Comparison of Field Measurements and DSM2 Simulation Results for 15-minute and Tidally Filtered Daily Average Flow at the Old River at Highway 4 and Turner Cut

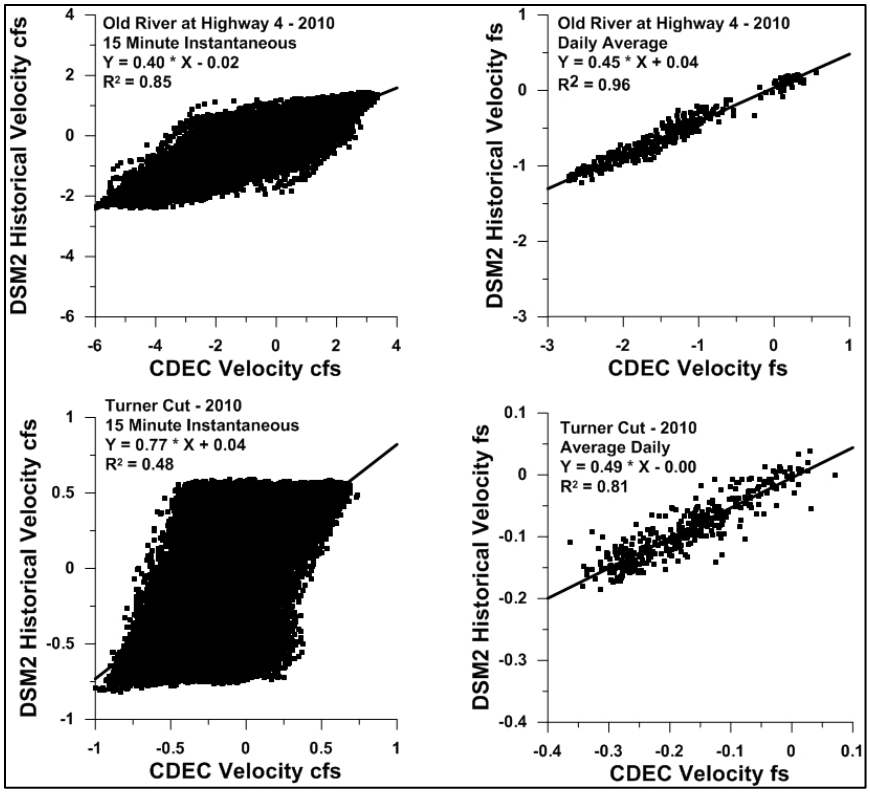

Figure B.3-9. Comparison of Field Measurements and DSM2 Simulation Results for 15-minute and Tidally Filtered Daily Average Velocity at the Old River at Highway 4 and Turner Cut

Table B.3-1. Regression Slope and Coefficients for a Comparison Between Empirical Flow and Velocity Data and Corresponding Modeled Results for Four Stations in the South Delta

Location	15-minute Flow Slope, r^2	15-minute Velocity Slope, r^2
West Canal near Clifton Court	0.995, 0.872	1.018, 0.829
Old River near Clifton Court	0.938, 0.847	1.137, 0.841
Old River at Highway 4	0.985, 0.888	0.340, 0.889
Turner Cut	0.754, 0.451	0.614, 0.451
Location	**Tidally Filtered Average Daily Flow Slope, r^2**	**Tidally Filtered Average Daily Velocity Slope, r^2**
West Canal near Clifton Court	1.044, 0.986	1.103, 0.990
Old River near Clifton Court	1.059, 0.981	1.317, 0.990
Old River at Highway 4	1.081, 0.986	0.447, 0.987
Turner Cut	0.504, 0.711	0.412, 0.716

Based on results of these analyses, we concluded that the agreement between DSM2 model predictions and measured flow and velocity is better at some locations than others in the South Delta. Results also show that the model predictions and measured values are in better agreement when using average daily values than when using 15-minute values. Furthermore, the agreement at one location can change over months and years such as the

case of Turner Cut (Figure B.3-10). The variation between modeled and measured values at a location could be the result of model input inaccuracies and over-simplified assumptions, consumptive use, bathymetry or inaccuracies, and drift in the meters used to measure velocities in the Delta.

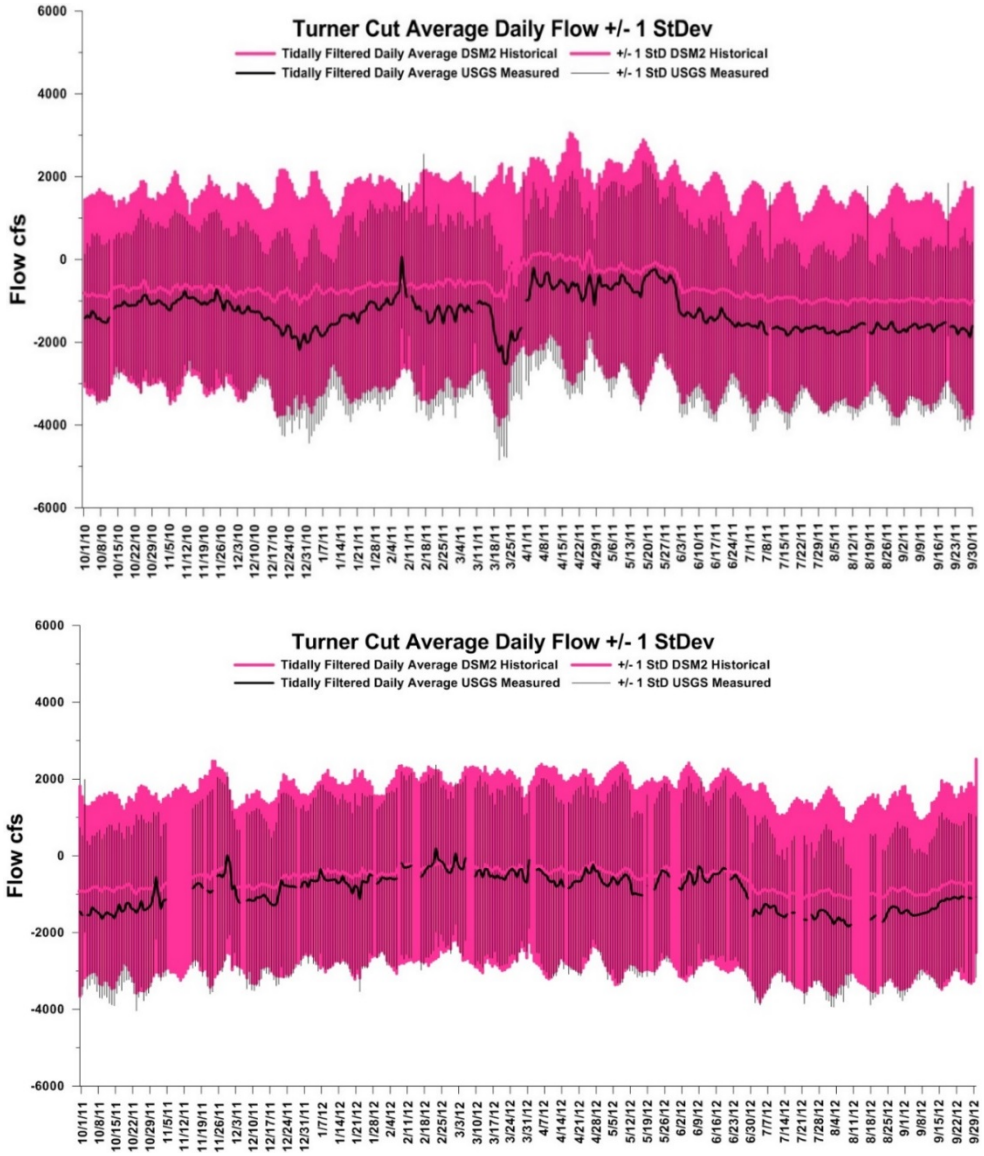

Figure B.3-10. Comparison of Field Measurements and DSM2 Simulation Results for 15-minute and Tidally Filtered Daily Average Flow at Turner Cut for Water Years 2011 and 2012

Numerous studies have been conducted in the last couple of decades to better document the hydrodynamics at complex locations in the Delta (Dinehart and Burau 2005a, 2005b; Paulsen and Chiang 2008; Brunell et al. 2010; DWR 2012, 2013). The purposes of these studies are to calibrate the hydrodynamic models at those locations, and to expand the results to other areas in the Delta. The USGS also regularly collects velocity transects at many locations in the Delta for the calibration of their flow stations.

B.3.2 Comparison of One-Dimensional and Two-Dimensional Model Results

While many hydrodynamic models have been applied in the Delta, the hydrodynamic models most extensively used in studies that have both hydrodynamic and particle tracking components are DSM2, RMA2, and UnTRIM. For this reason, available model comparisons performed to date have largely applied to these models.

The DSM2 and RMA2 hydrodynamic model performance in the Delta are compared by Bombardelli et al. (2011). The report concludes that while one model may perform better than the other at individual locations, both models performed well for a range of conditions including high and low tributary flow and high and low exports.

The Salmon Scoping Team (SST) requested a comparison between DSM2-1D and RMA-2D model simulations and measured flow and velocity data at 18 locations in the South Delta to help determine if there is a model that can be used at a short time scale and small geographic scale to complement the fine-scale acoustic tag fish data that have been collected. The complete report is included as Appendix C.

DSM2 is a 1-D longitudinal model with depth and cross section averaged. RMA-2D adds a second dimension, cross section, at the wider channels in the Delta. The depth dimension is still averaged, and one dimension is used in most of the South Delta where the channels are narrower. Model simulations of historical conditions were performed for the period from October 1, 2010 through September 30, 2012. Water year 2011 was a wet year and 2012 a below normal/dry year.

RMA compared three scenarios, DSM2-1D with their boundary conditions, RMA-2D with DSM2 boundary conditions, and RMA-2D with their own boundary conditions to the measured data. Most boundary conditions between DSM2 and RMA were similar, with the exception of Cache Slough/Yolo Bypass area (Appendix C, Pages 3 and 8 for a complete description).

The quality of fit between model results and measured data is presented in the form of time series of both 15-minute instantaneous and tidally averaged time scales in Appendix C. In addition, RMA used several model error metric statistics and model skill[2] to quantify the differences between model results and measured data. The error metrics were mean, lag, linear regression, and amplitude ratio. A summary of flow and velocity error metrics and

2 Model skill is a measure of hydrodynamic model performance that captures the degree to which deviations in the observed data about the observed data average correlate with deviations in the modeled data about the observed data average (Willmott 1981).

model skill are presented in Table B.3-2 and Table B.3-3 with colored cells for a quick assessment of goodness of fit with observed data. The colors range from green for better fit to red for worse fit.

The DSM2 and RMA models both compared favorably with measured data throughout much of the South Delta. The RMA model compared better with measured data than DMS2 with regard to mean difference from measured data (17.2% versus 54.2%, respectively) and lag (22 versus 28 minutes, respectively), while DSM2 model compared slightly better than RMA with regard to linear regression (0.941 versus 0.937 r^2, respectively) and amplitude ratio (0.940 versus 0.939, respectively). The two models were very close in terms of model skill (RMA=0.967 versus DSM2=0.957), both near the cusp of accurate and acceptable (0.95). There was little difference between the results of RMA in the South Delta using the DSM2 boundary conditions compared to their own RMA boundary conditions (see Table B.3-2 and Table B.3-3).

For the RMA model, the mean percent flow difference from measured data is about 10% or less at most locations analyzed with an average absolute difference of 17%. For DSM2, the mean percent difference from measured data was about 10% for the majority of stations as well, but there were a few more locations that did not validate well resulting in an average absolute difference of 54%. These stations are described in more detail below.

DSM2 flow lagged measured data at all locations, with an average lag of 28 minutes. The RMA model had a mix of positive and negative lags with an average of the absolute lag values of 12 minutes.

At most locations, r^2 values for flow exceeded 0.9 for both models and averaged about 0.94 for both models. Amplitude ratios and slopes ranged from 0.8 to 1.1 at most locations for both models and averaged 0.94.

During the lower flow periods within water year 2011 and 2012, DSM2 and RMA produced similar flow results at many locations. In comparison, there tended to be more disparity among the models and between the models and measured data during the high flow period in April 2011. Two contributing factors could be: 1) geometry in either model may not be as accurate at higher water levels; and 2) measured data gauges may not be as accurate at high flows for some locations.

Table B.3-2. Summary of Flow Error Metrics and Model Skill

	% diff from observed			lag (minutes)			ampRatio			R2			Model Skill		
Station	DSM2	RMA2 w DSM2 BC	RMA2	DSM2	RMA2 w DSM2 BC	RMA2	DSM2	RMA2 w DSM2 BC	RMA2	DSM2	RMA2 w DSM2 BC	RMA2	DSM2	RMA2 w DSM2 BC	RMA2
SJR at Brandt Bridge	5.9%	0.6%	2.8%	-24	2	2	1.013	1.047	1.045	0.987	0.985	0.990	0.994	0.996	0.997
SJR at Prisoners Point	149.9%	82.7%	84.4%	-44	-27	-27	0.808	0.970	0.970	0.975	0.972	0.973	0.945	0.978	0.979
SJR at Jersey Pt	-3.9%	3.4%	0.2%	-27	-14	-14	0.879	0.961	0.961	0.987	0.988	0.989	0.980	0.993	0.994
Old River at Franks Tr	-246.7%	-84.0%	-85.9%	-23	7	7	1.199	0.776	0.776	0.935	0.915	0.916	0.939	0.962	0.962
Holland Cut	90.9%	55.0%	55.6%	-28	-21	-20	0.670	1.007	1.007	0.974	0.973	0.974	0.938	0.983	0.984
Old River at Bacon	-4.8%	7.6%	8.0%	-17	-18	-17	0.934	1.058	1.059	0.973	0.977	0.979	0.987	0.987	0.988
Old River at Quimby	-305.5%	-23.3%	-21.8%	-11	-15	-15	0.900	1.023	1.023	0.965	0.967	0.969	0.979	0.987	0.987
Middle River at Middle River	-6.3%	2.4%	2.8%	-39	-11	-11	0.815	0.878	0.880	0.960	0.967	0.968	0.952	0.987	0.987
Turner Cut at Holt	41.6%	-8.8%	-9.1%	-90	-7	-7	1.103	0.568	0.569	0.907	0.816	0.816	0.811	0.900	0.901
Old River near DMC	23.7%	4.0%	3.8%	-30	7	7	0.875	0.892	0.894	0.894	0.901	0.900	0.953	0.973	0.973
Old River at Tracy	10.6%	13.2%	12.7%	-23	23	23	1.247	0.858	0.861	0.916	0.879	0.876	0.940	0.957	0.956
Old River at Hwy 4	-3.3%	-2.3%	-2.0%	-25	-9	-9	0.984	1.035	1.036	0.922	0.928	0.930	0.970	0.978	0.979
SJR at Rough-n-Ready	-1.6%	1.5%	-0.6%	-29	-4	-4	0.831	1.095	1.095	0.928	0.913	0.921	0.956	0.976	0.978
SJR at Garwood	4.6%	0.4%	-1.8%	-34	-12	-11	0.950	1.097	1.096	0.973	0.968	0.978	0.985	0.991	0.993
Old River at Head	-2.3%	-1.7%	-4.0%	-16	14	14	0.939	0.862	0.858	0.956	0.960	0.977	0.988	0.990	0.993
SJR nr Lathrop	14.6%	-9.1%	-11.5%	-20	4	4	0.914	0.970	0.967	0.954	0.955	0.959	0.982	0.986	0.986
Old R at Clifton Court Intake	-50.1%	-1.4%	1.5%	-11	9	9	0.879	0.879	0.879	0.858	0.859	0.859	0.958	0.960	0.960
West Canal at Clifton Ct Intake	-8.7%	1.0%	1.2%	-4	12	12	0.973	0.918	0.919	0.873	0.882	0.883	0.964	0.967	0.967
Average of absolute values	54.2%	16.8%	17.2%	28	12	12	0.940	0.939	0.939	0.941	0.934	0.937	0.957	0.975	0.976

Note: Shading ranges from green for better fit to red for worse fit.
Source: RMA (2015)

Table B.3-3. Summary of Velocity Error Metrics and Model Skill

	% diff from observed			lag (minutes)			ampRatio			R2			Model Skill		
Station	DSM2	RMA2 w DSM2 BC	RMA2	DSM2	RMA2 w DSM2 BC	RMA2	DSM2	RMA2 w DSM2 BC	RMA2	DSM2	RMA2 w DSM2 BC	RMA2	DSM2	RMA2 w DSM2 BC	RMA2
SJR at Brandt Bridge*	-6.6%	-8.8%	-7.4%	1	27	27	0.861	0.918	0.915	0.957	0.956	0.960	0.984	0.980	0.982
SJR at Prisoners Point	187.5%	97.7%	99.7%	-43	-26	-26	0.904	0.927	0.927	0.975	0.972	0.973	0.954	0.978	0.978
SJR at Jersey Pt	-33.2%	-8.9%	-6.5%	-27	-13	-13	0.652	0.953	0.953	0.987	0.987	0.989	0.940	0.993	0.993
Old River at Franks Tr	-253.3%	-69.1%	-70.9%	-22	6	6	0.993	0.592	0.593	0.936	0.917	0.918	0.956	0.920	0.920
Holland Cut	93.2%	64.7%	65.2%	-27	-20	-20	0.973	0.900	0.900	0.974	0.973	0.974	0.975	0.981	0.982
Old River at Bacon	2.3%	21.4%	21.8%	-17	-17	-17	0.879	0.909	0.909	0.972	0.977	0.979	0.985	0.986	0.987
Old River at Quimby	-394.6%	-18.0%	-16.5%	-12	-15	-14	0.899	0.910	0.911	0.967	0.968	0.969	0.979	0.985	0.986
Turner Cut at Holt	55.0%	-5.2%	-5.4%	-90	-8	-7	0.896	0.504	0.505	0.898	0.794	0.794	0.805	0.871	0.871
Old River near DMC	34.7%	13.2%	13.1%	-26	9	9	0.990	1.065	1.067	0.899	0.896	0.897	0.952	0.966	0.966
Old River at Tracy*	-18.6%	-18.3%	-17.8%	0	47	47	0.822	0.741	0.743	0.806	0.736	0.734	0.937	0.902	0.902
Old River at Hwy 4	58.9%	60.6%	60.7%	-24	-8	-8	0.395	0.403	0.404	0.920	0.927	0.928	0.778	0.785	0.786
SJR at Rough-n-Ready*	4.6%	-7.1%	-5.2%	-9	14	15	0.878	1.018	1.018	0.849	0.832	0.839	0.957	0.949	0.951
SJR at Garwood	8.4%	3.1%	5.1%	-32	-10	-10	0.989	1.110	1.110	0.973	0.971	0.978	0.983	0.991	0.993
Old River at Head*	-10.2%	-15.7%	-14.5%	18	40	41	0.748	0.625	0.619	0.922	0.922	0.921	0.969	0.958	0.960
SJR nr Lathrop*	-12.4%	-14.2%	-13.1%	21	43	44	0.584	0.655	0.656	0.804	0.838	0.854	0.931	0.932	0.937
Old R at Clifton Court Intake*	-95.2%	-23.8%	-21.4%	10	37	37	1.043	0.947	0.946	0.849	0.848	0.849	0.945	0.936	0.936
West Canal at Clifton Ct Intake*	-14.3%	-7.4%	-7.2%	28	40	40	1.006	0.973	0.974	0.860	0.860	0.861	0.949	0.940	0.940
Average of absolute values	72.8%	25.6%	25.3%	24	22	22	0.854	0.832	0.832	0.915	0.904	0.907	0.940	0.944	0.945

Notes: Asterisks after station names indicate that observed data are from CDEC, which can contain time shift errors. Shading ranges from green for better fit to red for worse fit.
Source: RMA (2015)

There were four locations in the South Delta where both models diverged from measured flow data: Old River at Franks Tract (Appendix C, Figures C24-C26), San Joaquin River at Prisoners Point (Appendix C, Figures 18-20), and Holland Cut (Appendix C, Figures 27-29). The largest differences between DSM2 and RMA and their divergence from measured data occurred at Old River at Franks Tract (-246.7 versus -85.9, respectively) (Table B.3-2), Old River at Quimby (-305.5 versus -21.8, respectively) (Table B.3-2; Appendix C, Figures 33-35), Turner Cut (+41.6 versus -9.1, respectively) (Table B.3-2; Appendix C, Figures 39-41), and Holland Cut (+90.9 versus +55.6, respectively) (Table B.3-2). At Turner Cut, both models were in the poor category for model skill (Table B.3-2). Refer to Appendix C (pages 14 through 16) for a detailed explanation of the difficulties at these locations.

There were larger disparities between modeled velocity and measured velocity relative to flow. For the RMA model, the average absolute difference was 25% (compared to 17% for flow), and for DSM2, the average absolute difference was 73% (compared to 54% for flow). The trend among the locations was mostly similar for both models with the exception of Old River at Highway 4. Old River at Highway 4 had a particularly higher percent difference between modeled velocity results and measured velocity (Appendix C, Figures 48-50 for flow and Figures 118-120 for velocity): about 60% for both models compared to about -3% for both models for flow.

B.4 TEMPORARY, OPERABLE, AND NON-PHYSICAL BARRIERS

As part of SWP and CVP operations, both temporary rock barriers (e.g., agricultural barriers in the South Delta, the Head of Old River Barrier [HORB]) and operable barriers (DCC radial gates) are used to regulate and manage water flows through Delta channels and reduce the effects of South Delta export operations on water elevation in South Delta channels. In recent years, use of non-physical barriers for guiding downstream migrating Chinook salmon and steelhead have been tested in the Sacramento River at Georgiana Slough and San Joaquin River at the head of Old River.

B.4.1 TEMPORARY BARRIERS

The South Delta Temporary Barriers Project has been in place since 1991 and has included the spring installation and subsequent fall removal of four rock barriers at a number of locations in the South Delta (DWR 2011a). The historical construction schedule can be found at http://baydeltaoffice.water.ca.gov/sdb/tbp/web_pg/tempbsch.cfm. The three agricultural barriers are used to increase water levels in South Delta channels (thereby reducing the effects of exports on water levels), and to improve water circulation and water quality for agricultural use. Temporary agricultural barriers are installed at Middle River, the head of Old River during the spring and fall, Grant Line Canal, and Old River at Tracy in the spring.

As part of the Delta Temporary Barriers Project evaluation (DWR 2011a, 2011b), the 1-D DSM2 model was used at a 15-minute time step to simulate changes in average daily flow in various Delta channels with and without the temporary barriers. The model was used to represent actual hydrologic boundary conditions during the period that the barriers were installed. Results of the model validation show that the model predictions and observed stage and flow generally agree at a majority of locations.

Results of the DSM2 simulations showed that installation of the temporary barriers resulted in significantly altered stage and flows in the South Delta (DWR 2011a, 2011b). The effects of barrier installation were typically localized to the channels in the immediate vicinity of each barrier and diminished with distance upstream and downstream from the barrier. The barriers were also found to diminish tidal variation in flows with the effect most pronounced in OMR when the Grant Line Canal barrier was installed. Model analyses of the effects of the temporary barriers on hydrodynamics in the South Delta in 2009 are presented in DWR (2011b).

B.4.2 Head of Old River Barrier

The HORB is used to increase flows and dissolved oxygen concentrations for adult fall-run Chinook migration, and reduce the proportion of juvenile salmon and steelhead migrating into Old River in the spring. Results of DSM2 simulations show that installation of the HORB significantly reduces the flow of water that enters Old River and Grant Line Canal (DWR 2011a, 2011b) from the lower San Joaquin River. The HORB increases flow in the mainstem of the San Joaquin River, decreases flow in Old River between the head and Grant Line Canal, and decreases minimum velocity in Middle River between the head and Tracy Boulevard (see section B.5.3 for details).

B.4.3 Delta Cross Channel

The USGS conducted a fine-scale hydrodynamic study, in conjunction with fine-scale fish tracking, on the Sacramento River near the head of the DCC. Prior to the study, fisheries researchers thought that smolts feeding along the west bank of the main channel during a rising tide would not be diverted into the DCC entrance. The purpose of the study was to compare hydrodynamic results to fish tracking results. In addition to the streamwise velocity, USGS identified lateral and vertical secondary circulation velocity patterns within the stream cross sections (Dinehart and Burau 2005b). The lateral and vertical velocity patterns were influenced by the difference in water surface elevation between the Sacramento River mainstem and channels east of the DCC. For example, towards the end of an outgoing tide in the Sacramento River, velocities in the Sacramento River and open DCC were both downstream. When the tide shifted to incoming in the Sacramento River, the velocity in the Sacramento River deceased, but the velocity was directed downstream north of the DCC and upstream south of the DCC. At the same time, velocity in the DCC increased

and was still directed downstream. At the start of the next outgoing tide on the Sacramento River, velocity in the Sacramento mainstem was downstream both north and south of the DCC, but the velocity north was slower than the velocity south, and the velocity in the DCC shifted to upstream and flowed into the Sacramento River (Figure B.4-1).

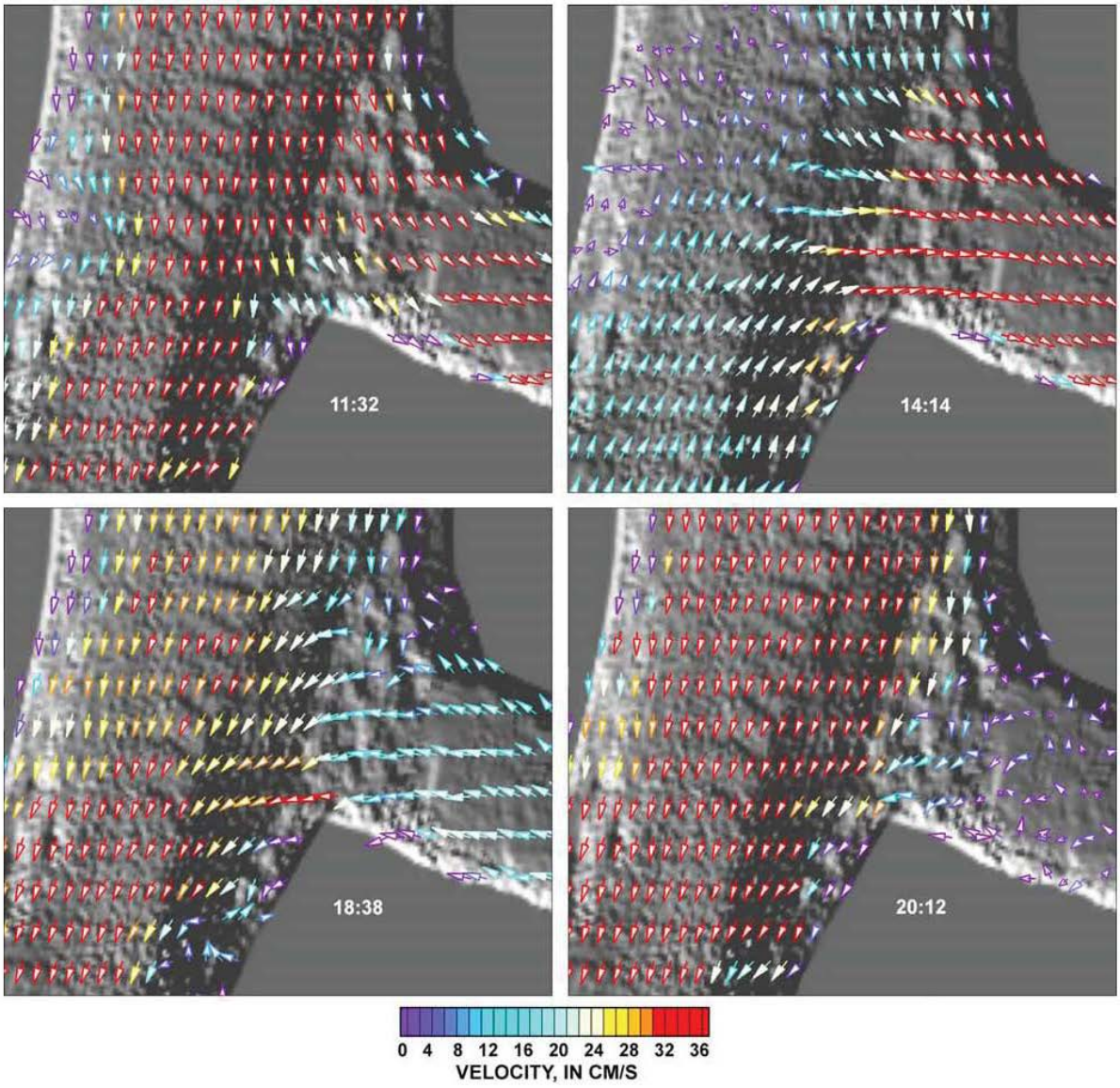

Figure B.4-1. Fine-scale Velocity Vectors in the Sacramento River at the Delta Cross Channel over a 9-hour Period

Note: Arrows illustrate the direction and color contours illustrate the magnitude.
Source: Dinehart and Burau (2005b)

Flow directions through time and space were illustrated with "streamtraces." Streamtraces simulate the paths of massless particles that follow the flow. A rake of streamtrace origins was placed from bank to bank across the Sacramento River just upstream of the DCC, for a

rising tide, to compare flow direction originating from the east versus west banks. The study results show that streamtraces originating near the west bank of the main channel entered the DCC for four hours during each diurnal tidal phase (Figure B.4-2(A)).

To examine the near-bed effects of flow toward the canal entrance, a rake of streamtrace origins was placed diagonally along the thalweg at a depth of 7 meters in the vector grid. The streamtraces indicated a vertical upward movement of 5 meters on paths from the thalweg into the DCC (Figure B.4-2(B)).

B.4.4 Georgiana Slough Non-Physical Barrier

The National Marine Fisheries Service (NMFS) 2009 Biological and Conference Opinion for the Long-Term Operations of the Central Valley Project and State Water Project (BiOp) included a reasonable and prudent alternative requiring DWR and the USBR to consider engineering solutions to reduce the diversion of juvenile salmonids from the Sacramento River into the interior and South Delta, Action IV.1.3 of the BiOp. After evaluating results of experimental tests using various alternative non-physical barrier technologies, DWR implemented the Georgiana Slough Non-Physical Barrier Studies in 2011, 2012, and 2014 to test the effectiveness of using a non-physical barrier, referred to as a behavioral Bio-Acoustic Fish Fence (BAFF). The BAFF combines three stimuli expected to deter juvenile Chinook salmon and steelhead from entering Georgiana Slough: sound, high-intensity modulated light (previously known as stroboscopic light), and a bubble curtain. As part of the studies, hydrodynamics and velocity were measured simultaneous to fine-scale fish movements in the study area Acoustic Doppler Current Profilers (ADCPs) were deployed along the non-physical barrier to assess velocity and general hydrodynamic conditions, and flow proportions entering Georgiana Slough. Six fixed ACDPs were deployed along the BAFF for the duration of the studies, and drifting ADCPs were deployed at several time periods to interpolate surface velocities between the fixed ADCP locations (Figure B.4-3).

The purpose of the studies was to determine the hydrodynamics that potentially affect fish entrainment into Georgiana Slough. The measured hydrodynamic data were used in a model to estimate velocity streamlines and 2-D velocity fields. Velocity fields are complex to assess, and were simplified using the entrainment zone and critical streakline concepts. A hydrodynamic model was developed and releases of drifters to validate particle transport streamtraces modeled with the temporally broader hydrodynamic model.

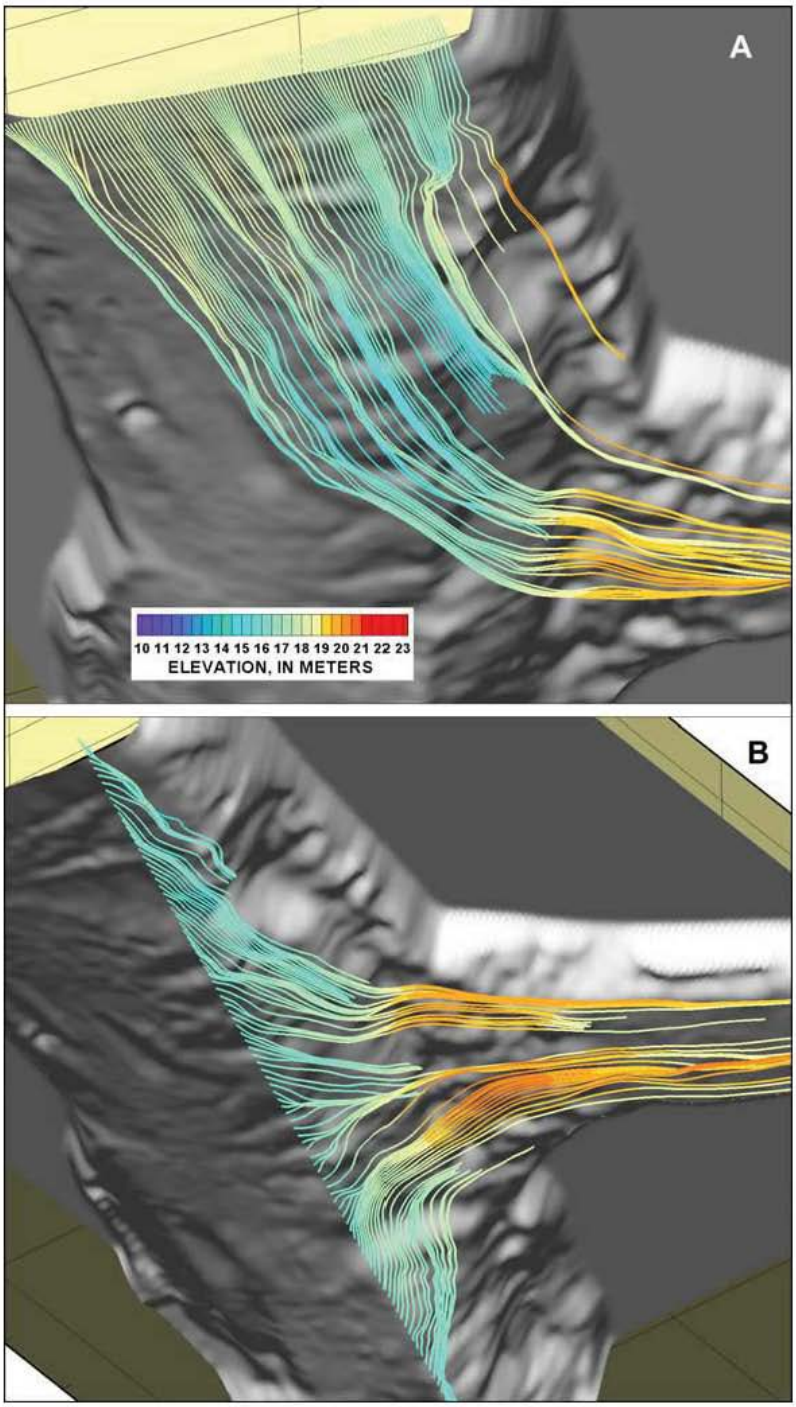

Figure B.4-2. Streamtraces in the Sacramento River at the Delta Cross Channel During a Rising Tide

Notes: Streamtraces are a visualization of flow direction through 3-D fields. The color contour represents the horizontal elevation.
Source: Dinehart and Burau (2005)

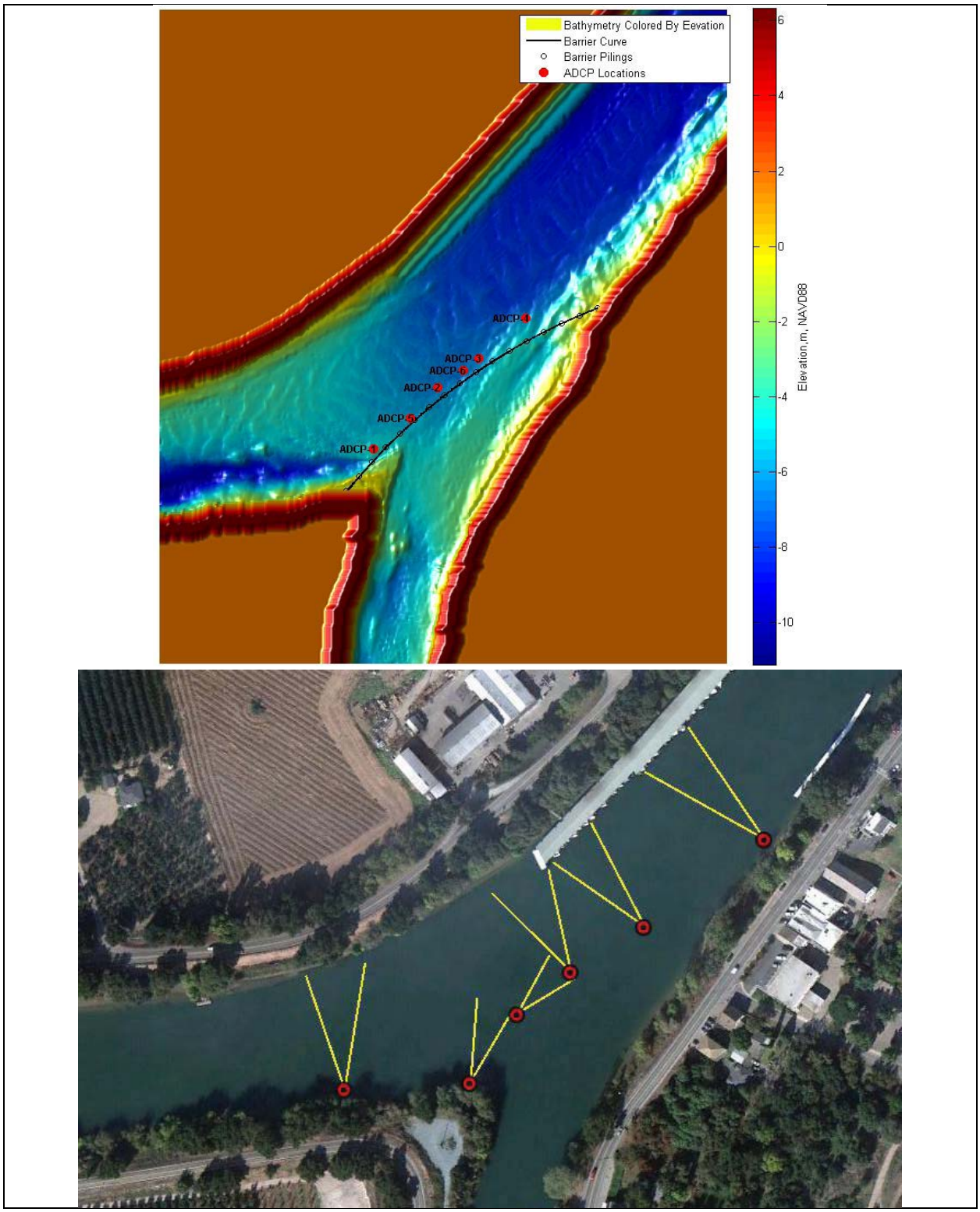

Figure B.4-3. ADCP Deployment Locations in the Sacramento River at Georgiana Slough for the 2011 (upper) and 2012 (lower) Non-physical Barrier Study

Source: DWR (2012)

Particles (or drifters) that enter the junction of the Sacramento River with Georgiana Slough are either transported into Georgiana Slough or bypass it during downstream flow conditions. Areas in the junction where a large percentage of particles share the same fate are called entrainment zones. The critical streakline is the spatial divide between the entrainment zones. In Figure B.4-4, the critical streakline (red) separates the entrainment zone for modeled particles that enter the Georgiana Slough and the entrainment zone for particles that remain in the Sacramento River during downstream flow conditions. Figure B.4-5 is an illustration of the critical streakline for upstream flow conditions, and Figure B.4-6 shows the critical streakline for converging flow conditions.

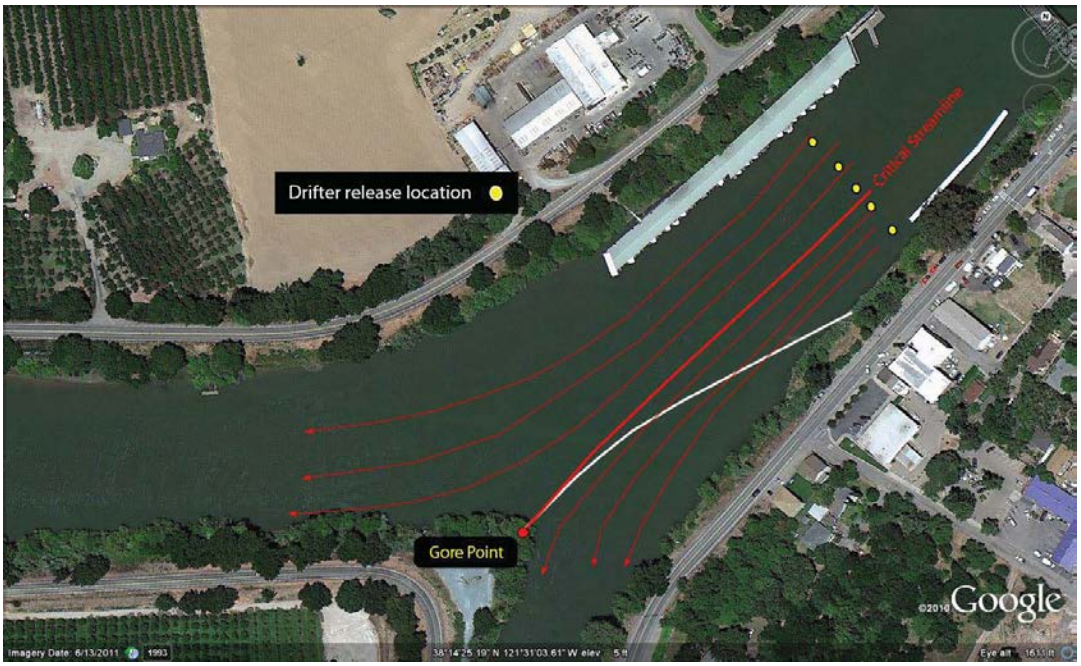

Figure B.4-4. Drifter Release Locations (yellow dots) During Ebb Tides and Modeled Particle Paths and Critical Streamline Under Downstream Conditions

Source: DWR (2013)

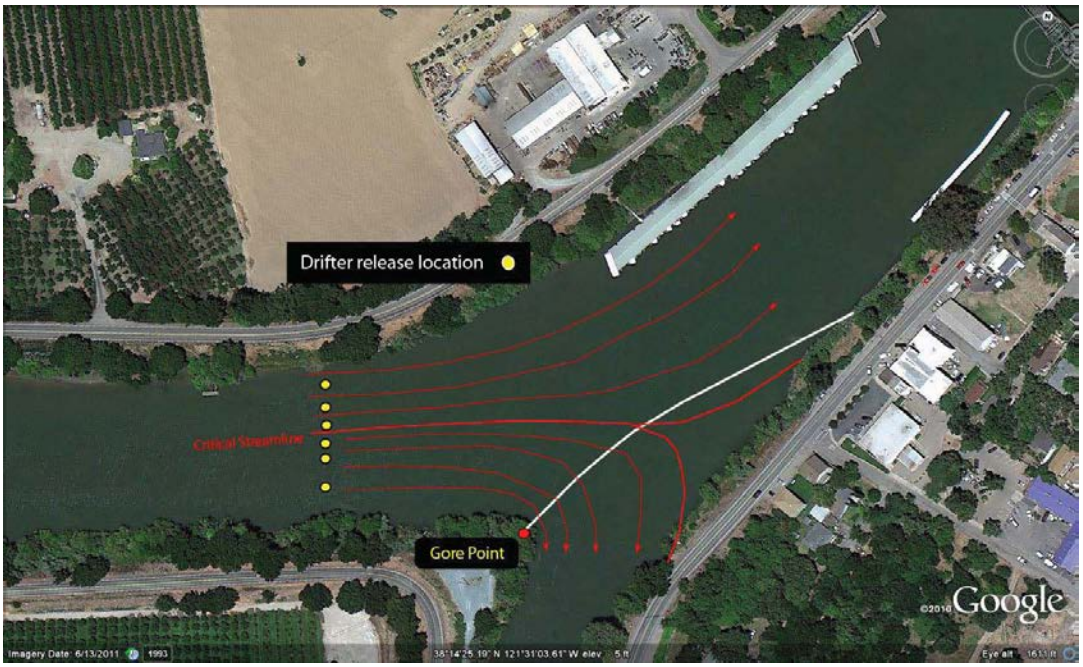

Figure B.4-5. Drifter Release Locations (yellow dots) During Flood Tides and Modeled Particle Paths and Critical Streamline Under Upstream Conditions

Source: DWR (2013)

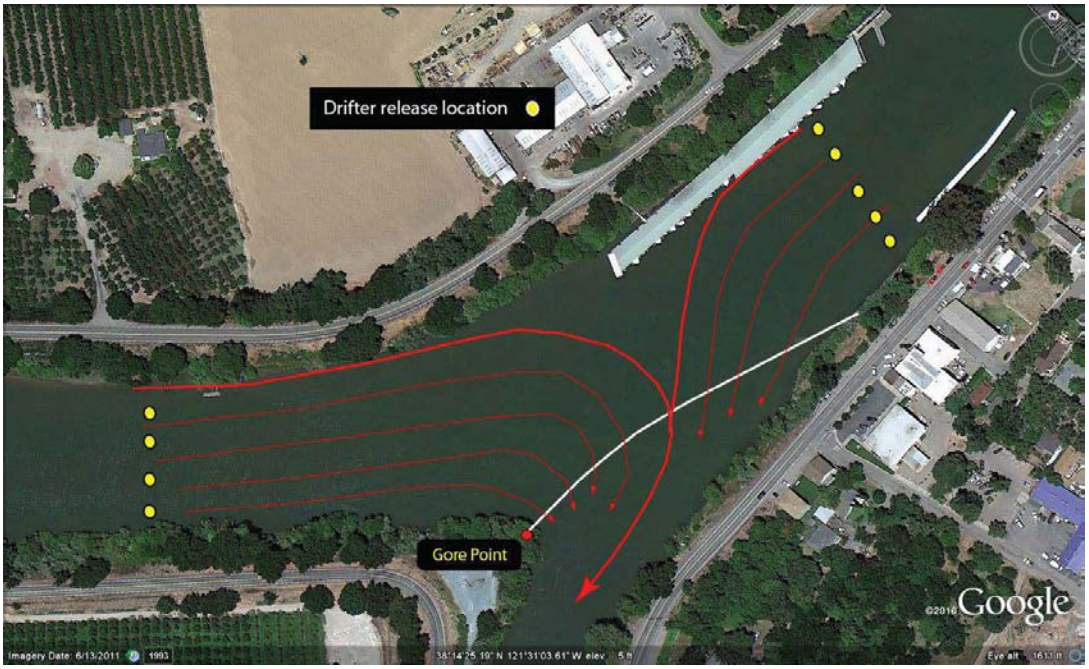

Figure B.4-6. Drifter Release Locations (yellow dots) During a Converging Stage and Modeled Particle Paths and Critical Streakline Under Converging Conditions

Source: DWR (2013)

The streakline positions are useful in understanding entrainment of particles. The streakline positions are related to the discharge ratio (the proportion of flow that enters Georgiana Slough from the Sacramento River) scaled by the channel width. There are potentially six tide conditions that must be considered to correctly compute the discharge ratio in junctions where the tidal currents are reversing: 1) upstream; 2) downstream; 3) converging flows when water is entering the side channel; 4) upstream; 5) downstream; and 6) converging flows when water is leaving the side channel. This is important when considering tidally averaged or longer time scales used in regulatory management actions. The correct calculation of the tidally averaged discharge ratio is the average of the ratio, not the ratio of the average. The ratio should be calculated at the shortest time scale appropriate for the intended use and then averaged over the time scale of interest. Typically in the Delta, the average of the components of the ratio is calculated and then the ratio is calculated. This often results in incorrect results (DWR 2013).

B.4.5 Clifton Court Forebay Gate Operations

CCF is operated as a regulating reservoir within the tidal region of the South Delta for SWP water export operations (Clark et al. 2009). CCF was constructed in 1969 with a surface area of 2,200 acres. Water is diverted from Old River and West Canal into the CCF intake through five radial gates (each 20 by 20 feet). Diversion (gate opening) is timed to occur as the flooding tide reaches the CCF intake and through the early part of the ebb tidal cycle. The frequency that the radial gates are opened to flood CCF depends on the SWP export rate, the volume of water storage in CCF, and tidal conditions. When the difference in water surface elevation between Old River and CCF is greatest, water velocities through Clifton Court Canal typically exceed 15 ft/sec at flow rates typically ranging between 10,000 and 15,000 cfs (Clark et al. 2009). After CCF has been filled, the radial gates are closed and water exports are made from storage within CCF.

B.5 HYDRODYNAMIC EFFECTS OF EXPORT OPERATIONS

B.5.1 Methods

The SST characterized the extent of the effect of the SWP and CVP South Delta export operations on flow along channels and at selected junctions in the South Delta and Georgiana Slough over a range of Delta inflows and HORB installation with the DCC closed using results of DSM2 simulation modeling. As discussed above, the accuracy of DSM2 modeling is better at some locations than others in the South Delta, and is better for average daily values than for 15-minute values. Accuracy can also change over months and years as has been observed at Turner Cut.

The South Delta was partitioned into three routes: 1) mainstem of the San Joaquin River; 2) Old River; and 3) Middle River. DSM2 model runs were used to examine changes in daily

average, minimum, and maximum water flow, and 15-minute instantaneous velocity, under three simulation scenarios, similar to Cavallo et al. (2013).

In assessing the effects of export rate on hydrodynamic conditions in the Delta, we evaluated the geographic area (i.e., footprint) where export-related changes in daily average, maximum, and minimum flow; and tidally averaged, maximum and minimum velocities associated with the low/low and high/high tides phases were detected based on the model results. The changes in flow within Delta channels were evaluated as a function of three levels of Delta inflow and three levels of SWP and CVP exports. Changes in velocity were evaluated as a function of two levels of Delta inflow and two levels of exports. The results were illustrated as both profile figures and color contour figures representing a "heat" map.

The model scenarios were developed by DWR for Kimmerer and Nobriga (2008) to evaluate particle transport over a wide range of exports and inflows, with the HORB in and out (the HORB was modeled as six culverts and water moving in both directions), and with the DCC gates closed and opened. We used the scenarios to isolate the effect of SWP and CVP export rate, Delta inflow, and HORB position on water flow and velocity and direction, over a range of Sacramento River and San Joaquin River basin inflow conditions. Thus, we were able to evaluate the effect of exports on flow and velocity over a range of inflow and barrier conditions and, alternatively, evaluate the effect of inflows over a range of exports and barrier conditions.

Cavallo et al. (2013) analyzed a subset of the DSM2 model scenarios originally developed by Kimmerer and Nobriga (2008) in order to examine changes in channel flow. These were the three lower inflow scenarios from Kimmerer and Nobriga (2008) with Delta inflow ranging from 12,000 cfs to 38,000 cfs; San Joaquin River flow ranging from 1,495 to 5,712; Sacramento River flow ranging from 10,595 to 32,288; and exports ranging from 2,000 cfs to 10,000 cfs. Conditions were compared when the HORB was in or out, the DCC was closed, and the agricultural barriers were not installed.

There were two limitations of the Cavallo et al. (2013) scenarios. First, the Sacramento River and San Joaquin River inflows were varied together proportionally; therefore, we were not able to independently evaluate the effect of Sacramento versus San Joaquin river inflow. Second, without the two higher inflow scenarios in Kimmerer and Nobriga (2008), we were not able to analyze a wide range of inflows.

B.5.2 Conceptual Model

The conceptual model that was developed for the hypothesized relationships between water project operations and Delta hydrodynamics is illustrated in Table B.5-1. The relationships shown in black text in the model were examined using available information and modeling results. The relationships shown in red text were not examined due to lack of resources.

Table B.5-1. Hydrodynamics Drivers, Linkages, and Outcomes [DLOs] Components for Analysis (DLOs not included in the analysis are shown in red italic text)

Drivers	Linkages	Outcomes
• Exports • River inflow; Sacramento and San Joaquin • Tide • *Channel morphology*	• Proximity to exports • Channel configuration/barrier deployment • *CCF operation radial gate operations (e.g., opening to fill CCF and then closing to isolate the pumping plant operations from the Delta)*	• Instantaneous velocities or flows • Net daily flow • Sub-daily velocity • *Percent positive flow* • *Water temperature* • *Salinity* • *Residence time* • *Source/origin of water*

Note: Red italicized text indicates Drivers, Linkages, and Outcomes that were not analyzed.

Results of the examinations were characterized as follows: 1) the results of studies and analyses are consistent and supportive of the relationship predicted based on the conceptual model; 2) the results of studies and analyses were not consistent or did not support the predicted relationships based on the conceptual model, suggesting that alternative hypotheses and relationships should be considered; or 3) the available information was inconsistent or inadequate to support or refute a predicted relationship, which was identified as a data or information gap that could be addressed in the future.

The following predictions were made based on the conceptual model:

- The effect of exports and inflows, within the context of tides, on average, maximum, and minimum daily flows, varies with proximity to the exports.
- The effect of exports and inflows, within the context of tides, on average, maximum, and minimum daily flows, varies with channel configuration.
- The effect of exports and inflows, within the context of tides, on average, maximum, and minimum daily flows, varies with barrier deployment.
- The effect of exports and inflows, within the context of tides, on average daily, maximum, and minimum flows, varies with Clifton Court radial gate operations.

B.5.3 Export Effects on Flow

Results of the modeling showing daily average, maximum, and minimum flows and differences between scenarios are presented as profile illustrations in Figure B.5-1 through Figure B.5-7, as a table in Table B.5-2, and as a "heat" map in Figure B.5-8. These are presented together and used to illustrate the subsequent narrative regarding the effects of SWP and CVP exports on hydrodynamic conditions in the mainstem San Joaquin River, Old River, Middle River, and Georgiana Slough in the sections below.

The basis of knowledge for the relationship between different routes' hydrodynamic metrics and drivers such as exports, barriers or Clifton Court radial gate operations is low because it

is based on non-peer reviewed agency reports. Understanding for the relationship between migration route and hydrodynamic metrics is based on non-peered reviewed agency reports and information presented in this report.

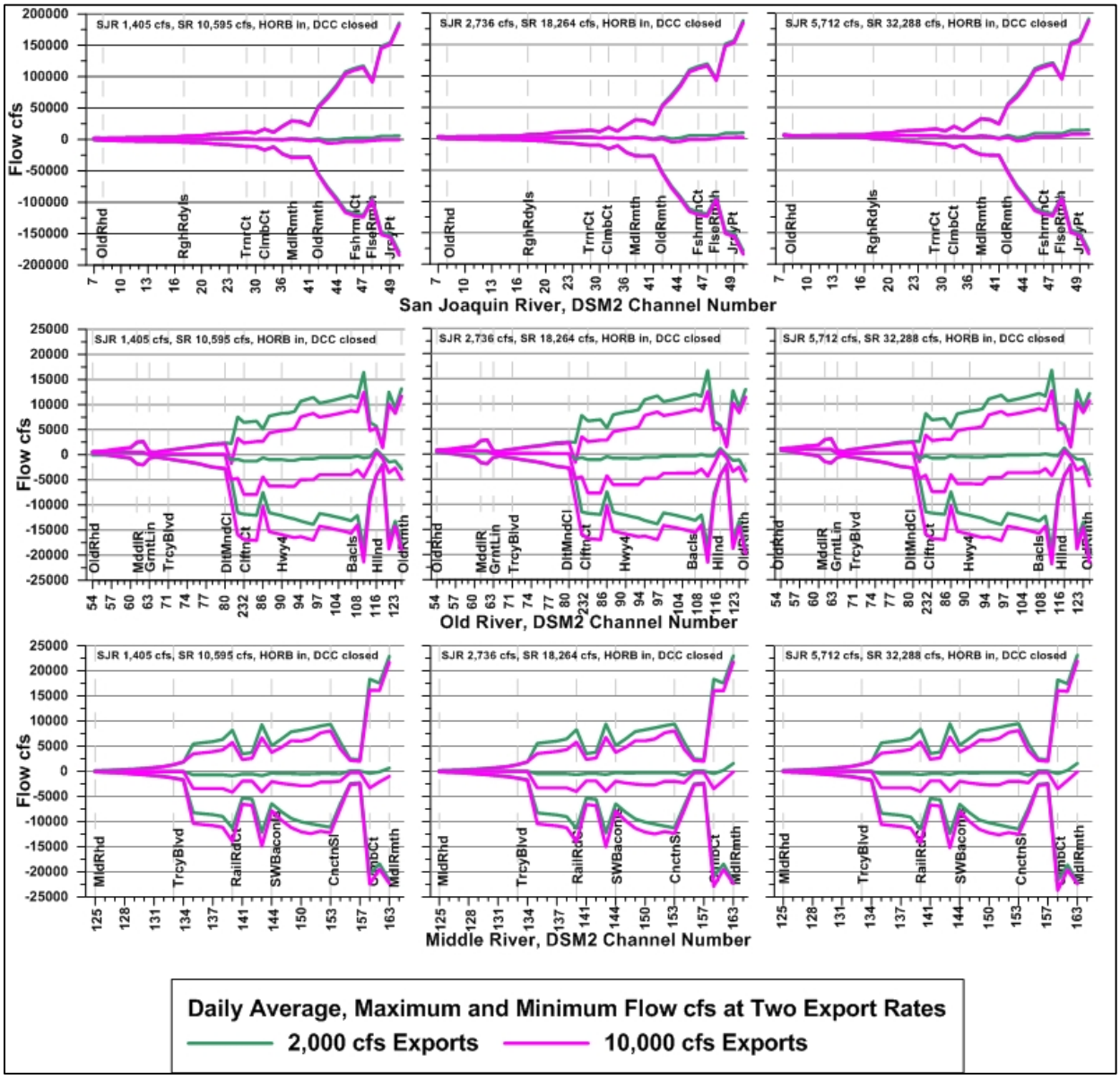

Figure B.5-1. DSM2 Modeled Daily Average, Maximum, and Minimum Flow in Each DSM2 Channel Reach for Each of Six Model Scenarios in Each of Three Routes in the South Delta With the HORB In

Notes: The six scenarios were low inflow/low exports, low inflow/high exports, medium inflow/low exports, medium inflow/high exports, high inflow/low exports, and high inflow/high exports. These exports represent the most extreme modeled scenarios and, therefore, capture the maximum difference in flow. The three routes were the San Joaquin River mainstem, Old River, and Middle River. The x axis is serial DSM2 channel reach number.

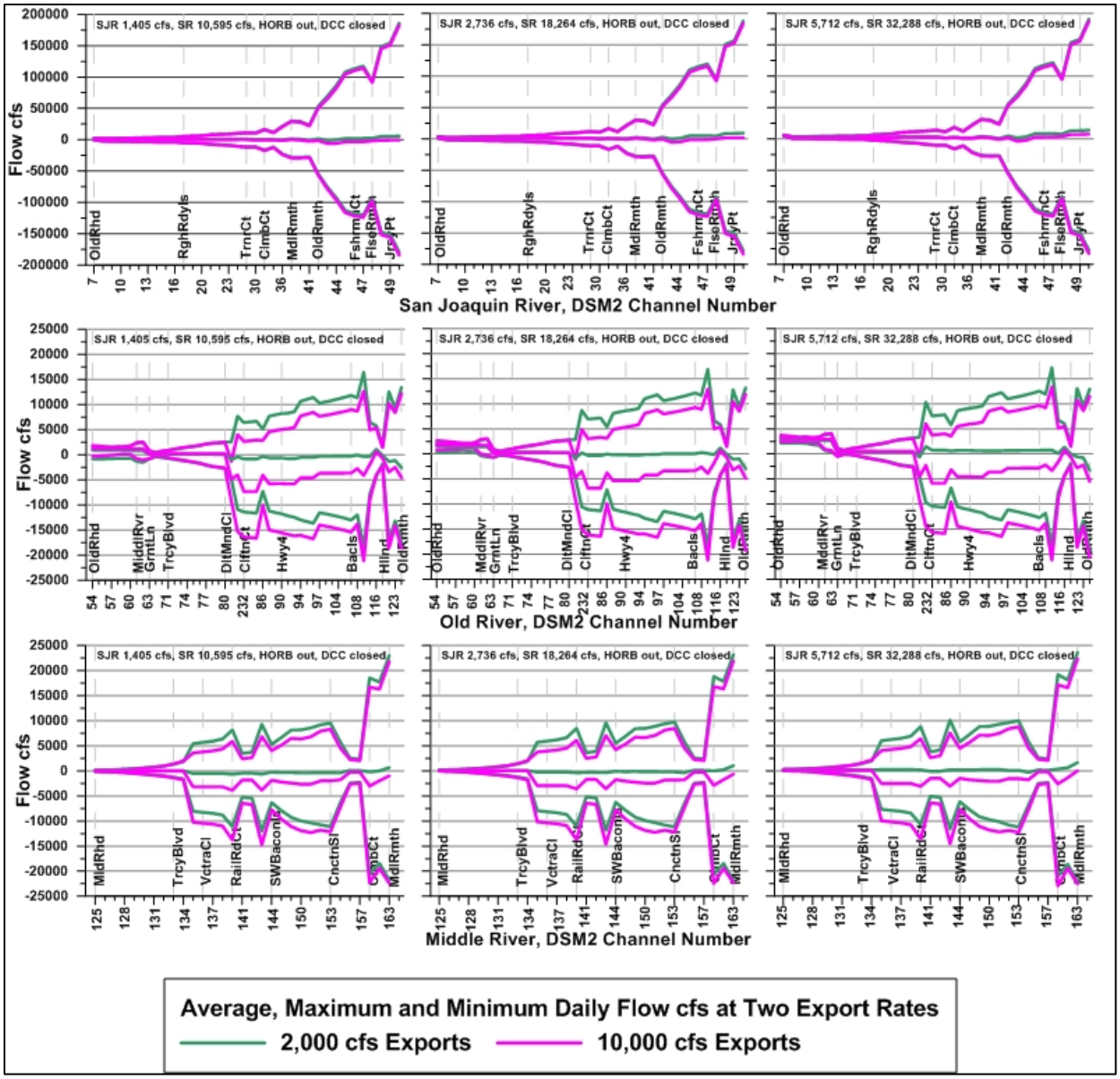

Figure B.5-2. DSM2 Modeled Daily Average, Maximum, and Minimum Flow in Each DSM2 Channel Reach for Each of Six Model Scenarios in Each of Three Routes in the South Delta With the HORB Out

Notes: The six scenarios were low inflow/low exports, low inflow/high exports, medium inflow/low exports, high inflow/medium exports, low inflow/high exports, and high inflow/high exports. These exports represent the most extreme modeled scenarios and, therefore, capture the maximum difference in flow. The three routes were the San Joaquin River mainstem, Old River, and Middle River. The x axis is serial DSM2 channel reach number.

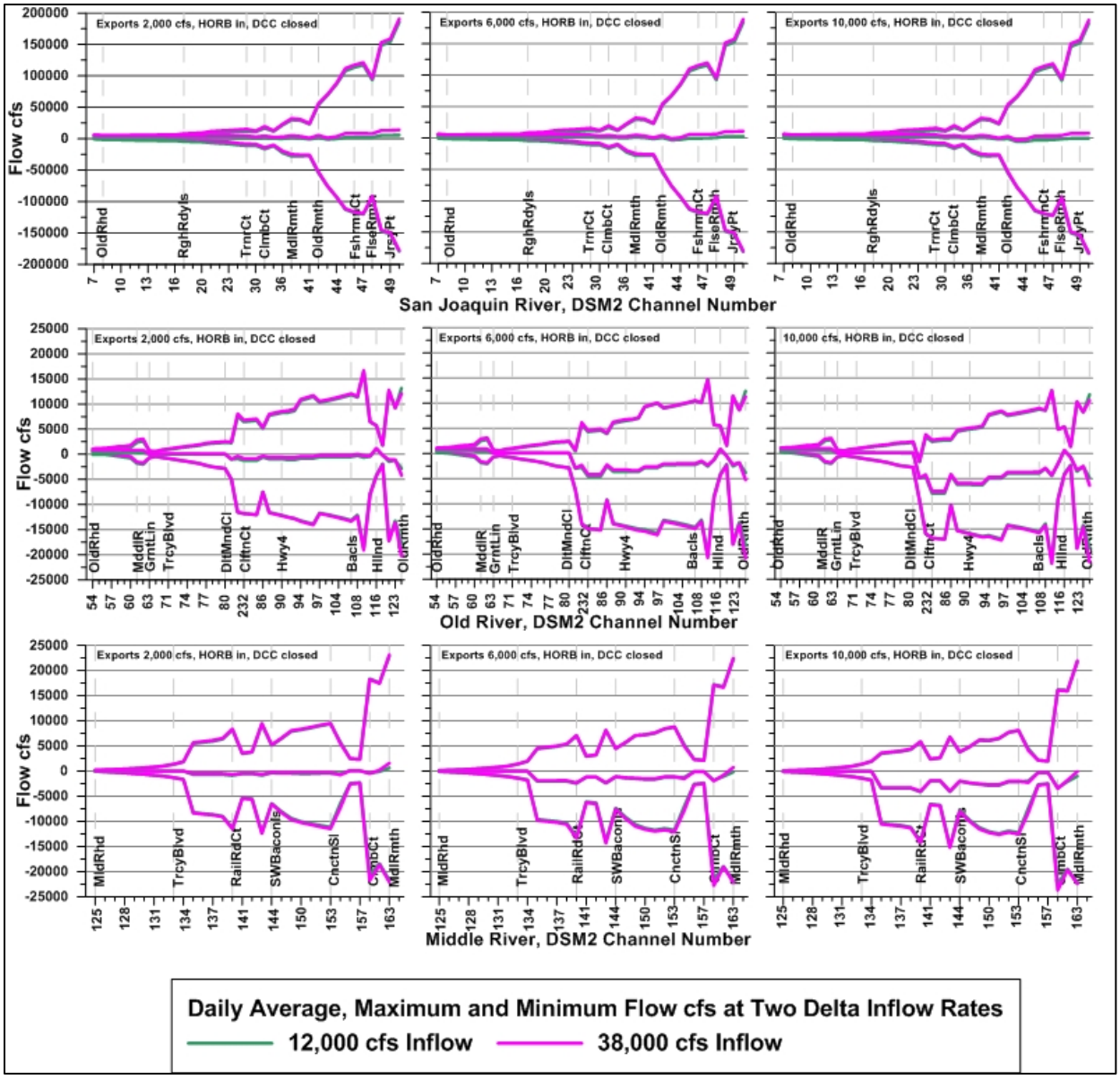

Figure B.5-3. DSM2 Modeled Daily Average, Maximum, and Minimum Flow in Each DSM2 Channel Reach, in Each of Six Scenarios, in Each of Three Routes in the South Delta

Notes: The six scenarios were low inflow/low exports, high inflow/low exports, low inflow/medium exports, high inflow/medium exports, low inflow/high exports, and high inflow/high exports. These inflows represent the most extreme modeled scenarios and, therefore, capture the maximum difference in flow. The three routes were the San Joaquin River mainstem, Old River, and Middle River. The x axis is serial DSM2 channel reach number.

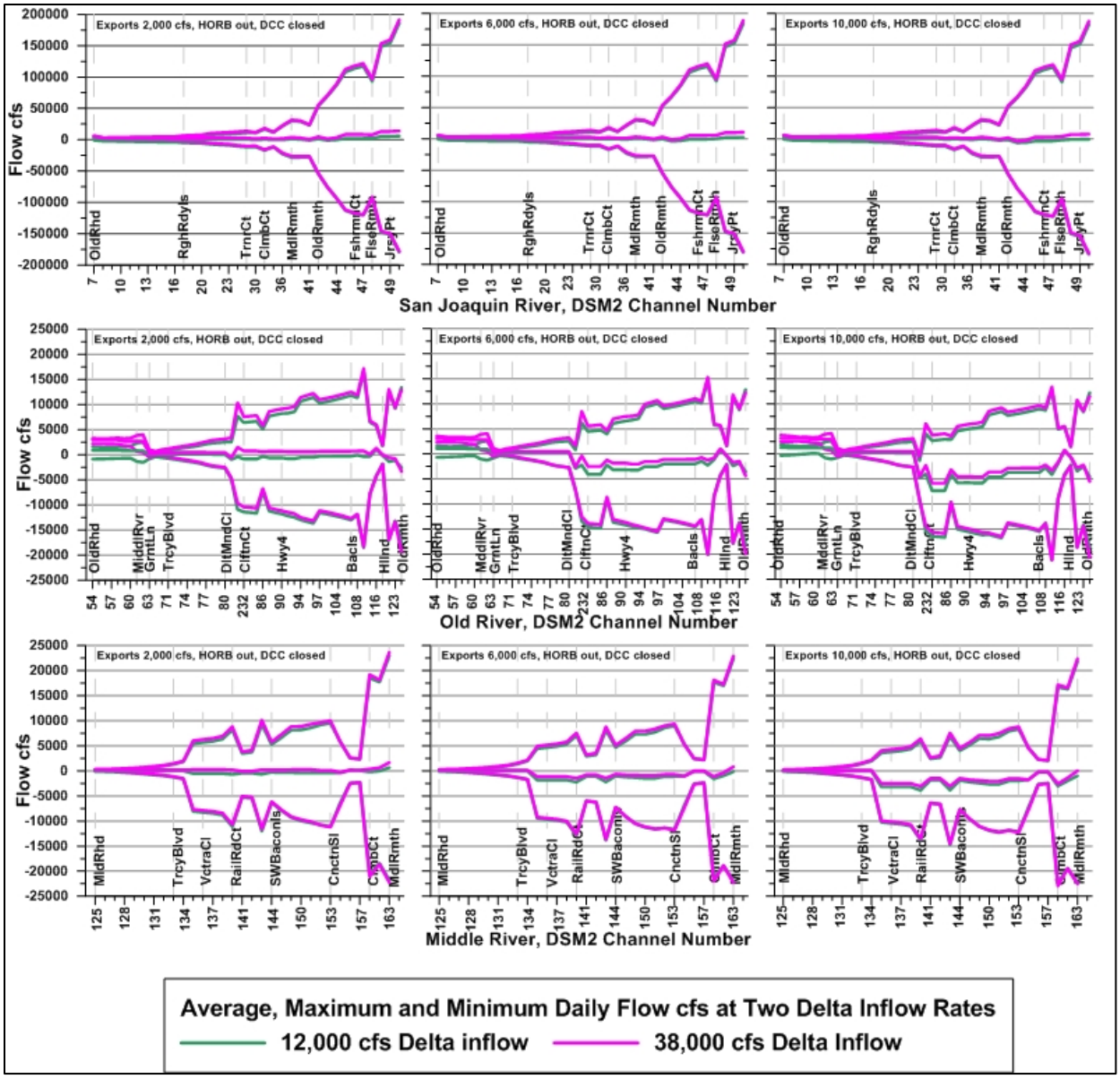

Figure B.5-4. DSM2 Modeled Daily Average, Maximum, and Minimum Flow in Each DSM2 Channel Reach, for Each of Six Model Scenarios, for Each of Three Routes in the South Delta With the HORB Out

Notes: The six scenarios were low inflow/low exports, high inflow/low exports, low inflow/medium exports, high inflow/medium exports, low inflow/high exports, and high inflow/high exports. These inflows represent the most extreme modeled scenarios and, therefore, represent the maximum difference in flow. The three routes were the San Joaquin River mainstem, Old River, and Middle River. The x axis was serial DSM2 channel reach number.

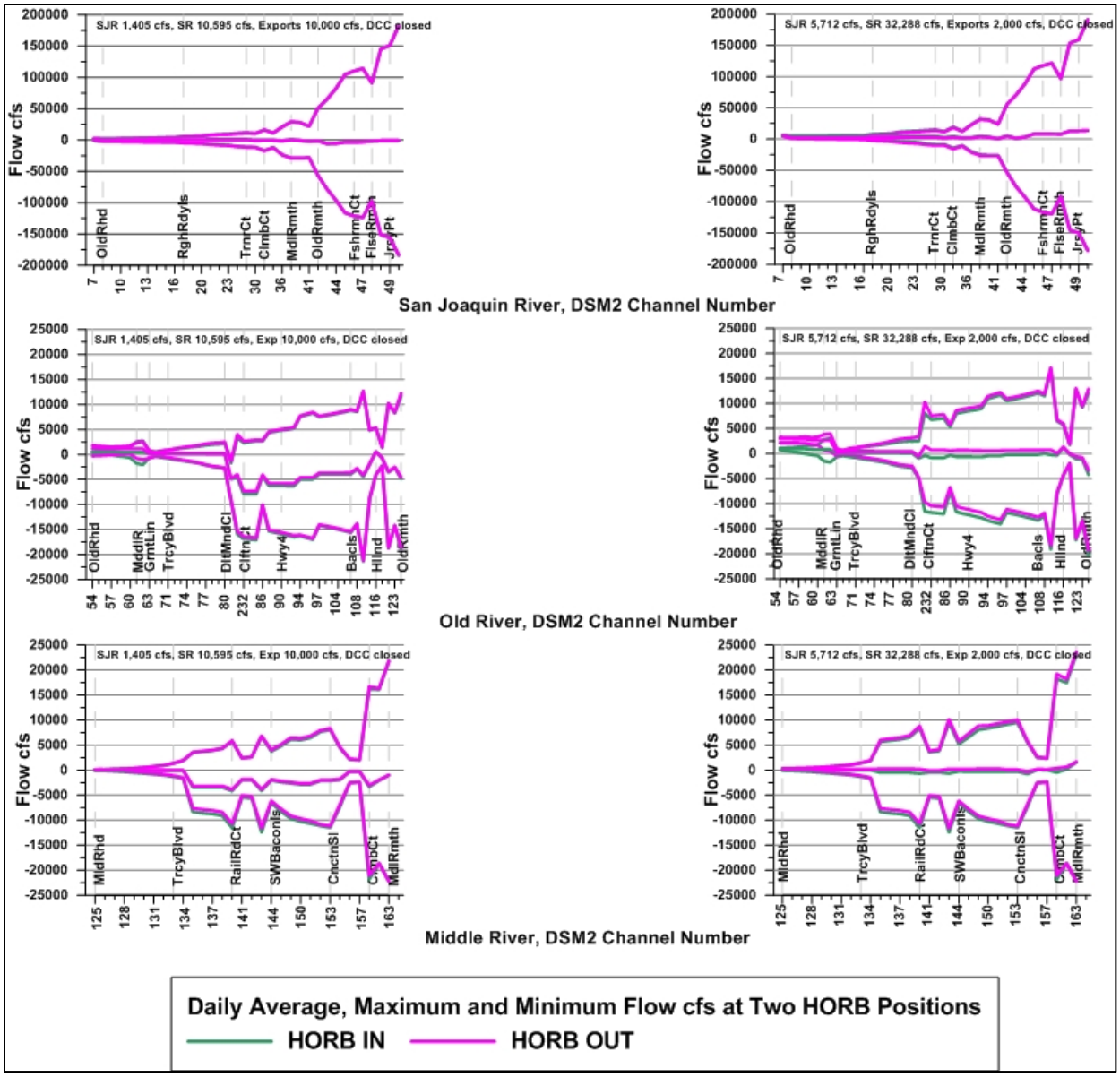

Figure B.5-5. DSM2 Modeled Daily Average, Maximum, and Minimum Flow in Each DSM2 Channel Reach, for Each of Four Scenarios, in Each of Three Routes in the South Delta, With and Without the HORB

Notes: The four scenarios were low inflow/high exports/HORB in, low inflow/high exports/HORB out, high inflow/low exports/HORB in, and high inflow/low exports/HORB out. These inflow, exports, and HORB positions represent the most extreme modeled scenarios and, therefore, the maximum difference in flow. The three routes were the San Joaquin River mainstem, Old River, and Middle River. The x axis is serial DSM2 channel reach number.

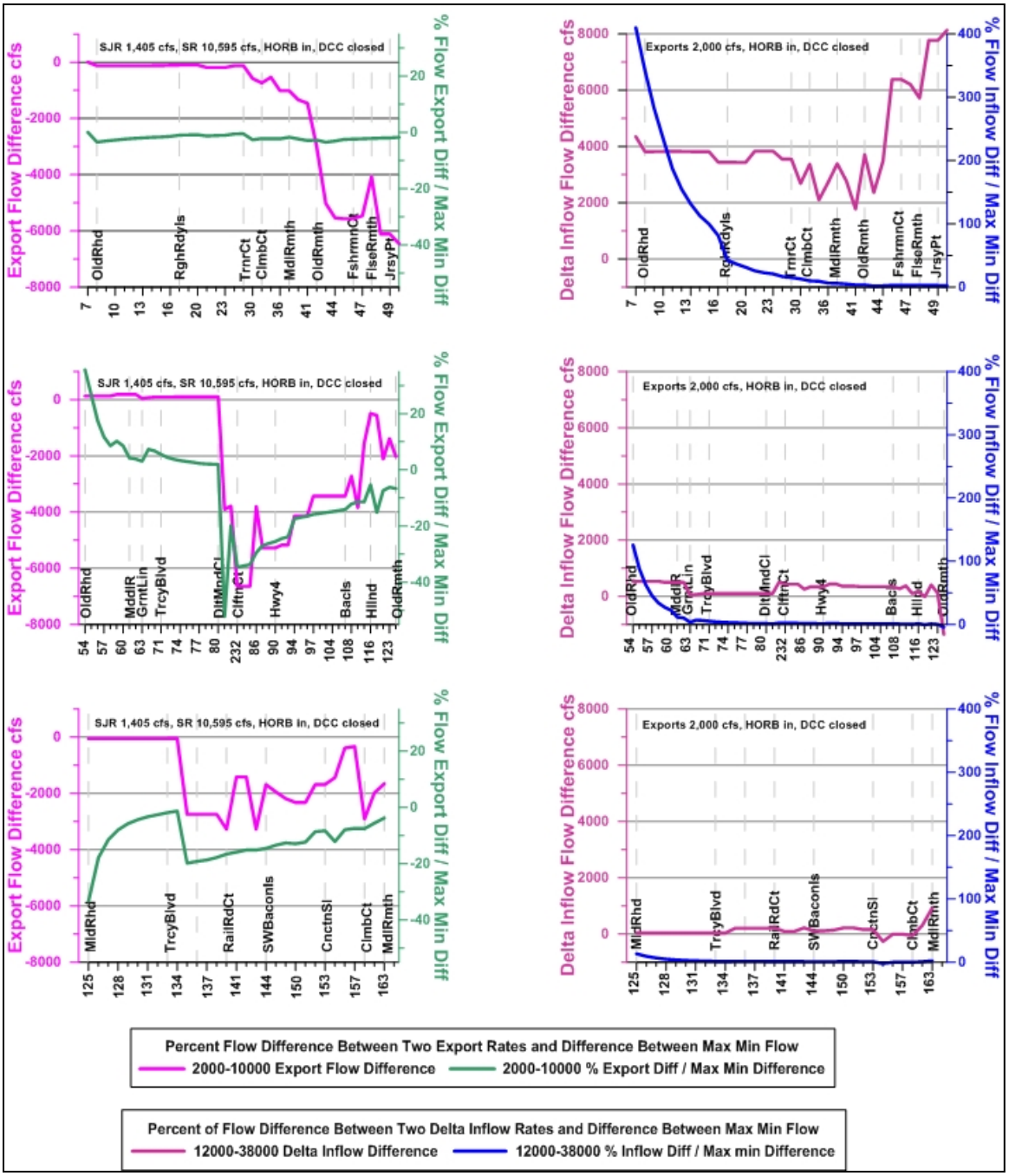

Figure B.5-6. Effect of Export Rate and Delta Inflow on Percent of Flow and Export Difference in the Lower San Joaquin River

Notes: All left panels represent the represent the high inflow scenario, the difference in daily average flow between low and high export rate (left y axis), and the difference in daily average flow between low and high export rate divided by the difference between daily minimum and maximum flow at the low export rate (right y axis) with the HORB installed. The right panels represent the difference in daily average flow between low and high inflow rate (left y axis) and the difference in daily average flow between low and high inflow rate divided by the difference between daily minimum and maximum flow at the low at the low inflow rate with the HORB installed. All right panels represent the low export scenario. The three routes were the San Joaquin River mainstem, Old River, and Middle River. The x axis is serial DSM2 channel reach number.

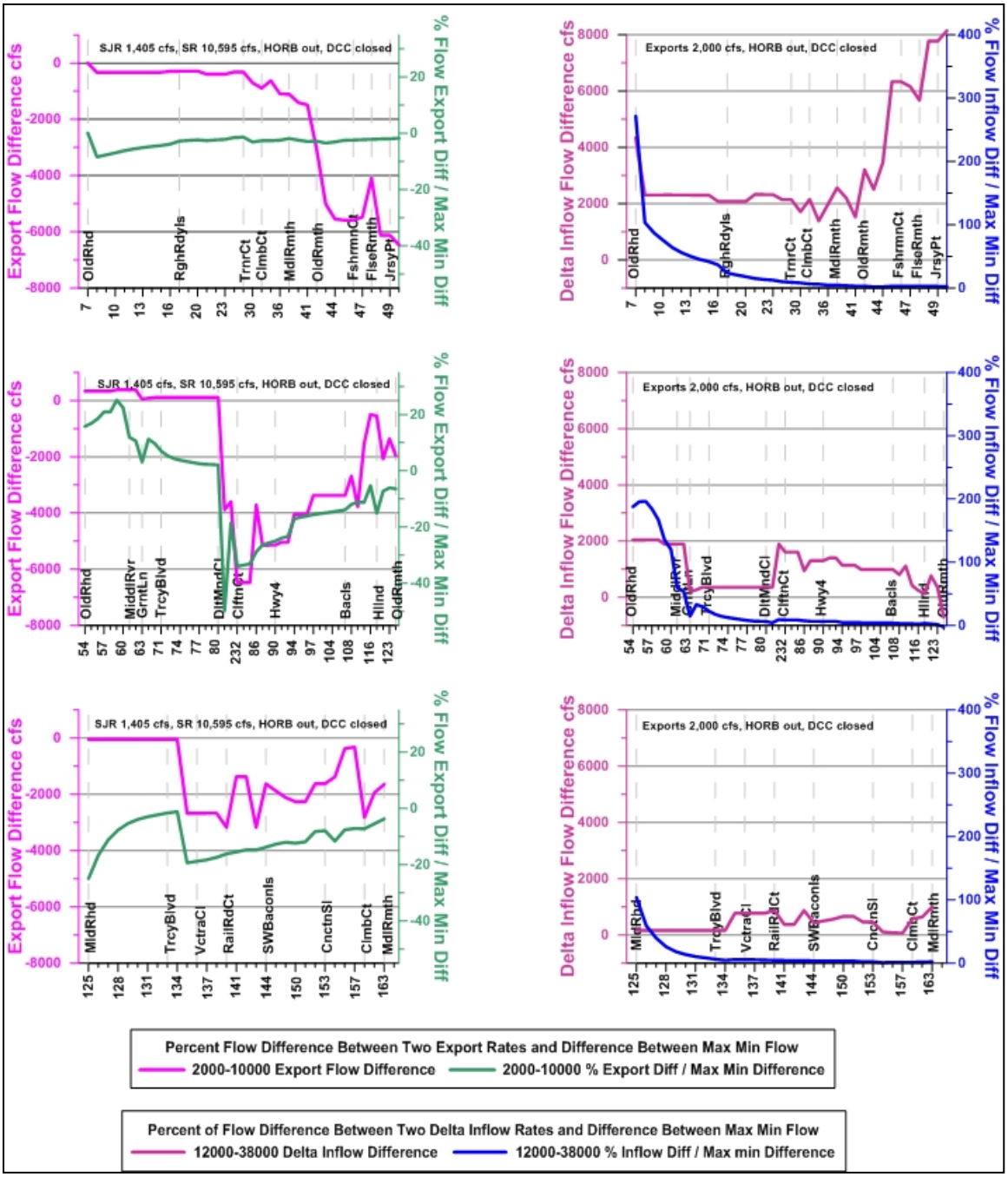

Figure B.5-7. Effect of Export Rate and Delta Inflow on Percent of Flow and Export Difference in the Lower San Joaquin River

Notes: All left panels represent the high inflow scenario, the difference in daily average flow between low and high export rate (left y axis), and the difference in daily average flow between low and high export rate divided by the difference between daily minimum and maximum flow at the low export rate (right y axis) without the HORB. The right panels represent the difference in daily average flow between low and high inflow rate (left y axis) and the difference in daily average flow between low and high inflow rate divided by the difference between daily minimum and maximum flow at the low inflow rate (right y axis) without the HORB. All right panels represent the low export rate scenario. The three routes were the San Joaquin River mainstem, Old River, and Middle River. The x axis is serial DSM2 channel reach number.

Table B.5-2. Summary of Hydrodynamic Simulation Model Results for Flows and Changes in Flow at Various Locations Within the South Delta With and Without the Head of Old River Barrier

Metric	San Joaquin River Route Head of Old River to Jersey Point		Middle River Route Head to Mouth of Middle River		Old River Route Head to Mouth of Old River	
Barrier Status	**HORB In**	**HORB Out**	**HORB In**	**HORB Out**	**HORB In**	**HORB Out**
Locations of high and low daily average flow in route at export of 10,000 cfs and Delta inflow of 12,000 cfs	+1,346 cfs upstream of head of Old River; -6,062 cfs between mouths of Middle and Old rivers	+1,341 cfs upstream of head of Old River; -6,004 cfs downstream of mouth of Old River	-29 cfs at head of Middle River; -4,153 cfs at Railroad Cut	+8.42 cfs at head of Middle River; -3,845 cfs at Railroad Cut	-7,905 cfs downstream of SWP intake; +557 cfs at Holland Cut	+1,241 cfs downstream of CVP intake; -7,330 cfs downstream of SWP intake
Locations of high and low daily maximum flow in route at export of 10,000 cfs and Delta inflow of 12,000 cfs	+2,118 cfs downstream of head of Old River; +182,393 cfs downstream of Jersey Point	+1,762 cfs downstream of head of Old River; +182,446 cfs downstream of Jersey Point	+35 cfs at head of Middle River; +21,718 cfs at mouth of Middle River	+78 cfs at head of Middle River; +21,814 cfs at mouth of Middle River	-1,702 cfs downstream of CVP intake; +12,437 cfs downstream of Bacon Island	-1,328 downstream of CVP intake; -12,671 cfs downstream of Bacon Island
Locations of high and low daily minimum flow in route at export of 10,000 cfs and Delta inflow of 12,000 cfs	-555 cfs upstream of head of Old River; -184,193 cfs downstream of Jersey Point	-337 cfs upstream of head of Old River; -183,975 cfs downstream of Jersey Point	-126 cfs at head of Middle River; -22,472 cfs at Columbia Cut	-114 cfs at head of Middle River; -22,389 cfs at mouth of Middle River	+276 cfs at head of Old River; -21,333 cfs downstream of Bacon Island	+133 cfs at head of Middle River; -21,100 cfs downstream of Bacon Island
Locations of high and low change in daily average flow in route due to increasing exports from 2,000 cfs to 10,000 cfs at Delta inflow of 12,000 cfs	+0.94 cfs upstream of head of Old River; -6,449 cfs downstream of Jersey Point	+0.78 cfs upstream of head of Old River; -6,461 cfs downstream of mouth of Old River	-47 cfs upstream of Victoria Canal; -3,270 cfs upstream of southwest Bacon Island	-42.2 cfs upstream of Victoria Canal; -3,175 cfs at Railroad Cut	+184 cfs upstream of Grant Line Canal; -6,642 cfs at SWP intake	+381 cfs at head of head of Middle River; -6,472 cfs at SWP intake
Locations of high and low difference between daily minimum and maximum flow in route at export of 10,000 cfs and Delta inflow of 12,000 cfs	+2,980 cfs upstream of head of Old River; +366,596 cfs downstream of Jersey Point	+3,004 cfs upstream of head of Old River; +369,752 cfs downstream of Jersey Point	+161 cfs at head of Middle River; +44,048 cfs at mouth of Middle River	+237 cfs at head of Middle River; +45,363 cfs at mouth of Middle River	+358 cfs at head of Old River; +33,770 cfs downstream of Bacon Island	+709 cfs upstream of Grant Line; +37,536 cfs downstream of Bacon Island
Locations of high and low change in daily average flow in route due to increasing Delta inflow from 12,000 to 38,000 cfs at export of 2,000 cfs	+1,777 cfs upstream of mouth of Old River; +8,130 cfs downstream of mouth of Old River	+1,381 cfs downstream of Columbia Cut; +8,145 cfs downstream of Jersey Point	-262 cfs downstream of Connection Slough; +928 cfs at mouth of Middle River	+67 cfs upstream of Columbia Cut; +1,001 cfs upstream of Columbia Cut	+540 cfs downstream of head of Old River; -1345 cfs at mouth of Old River	+2,050 cfs upstream of head of Middle River; -702 cfs at mouth of Old River
Locations of high and low difference between daily minimum and maximum flow in route at export of 2,000 cfs and Delta inflow of 38,000 cfs	+1,060 cfs upstream of head of Old River; +368,502 cfs downstream of Jersey Point	+1,600 cfs upstream of head of Old River; +368,767 cfs downstream of Jersey Point	+282 cfs at head of Middle River; +45,218 cfs at mouth of Middle River	+155 cfs at head of Middle River; +42,825 cfs at mouth of Middle River	+427 cfs at head of Old River; +35,753 cfs downstream of Bacon Island	+817 cfs upstream of Grant Line; +35,495 cfs downstream of Bacon Island

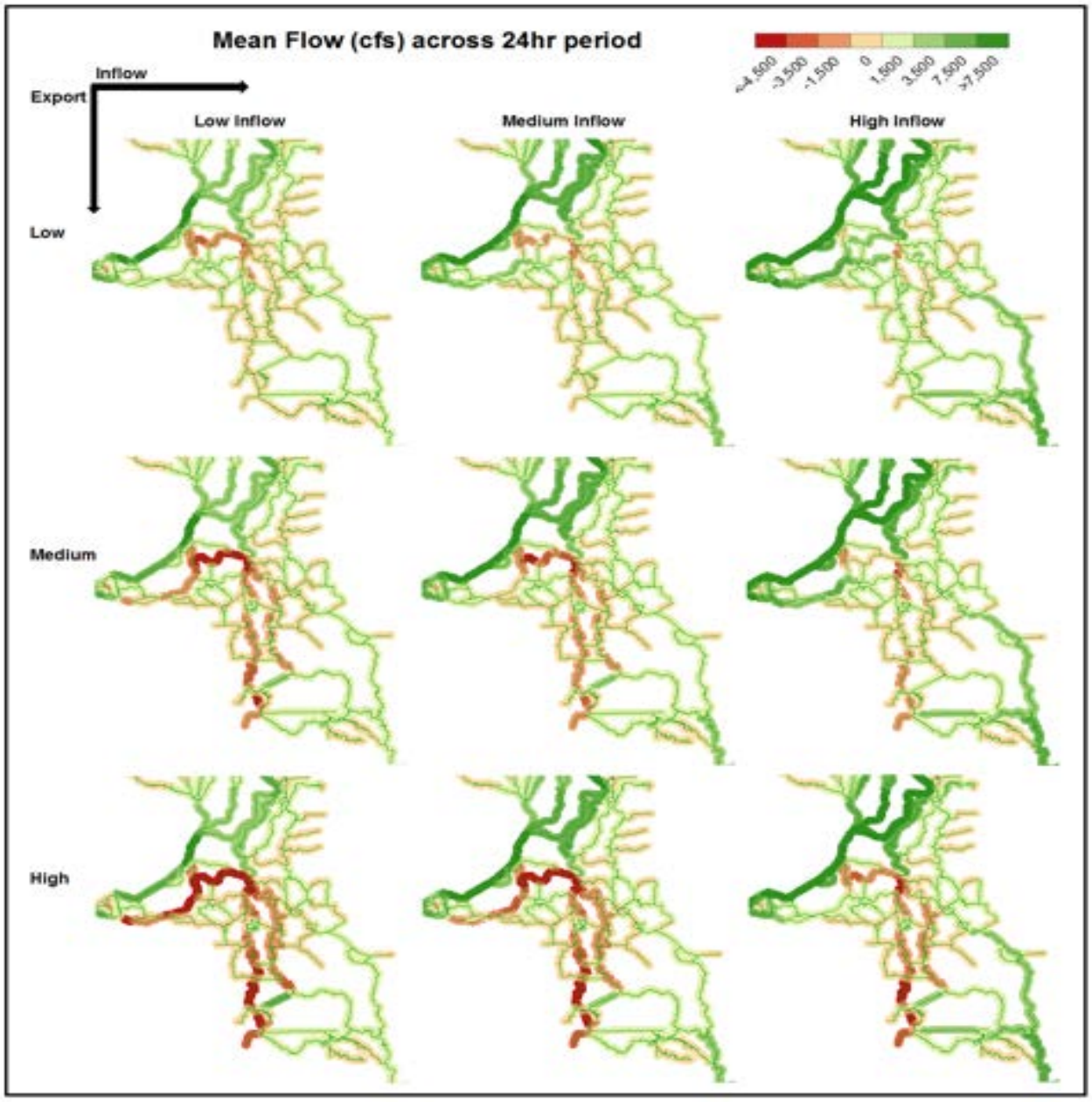

Figure B.5-8. DSM2 Modeled Daily Average Flow at Each DSM2 Channel Reach in the South Delta at Three Export Rates and Three Delta Inflow Rates. The Export Rates Were 2,000, 6,000 and 10,000 cfs, and the Delta Inflow Rates Were 12,000, 21,000, and 38,000 cfs.

Note: The magnitude of flow is illustrated as a color from red to green (see legend at top of figure).

B.5.3.1 San Joaquin River Mainstem

In the context of the three South Delta routes, the mainstem San Joaquin River, on average, had the least negative change in modeled flow due to exports with and without the HORB, and the most positive change in flow due to Delta inflow with the HORB installed under the scenarios modeled (Figures B.5-1 through B.5-4 and B.5-6 through B.5-8).

- The modeled tidal influence on flow in the lower half of the San Joaquin River was about eight times greater than in OMR (the y axis for the San Joaquin River is ±200,000 cfs, whereas the y axis for OMR is ±25,000 cfs) (Figure B.5-1). As an example, the difference in average daily flow on the San Joaquin River at the mouth of Old River was similar in magnitude to the Old River at Clifton Court, but the ratio of the change in average daily flow due to exports compared to the change in flow due to daily tide is an order of magnitude less in the San Joaquin River at the mouth of Old River (3.5% compared to 35%).
- At the head of Old River junction, the effect of increasing exports on flow within the junction was a decrease in flow downstream towards the riverine San Joaquin River and an increase in flow downstream in Old River (towards the exports) corridor. The change in daily average flow into Old River, due to increasing exports from 2,000 to 10,000 cfs, increased by 217 cfs, which was 10% of the difference between the daily minimum and maximum flow of 2,300 cfs at the lower export rate (Cavallo et al. 2013; Figure B.5-9).
- At the Turner Cut junction, the effect of increasing exports on flow within the junction was an increase in flow in Turner Cut towards the exports (or interior Delta) corridor. The change in daily average flow into the Turner Cut, due to an increase in exports from 2,000 to 10,000 cfs, increased by 589 cfs, which was 7.5% of the difference between the minimum and maximum flow of 7,800 cfs at the lower export rate (Cavallo et al. 2013; Figure B.5-10).
- At the Columbia Cut junction, the effect of increasing exports on flow within the junction was an increase in flow in Columbia Cut towards the exports (interior Delta). The change in average daily flow into Columbia Cut, due to an increase in exports from 2,000 to 10,000 cfs, increased by 1,360 cfs, which was 9% of the difference between the daily minimum and maximum flow of 14,640 cfs at the low export rate (Cavallo et al. 2013; Figure B.5-11). The modeled effect of Delta inflow on flow in the upper San Joaquin River route, with the HORB installed, was about four times greater than in upper Old River route (Figure B.5-7). As an example of the positive effect of inflow in the upper San Joaquin River route with the HORB installed (low exports), upstream of the head of Old River, the difference in average daily flow due to a change in inflow from 12,000 to 38,000 cfs was +1,777 cfs, and that was 165% of the difference between the maximum and minimum flow of 1,060 cfs. For comparison, in Old River near the head, the average daily flow difference due to a change in inflow from 12,000 to 38,000 cfs was +540 cfs, and that was 126% of the difference between the maximum and minimum flow of 427 cfs (Table B.5-7). Without the HORB, the difference between the San Joaquin River and Old River was much less (Figure B.5-7; Table B.5-7).

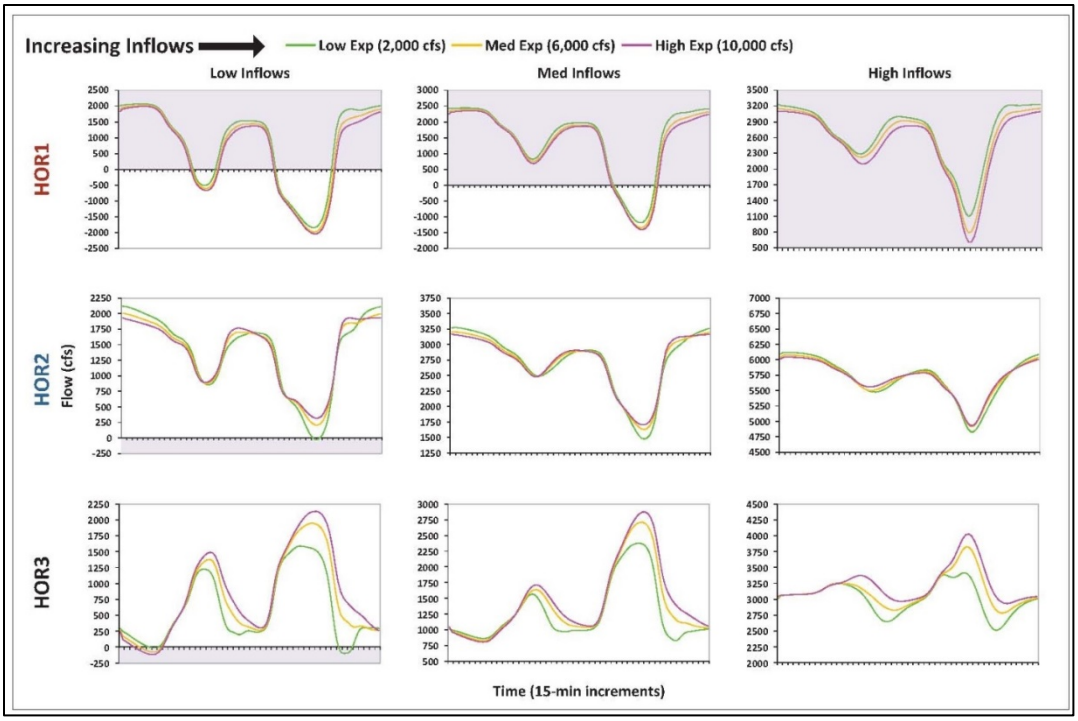

Figure B.5-9. DSM2 Modeled Instantaneous 15-minute Flow Versus Time Over 24 Hours at the Junction of the San Joaquin River and Head of Old Rivers in Three DSM2 Channel Reaches for Nine Model Scenarios

Notes: The three DSM2 channel reaches are in the vertical panel direction. The nine model scenarios include three Delta inflow rates in the horizontal panel direction (12,000, 21,000, and 38,000 cfs), and three export rates within each panel (2,000, 6,000, and 10,000 cfs). HOR1 is the San Joaquin River downstream of the junction, HOR2 is the San Joaquin River upstream of the junction, and HOR3 is Old River downstream of the junction (Cavallo et al. 2013).

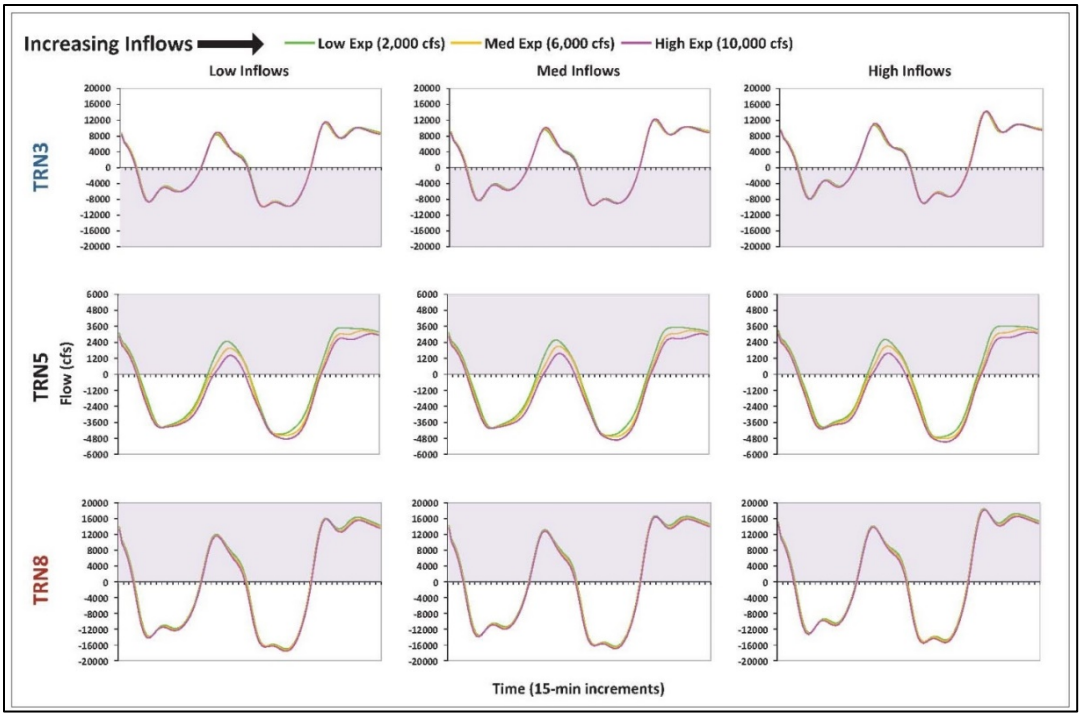

Figure B.5-10. DSM2 Modeled Instantaneous 15-minute Flow Versus Time Over 24 Hours at the Junction of San Joaquin River and Turner Cut in Three DSM2 Channel Reaches for Nine Model Scenarios

Notes: The three DSM2 channel reaches are in the vertical direction. The nine model scenarios include three Delta inflow rates in the horizontal direction (12,000, 21,000, and 38,000 cfs), and three export rates within each panel (2,000, 6,000, and 10,000 cfs). TRN3 is the San Joaquin River upstream of the junction, TRN5 is Turner Cut downstream of the junction, and TRN8 is the San Joaquin River downstream of the junction (Cavallo et al. 2013).

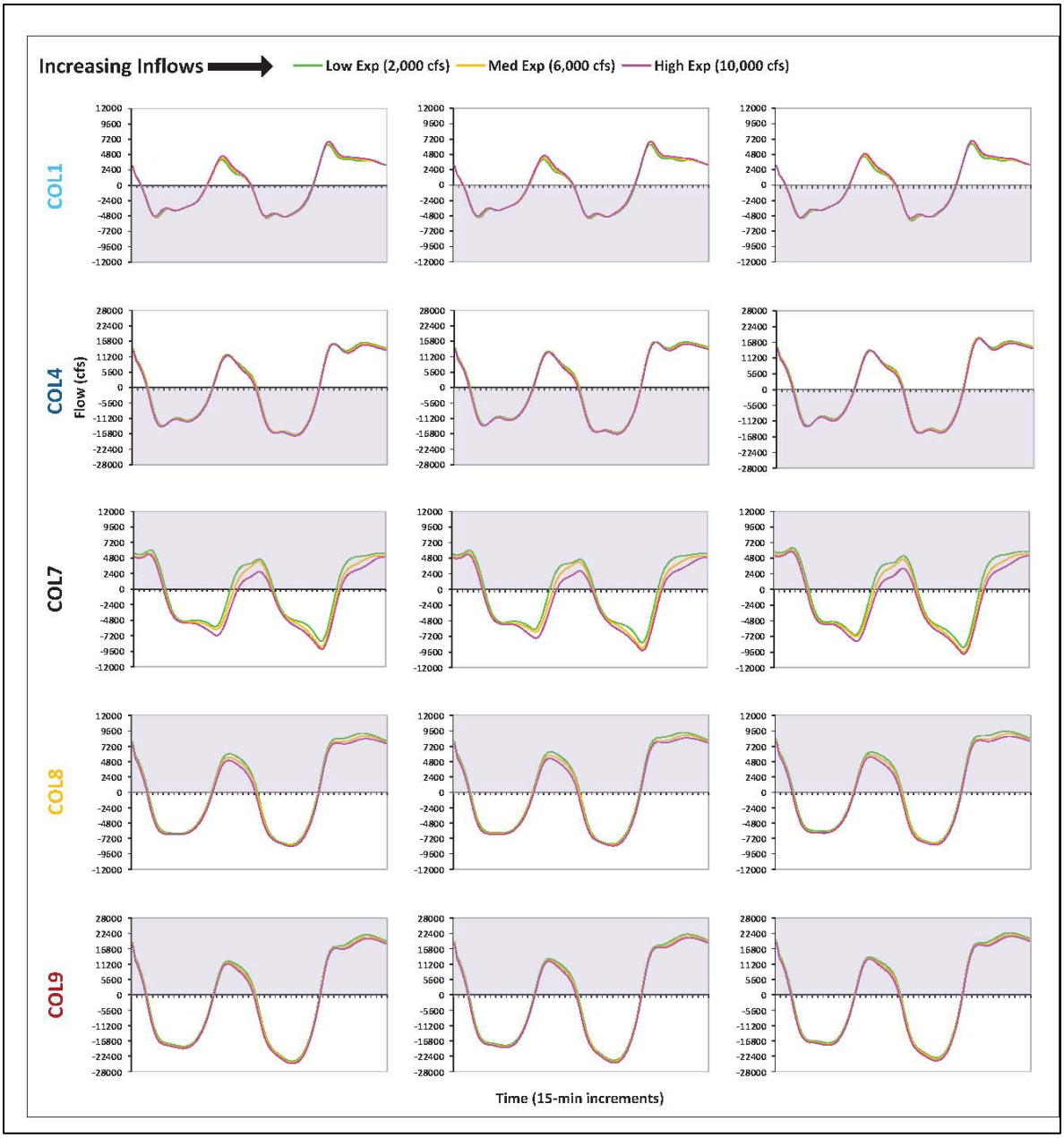

Figure B.5-11. DSM2 Modeled Instantaneous 15-minute Flow Versus Time Over 24 Hours at the Junction of San Joaquin River and Columbia Cut in Five DSM2 Channel Reaches for Nine Model Scenarios

Notes: The five DSM2 channel reaches are in the vertical direction. The nine model scenarios include three Delta inflow rates in the horizontal direction (12,000, 21,000, and 38,000 cfs), and three export rates within each panel (2,000, 6,000, and 10,000 cfs). COL1 is Disappointment Slough upstream of the junction, COL4 is the San Joaquin River upstream of the junction, COL7 is Columbia Cut downstream of the junction, COL8 is the San Joaquin River downstream of the junction, and COL9 is the San Joaquin River downstream of the junction (Cavallo et al. 2013).

B.5.3.2 Old River

In the context of the three South Delta routes, Old River, on average, had the greatest change in modeled flow due to exports with and without the HORB, under the scenarios modeled (Figures B.5-1 through B.5-4 and B.5-6 through B.5-8).

- Old River had the greatest negative change in daily average, minimum, and maximum modeled flow due to an increase in exports with or without the HORB, compared to the other two routes. The largest relative changes occurred downstream of the CVP and SWP export facilities and dissipated toward the mouth (Figures B.5-1, B.5-2, B.5-6, and B.5-7; Table B.5-2).
- Exports draw water toward the export facilities from upstream and downstream locations in Old River. The mid-route location of the export facilities in Old River causes exports to increase downstream flows in Old River upstream of the facilities (particularly with no HORB) and decrease downstream flows downstream of the facilities (Figures B.5-2 and B.5-7).
- Without the HORB, flow was more positive in Old River between the head of Old River and Grant Line Canal due to increasing exports. For instance, at exports of 2,000 cfs, Delta inflow of 12,000 cfs, and HORB in place, the daily average flow between the head of Old River up to Grant Line Canal ranged between 407 and 323 cfs, whereas without the HORB it ranged between 907 and 790 cfs (Figure B.5-5; Table B.5-2).
- At Clifton Court (low inflow and HORB in), the difference in average daily flow due to a change in exports from 2,000 to 10,000 cfs was -6,642 cfs, which was 35% of the difference between the minimum and maximum flow of 19,209 cfs (Table B.5-2). At the mouth of Old River, the average daily flow difference due to a change in exports from 2,000 to 10,000 cfs was -2,029 cfs, which was 7% of the difference between the daily minimum and maximum flow of 30,606 cfs (Table B.5-2).
- Upstream of CVP and SWP intakes, the effect of increasing exports is positive flows towards the export facilities. Just upstream of Grant Line Canal, the average daily flow difference due to increasing exports from 2,000 to 10,000 cfs was +184 cfs, which was 4% of the difference between minimum and maximum flow of 4,742 cfs (Table B.5-2).
- Increasing exports increases flow upstream of the CVP and SWP intakes and reduces flow downstream, but the negative effect just downstream was 36 times greater than the positive effect upstream (Figures B.5-1, B.5-2, and B.5-7; Table B.5-2).
- For comparison, in Middle River at Railroad Cut, the average daily flow difference due to a change in exports from 2,000 to 10,000 cfs was -3,270 cfs, and that was 16% of the difference between the minimum and maximum flow of 19,726 cfs. At the mouth of Middle River, the average daily flow difference due to a change in exports from 2,000 to 10,000 cfs was -1,657 cfs, and that was 4% of the difference between the minimum and maximum flow of 44,048 cfs (Table B.5-2).
- Exports decrease minimum flow more than maximum flow immediately downstream of the SWP export facility (Table B.5-2). For instance, at Delta inflow of 12,000 cfs and HORB in place, as exports increase from 2,000 to 10,000 cfs, the maximum flow decreases

by approximately 4,000 cfs whereas the minimum flow decreases by approximately 5,000 cfs (Table B.5-2).

B.5.3.3 Middle River

In the context of the three South Delta routes, Middle River, on average, had the least change in modeled flow due to inflow, and an intermediate change in flow due to exports, with and without the HORB installed, under the scenarios modeled (Figures B.5-1 through B.5-4 and B.5-6 through B.5-8).

- Increasing exports caused an increase in reverse daily average, minimum, and maximum flow while increasing inflow increased daily average, maximum, and minimum flow. Modeled relative daily changes in these metrics due to an increase in exports were intermediate between changes found in the San Joaquin River and Old River, and modeled relative daily changes due to an increase in Delta inflow were the least among the three rivers (Figure B.5-1 through B.5-8; Table B.5-2).
- Although the negative changes in flow due to exports were least among the three routes, the greatest changes within Middle River occurred at Victoria Canal, downstream of Railroad Cut, and again at Columbia Cut (Figures B.5-1 through B.5-8). The tidal influence at these locations increased between Victoria Canal and Columbia Cut.

B.5.3.4 Georgianna Slough

In Georgiana Slough, the effect of increasing exports on flow within the slough was an increase in flow towards the Interior Delta. The change in daily average flow into the Interior Delta was an increase of 124 cfs, which was 2% of the difference between minimum and maximum flow of 6,765 cfs (Figure B.5-12; Cavallo et al. 2013). Observed flow data on the Sacramento River, upstream and downstream of Georgiana Slough, indicate that there was no visible change in flow on the Sacramento River due to an increase in exports.

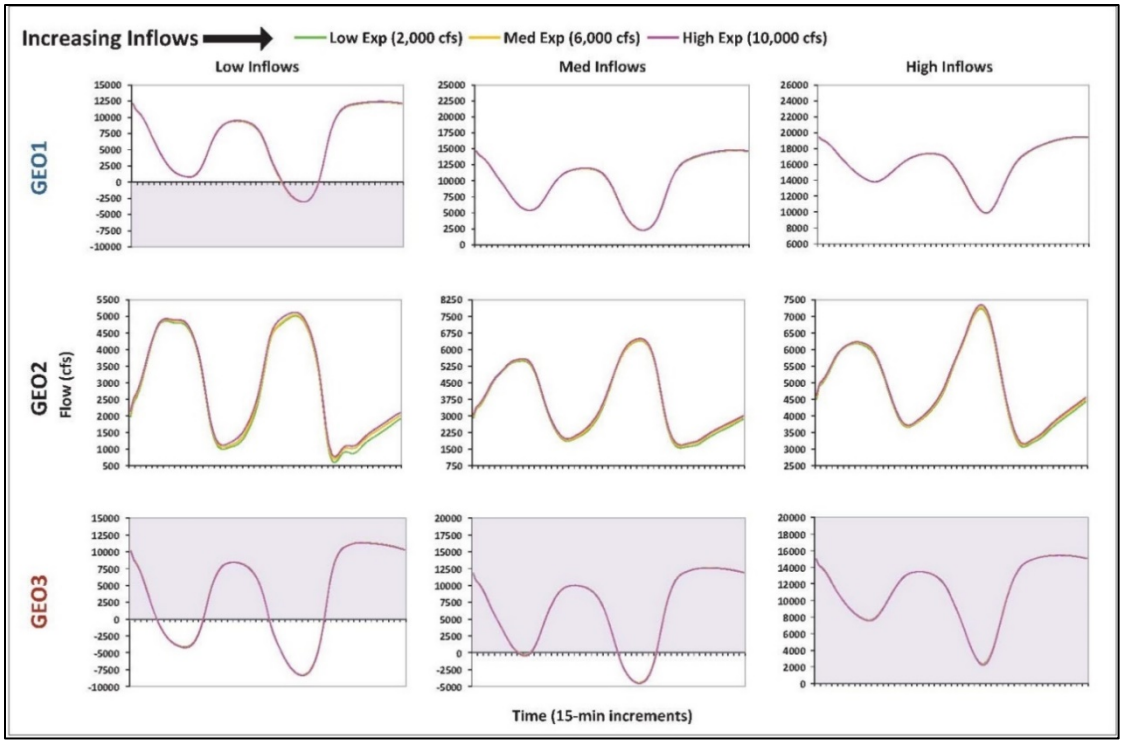

Figure B.5-12. Flow at Georgiana Slough Junction Channels Over 24 Hours

Notes: Time of day in 15-minute increments is on the x axis and magnitude of flow is on the y axis. Curve color indicates export level (Cavallo et al. 2013).

B.5.3.5 Conclusions

Hydrologic simulations provide a means for evaluating local and regional changes in Delta hydrodynamic conditions associated with alternative water project management; however, the Delta channels and channel junctions are characterized by complex and dynamic conditions, which complicate the development and interpretation of modeling results.

Model results support the conceptual model prediction that the effect of exports and inflows, within the context of tides, on average daily flows varies with proximity to the exports, channel configuration and barrier deployment, and CCF radial gate operations. Exports, within the context of tides, have the greatest effect on average daily flows in Old River immediately downstream of the exports and gradually dissipating towards the mouth. Exports have a positive effect upstream of the exports compared to a negative effect downstream. Upstream, the average daily flow increases towards the exports, whereas downstream average daily flow decreases, particularly immediately downstream of exports. If the HORB is deployed, exports have less of an effect on flow upstream (between the head of Old River and Grant Line Canal).

Exports, within the context of tides, have the least effect on average daily flows in the San Joaquin River mainstem. While it is accurate that near Jersey Point, if exports increase

from 2,000 to 10,000 cfs, the change in average daily flow is about -6,500 cfs, the difference between the daily minimum and maximum flow is 360,000 cfs, which is due predominately to the tides. The -6,500 cfs change in average daily flow is 2% of the daily change between daily minimum and maximum flow.

Inflows, within the context of tides, have the greatest effect on average daily flows in the San Joaquin River mainstem between the head of Old River and Columbia Cut with the HORB deployed, and some effect on Old River between the head and Grant Line Canal if the HORB is not deployed. Inflows had the least effect on Middle River.

The positive effect of Delta inflows in the San Joaquin River mainstem, within the context of tides, had a greater effect on average daily flows than the negative effect of exports on Old River.

1-D DSM2, in particular, provides a tool for assessing changes in Delta hydrodynamic conditions and has been used extensively for water supply planning. Validation tests indicate that DSM2 is more accurate for predicting average daily metrics than 15-minute time step metrics. The model validates well at some locations with weaker agreement between observed and predicted flow and velocity at other locations. Factors such as simplifying assumptions for Delta consumptive water use, channel bathymetry, complex geometry, and dynamic tidal conditions contribute to variability in model validation. More complex 2-D or 3-D simulation models may be needed to represent more complex hydrodynamic conditions on a finer time scale experienced by juvenile salmonids migrating through the Delta (Section B.3; Appendix C).

Selection of the appropriate simulation modeling tool should be based on the specific goals and objectives of an analysis, the level of resolution needed in model results, the complexities of the areas being modeled in terms of dynamic tidal and flow conditions, and channel geometry. The selected modeling tool should be calibrated and independently validated at a temporal and spatial scale appropriate for the desired analysis.

B.5.3.6 Gaps in Information

Gaps associated with the hydrodynamic simulation modeling and monitoring stations are described below:

- The flow and velocity of water in Clifton Court channel are not measured directly—they are estimated.
- Delta Consumptive Use, diversions on to and returns from the Delta islands, is not estimated adequately. Delta Consumptive Use becomes extremely important at low net Delta outflows. There are ongoing efforts to improve the estimations.
- Channel bathymetry in the South Delta are inadequate. Channel configuration has a major effect on the influence of inflow and exports on the magnitude, direction, and

proportion of flow entering downstream channels through the Interior, Central, and South Delta.

B.5.4 Export Effects on Velocities

Similar to the analyses regarding flow, the SST characterized the extent of the effect of the SWP and CVP South Delta export operations on velocity along the channels in the South Delta over a range of Delta inflows with no HORB (Figure B.5-13 through Figure B.5-17; Table B.5-3). Due to limited resources, we evaluated fewer scenario options. The scenarios were limited to low Sacramento River and San Joaquin River inflow (10,595 and 1,405 cfs, respectively) and low export (2,000 cfs), high inflow (32,288 and 5,712 cfs respectively) and low export, and high inflow/high export (10,000 cfs). The low inflow/high export scenarios were not examined because they are not realistic from an operations perspective.

The availability of the 15-minute output demonstrates the complexity of the hydrodynamics in the South Delta. Figure B.5-13 is an illustration of the complete tidal cycle for each DSM2 channel reach in each route. The multiple lines in each graph are the individual channel reaches in the route and represent the 15-minute instantaneous velocity over the tidal cycle. The graphs show how the tide phase reaches the upstream channels several hours later than the downstream channels (up to 7 hours later in the San Joaquin River mainstem). They also show that, within a route, there are groups of channel reaches that are similar, in terms of curve shape and tide phase timing, compared to other channel reaches. Old River demonstrates the most complex characteristics. Two channels in Old River actually run in the opposite direction compared to the majority of channels: near Grant Line Canal and at the north boundary of Bacon Island. This level of complexity makes it difficult to develop metrics for assessment, particularly in the Old River route.

Similar to the flow section above, Figures B.5-14 and B.5-15 present profiles for each route. For velocity, we graphed the minimum and maximum velocity associated with the flood and ebb high/high and low/low tide phase, respectively. For the two channels in Old River that flow in the opposite direction, the minimum and maximum of the low/low and high/high tide phases were selected.

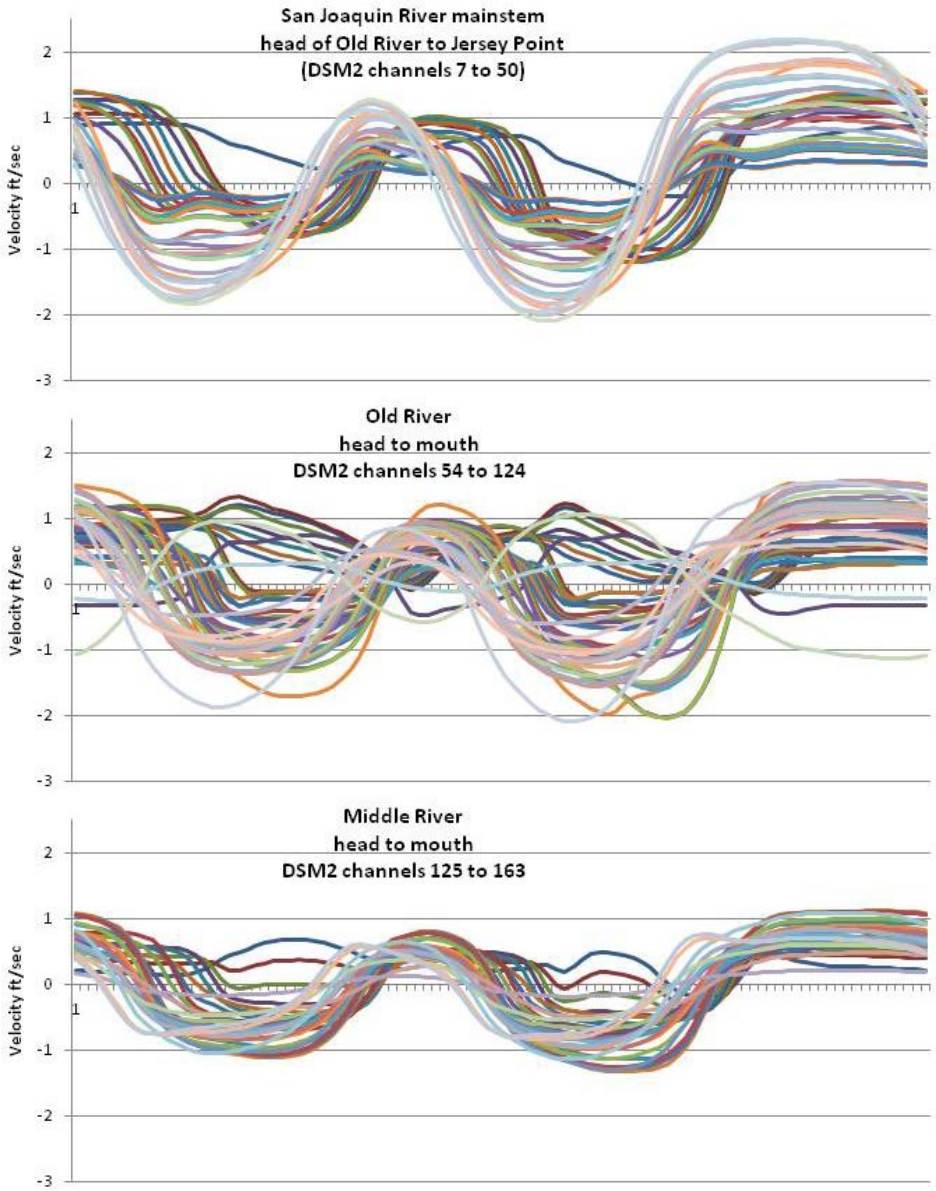

Figure B.5-13. DSM2 Modeled Instantaneous 15-minute Interval Velocity Versus Time Over One Tidal Cycle (~25 Hours) in DSM2 Channel Reaches in Three Routes of the South Delta.

Notes: The DSM2 channel reaches are reaches of river as defined in the DSM2 model grid. The routes are San Joaquin River mainstem, Old River, and Middle River. Each line represents one DSM2 channel reach within the route at the low inflow/low export model scenario.

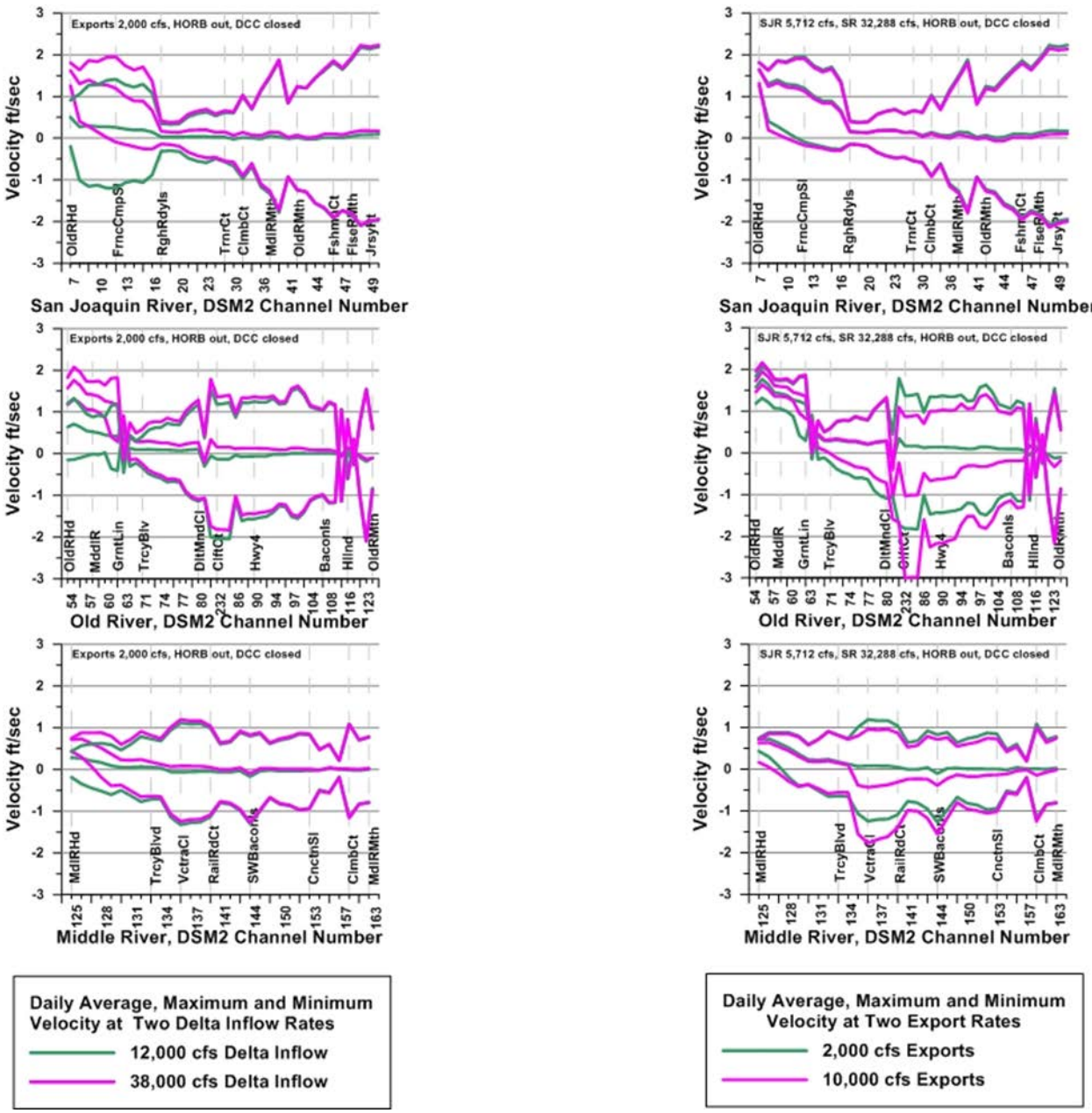

Figure B.5-14. DSM2 modeled average daily velocity and instantaneous maximum velocity associated in each channel reach, in each of two routes in the south Delta. The two model scenarios were, left panels - low exports at low and high inflows, and right panels - high inflows at low and high exports. We limited the export scenarios to low exports and the inflow scenario to high inflows because high exports are not permitted at low inflows. In each graph, the upper set of lines represents the maximum velocities for the scenario, and middle set on lines represents the daily average velocities for the scenario and the lower set of lines represents the minimum velocities for the scenario. The minimum and maximum velocities are associated with the flood and ebb tides, respectively.

Note: The three routes are San Joaquin mainstem, Old River and Middle River. The x axis is the serial DSM2 model channel number.

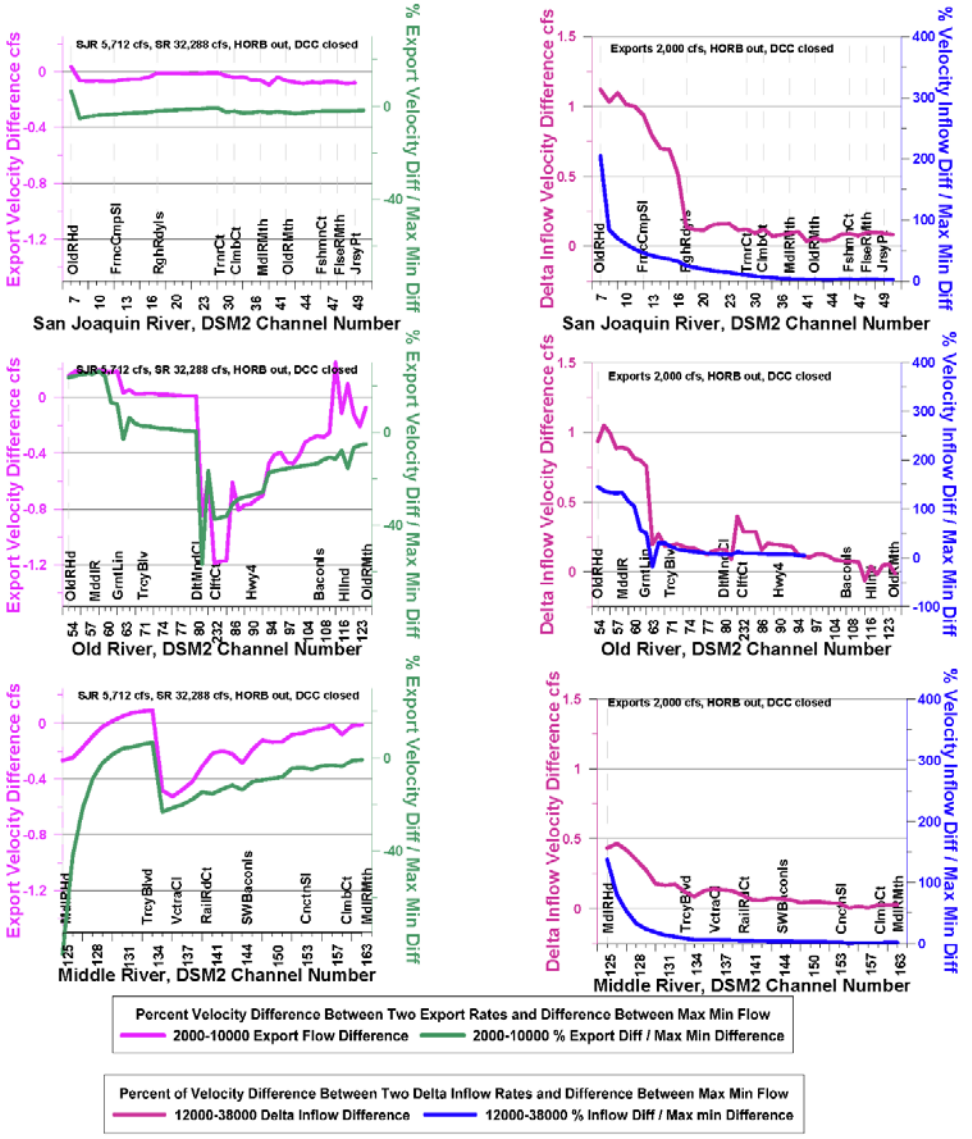

Figure B.5-15. Effect of Export Rate and Delta Inflow on Percent of Flow and Export Difference in the Lower San Joaquin River

Notes: The three routes are San Joaquin River mainstem, Old River, and Middle River. The x axis is the serial DSM2 model channel number. The left panels represent the high inflow scenario, the difference in average tidal velocity between low and high export rate (left y axis), and the difference in daily average velocity between low and high export rate divided by the difference between instantaneous maximum and minimum velocity at the low export rate (right y axis) without the HORB. The right panels represent the difference in daily average velocity between low and high inflow rate (left y axis) and the difference in daily average velocity between low and high inflow rate divided by the difference between daily maximum and minimum velocity at the low at the low inflow rate without the HORB. All right panels represent the low export scenario.

Similar to the flow section above, Figure B.5-16 is a "heat" map of the minimum and maximum velocity associated with the flood and ebb tides, respectively. The upper three panels are the minimum velocities associated with the flood tide phase throughout the South Delta for the three scenarios: low inflow/low export, high inflow/low export, and high

inflow/high export. The lower three panels are the maximum velocities associated with the ebb tide phase throughout the South Delta for the three scenarios.

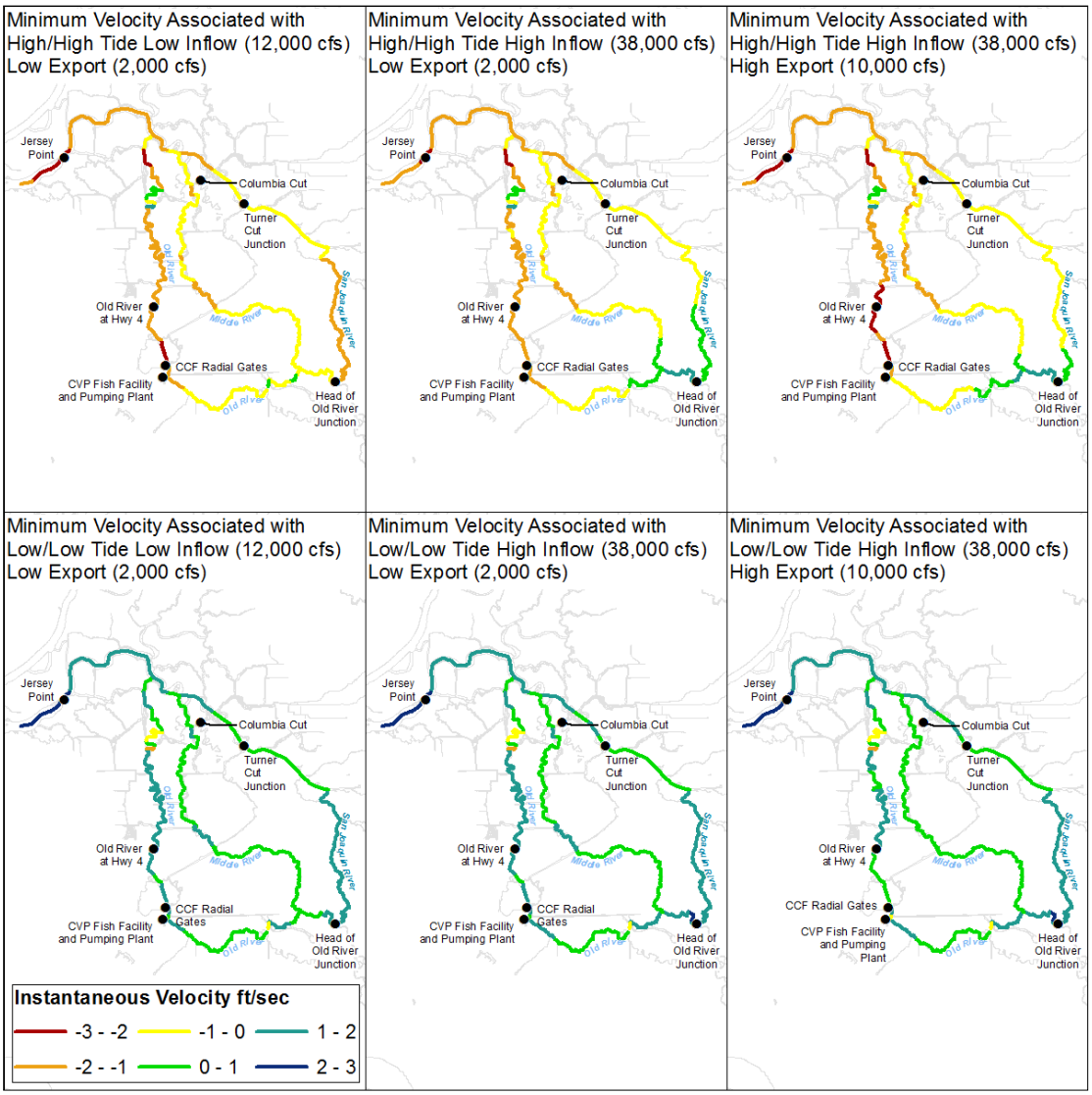

Figure B.5-16. DSM2 Modeled Instantaneous Minimum and Maximum Velocity Associated With the Ebb and Flood Tide Phases, Respectively, in Each Channel for Each of Three Model Scenarios, in Each of Three Routes in the South Delta

Notes: The three scenarios are low inflow/low export, high inflow/low export, and high inflow/high export. The three routes are the San Joaquin River mainstem, Old River, and Middle River. The upper three panels are the flood tide, and the lower three panels are the ebb tide.

Figure B.5-17 is a "heat" map of the difference between scenarios illustrated in Figure B.5-16. The upper three panels are the difference in minimum velocity between: 1) the high inflow/low export scenario and the low inflow/low export scenario (the first and second panels in the upper half of Figure B.5-16); 2) the high inflow/high export and the high inflow/low export scenario (the second and third panels in the upper half of Figure B.5-16); and 3) the high inflow/high export and low inflow/low export scenario (the first and third

panels in the upper half of Figure B.5-16). The lower three panels are the difference in maximum velocity between the three scenarios as described in the previous sentence.

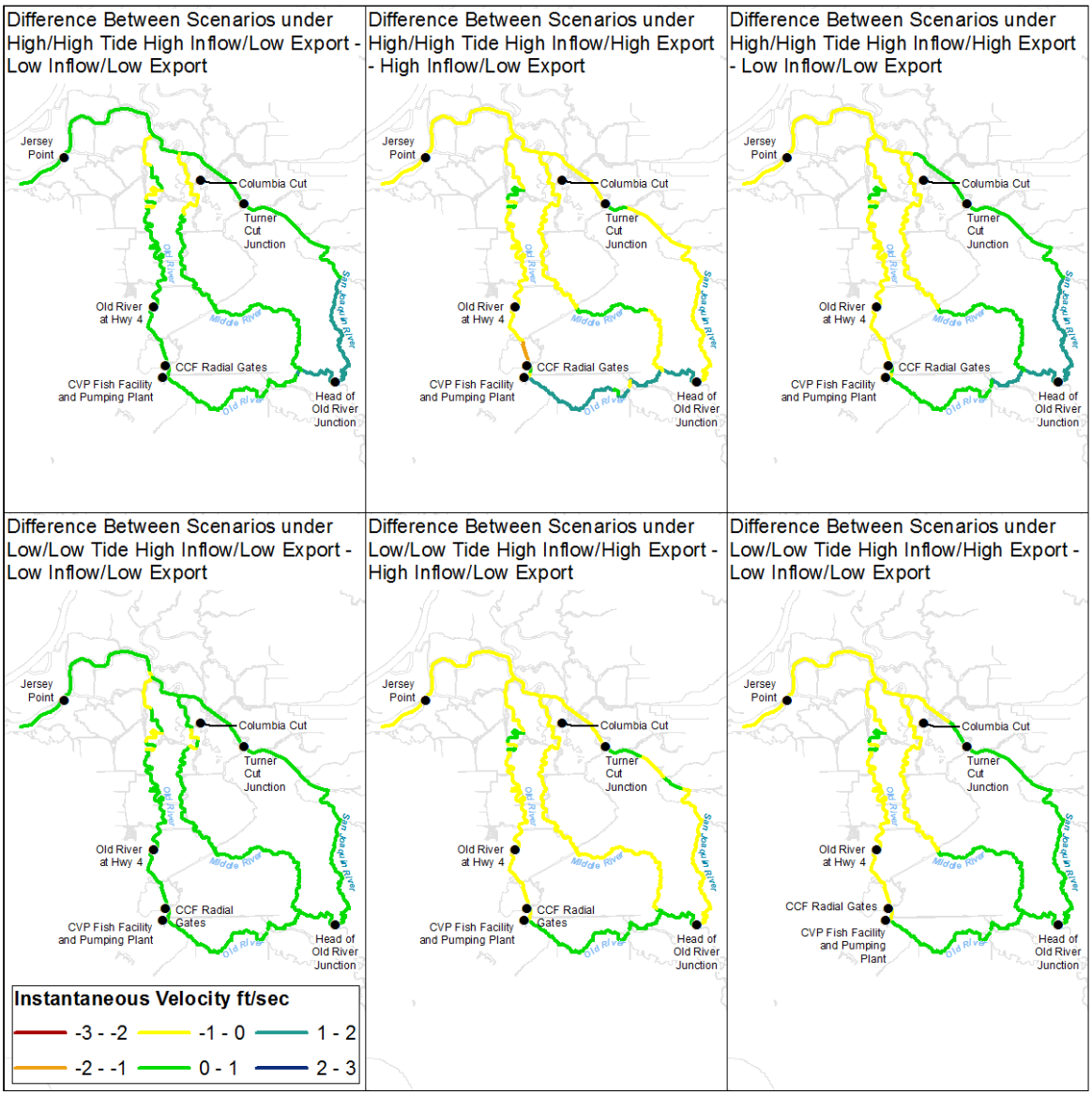

Figure B.5-17. Difference Between DSM2 Modeled Scenarios of Instantaneous Minimum and Maximum Velocity Associated With the Ebb and Flood Tide Phases, Respectively, in Each Channel for Each of Three Model Scenarios, in Each of Three Routes in the South Delta

Notes: The three scenarios are low inflow/low export, high inflow/low export, and high inflow/high export. The three routes are the San Joaquin River mainstem, Old River, and Middle River. The upper three panels are the difference of the minimum velocities and the lower three panels are the difference of the maximum velocities.

Table B.5-3 is a tabulation of the range of minimum and maximum instantaneous velocities in each route and all scenarios, and the differences in velocity between scenarios as a function of increased Delta inflow and export.

Results were further examined for each of three routes to describe changes in instantaneous minimum and maximum velocities associated with the low/low and high/high tide phase. The basis of knowledge for the relationships between different routes' maximum and minimum velocities and drivers such as exports, barriers, or Clifton Court radial gate operations is low because it is based on non-peer reviewed agency reports. Understanding the relationship between the migration route's velocity and these drivers is based on non-peer reviewed agency reports and information presented in this report. Results of simulation model predictions (DMS2) of the effects of SWP and CVP exports, and Sacramento River and San Joaquin River inflows, on hydrodynamic conditions in the San Joaquin River, Old River, and Middle River are summarized below.

B.5.4.1 San Joaquin River Mainstem

In the context of the three South Delta routes, the mainstem San Joaquin River, on average, had the least change in modeled velocity due to exports without the HORB, under the scenarios modeled. The change in velocity due to Delta inflow was more similar among the three routes (Figures B.5-14 through B.5-17).

- Similar to flow, the San Joaquin River had the least negative change in instantaneous velocity due to exports relative to OMR (Figure B.5-14 through Figure B.5-16; Table B.5-3). As an example of the difference between the San Joaquin River and OMR, the difference in minimum velocity due to an increase in exports from 2,000 to 10,000 cfs (high inflow, no HORB) in the San Joaquin River was greatest just downstream of the head of Old River (-0.21 ft/sec). For comparison, in Old River, the difference in minimum velocity due to the export increase was greatest at CCF (-1.19 ft/sec) (Figure B.5-17; Table B.5-3). In Middle River, at Victoria Canal, the difference in minimum velocity was -0.53 ft/sec (Table B.5-3). The differences in maximum velocity for the above analysis were similar in trend, but smaller in magnitude.
- From upstream to downstream, in the San Joaquin River route, the change in instantaneous minimum velocity due to increasing exports was greatest just downstream of the head of Old River (-0.21 ft/sec), then dissipated to less than -0.1 ft/sec upstream of French Camp Slough (Figure B.5-15 and Figure B.5-17).
- The San Joaquin River had a positive change in instantaneous velocity due to increasing Delta inflow that was similar to Old River, but greater than Middle River (
- Figure B.5-14 through Figure B.5-17; Table B.5-3). Increasing Delta inflow from 12,000 to 38,000 cfs (low export, no HORB) affected the instantaneous minimum and maximum velocities the most from the head of Old River to Rough and Ready Island, and then dissipated towards Jersey Point (Figure B.5-14 through Figure B.5-17). At the head of Old River the positive change in minimum velocity was +1.45 ft/sec, and then dissipated to less than +0.2 ft/sec downstream of Rough and Ready Island (Figure B.5-15 and Figure B.5-17).

Table B.5-3. Summary of Hydrodynamic Simulation Model Results for Changes in Water Velocities at Specific Locations Within the South Delta Without the Head of Old River Barrier for the Three Scenarios: 1) Low Inflow/Low Export; 2) High Inflow/Low Export; and 3) High Inflow/High Export

Metric	San Joaquin River Route Head of Old River to Jersey Point	Middle River Route Head to Mouth of Middle River	Old River Route Head to Mouth of Old River
Barrier Status	**HORB out**	**HORB out**	**HORB out**
Locations of high and low minimum velocity (associated with high/high tide) in the route for scenarios 1, 2, and 3	Upstream of head of Old River -0.20, +1.25, +1.31 ft/sec Downstream of mouth of False River -2.10, -2.08, -2.14 ft/sec	Head of Middle River -0.19, +0.44, +0.17 ft/sec Victoria Canal -1.32, -1.24, -1.77 ft/sec	Downstream of head of Old River -0.14, +1.31, +1.63 ft/sec CCF -2.04, -1.81, -3.01 ft/sec
Locations of low and high maximum velocity (associated with low/low tide) in the route for scenarios 1, 2, and 3	Downstream of Rough and Ready Island +0.33, +0.38, +0.37 ft/sec Downstream of Jersey Point +2.19, +2.23, +2.13 ft/sec	Columbia Cut +0.21, +0.21, +0.19 ft/sec Victoria Canal +1.11, +1.19, +0.96 ft/sec	Downstream of Delta Mendota Canal +0.38, +0.44, -0.41 ft/sec Downstream of head of Old River +1.33, +2.08, +2.16 ft/sec
Locations of high and low difference in minimum velocity between Scenarios 2 and 1 (effect of increasing inflow at low export)	Upstream of head of Old River +1.45 ft/sec Downstream of mouth of Old River 0.00 ft/sec	Downstream of head of Middle River +0.64 ft/sec Downstream of Connection Slough -0.03 ft/sec	Downstream of head of Old River +1.44 ft/sec Mouth of Old River -0.03 ft/sec
Locations of high and low difference in maximum velocity between Scenarios 2 and 1 (effect of increasing inflow at low export)	Upstream of head of Old River +0.89 ft/sec Downstream of mouth of Old River 0.00 ft/sec	Downstream of head of Middle River +0.31 ft/sec Downstream of Connection Slough -0.01 ft/sec	Upstream of head of Middle River +0.84 ft/sec Mouth of Old River -0.03 ft/sec
Locations of low and high difference in minimum velocity between Scenarios 3 and 2 (effect of increasing export at high inflow)	Downstream of head of Old River -0.21 ft/sec Upstream of head of Old River +0.05 ft/sec	Downstream of Victoria Canal -0.53 ft/sec Upstream of Victoria Canal +0.09 ft/sec	Downstream of Clifton Court -1.19 ft/sec Downstream of Paradise Cut +0.54 ft/sec
Locations of low and high difference in maximum velocity between Scenarios 3 and 2 (effect of increasing export at high inflow)	Downstream of Jersey Point -0.09 ft/sec Upstream of head of Old River +0.01 ft/sec	Downstream of Victoria Canal -0.24 ft/sec Upstream of Tracy Boulevard +0.09 ft/sec	Downstream of Delta Mendota Canal -0.85 ft/sec Downstream of head of Old River +0.13 ft/sec

- At the head of Old River junction, the effect of increasing exports from 2,000 cfs to 10,000 cfs (high inflow, no HORB) was an increase in instantaneous velocity in Old River just downstream of the head towards the Interior Delta. The maximum increase was 0.35 ft/sec. Increasing exports also increased instantaneous velocity in the San Joaquin River upstream of the junction a maximum of 0.08 cfs, and decreased velocity downstream of the junction by a maximum of -0.2 ft/sec. The effect of increasing inflow from 12,000 cfs to 38,000 cfs (low export, no HORB) was an increase in velocity upstream and downstream of the head of Old River and just downstream in Old River of about 1.5 ft/sec (Figure B.5-18).
- At the Turner Cut junction, the effect of increasing exports from 2,000 cfs to 10,000 cfs (high inflow, no HORB) was an increase in velocity in Turner Cut towards the Interior Delta. The maximum increase was +0.16 ft/sec. Increasing exports also decreased instantaneous velocity in the San Joaquin River upstream and downstream of the junction by a maximum of about -0.01 ft/sec. The effect of increasing inflow from 12,000 cfs to 38,000 cfs (low export, no HORB) was an increase in velocity in the San Joaquin River above and below the Turner Cut junction of about +0.15 ft/sec, and in Turner Cut of about +0.01 ft/sec (Figure B.5-19).
- At the Middle River junction, the effect of increasing exports from 2,000 cfs to 10,000 cfs (high inflow, no HORB) was a decrease in velocity in Middle River towards the Interior Delta (note: the default direction in that channel is away from the Interior Delta). The maximum increase was -0.16 ft/sec. The effects of increasing exports and increasing inflow from 12,000 cfs to 38,000 cfs in the other channels was about 0.05 to 0.01 ft/sec (Figure B.5-20).

B.5.4.2 Old River

Relative to the three routes, in the context of tides, Old River had the greatest negative change in instantaneous minimum and maximum modeled velocity due to an increase in exports:

- The largest relative changes occurred downstream of the CVP and SWP export facilities and then dissipated toward the mouth (Figure B.5-14 and Figure B.5-15; Table B.5-3).
- From upstream to downstream, in the Old River route, the change in instantaneous minimum velocity due to increasing exports was positive upstream of the delta Mendota Canal, and then became negative downstream. The greatest negative change in instantaneous minimum velocity was just downstream of Clifton Court, then dissipated to less than -0.2 ft/sec downstream of Bacon Island (Figure B.5-15 and Figure B.5-17).

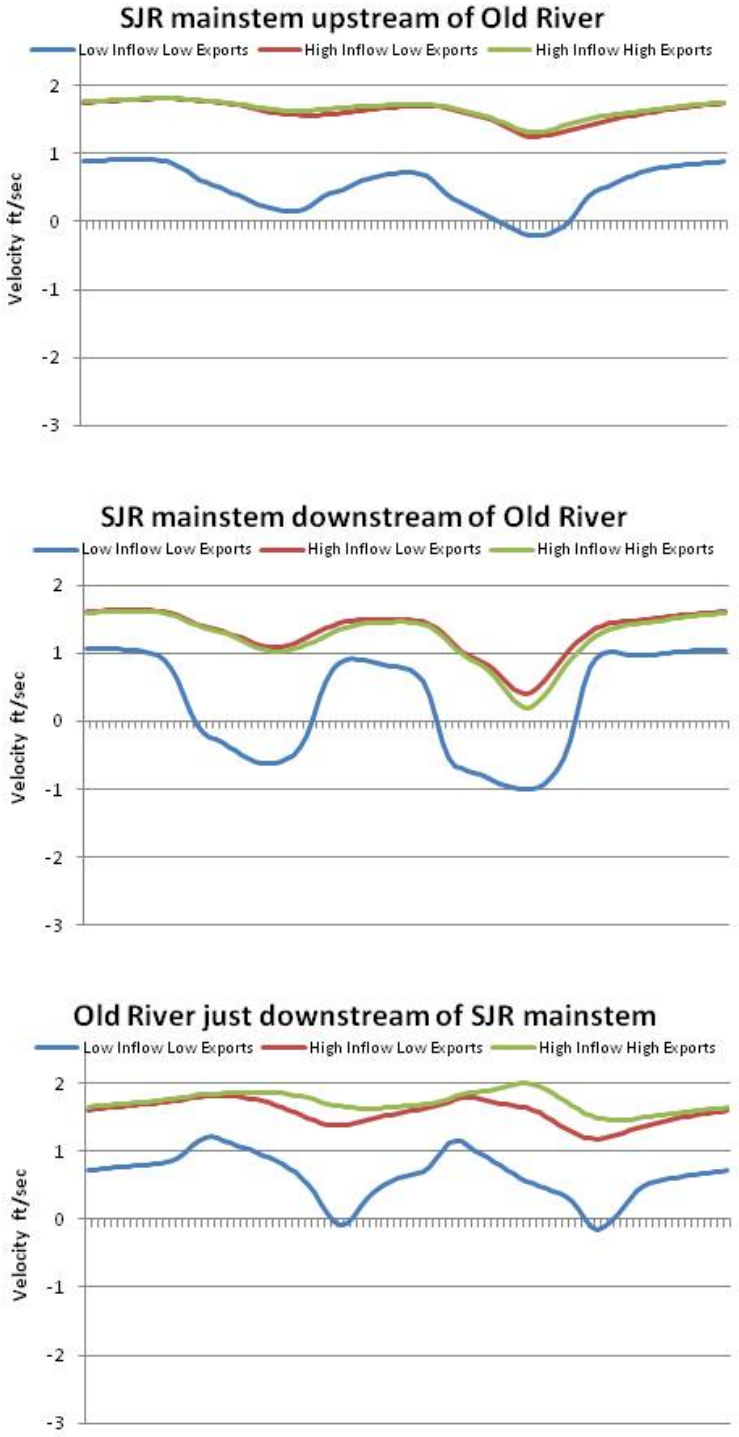

Figure B.5-18. DMS2 Modeled Instantaneous 15-minute Velocity Versus Time Over a Complete Tidal Cycle (~25 Hours) in Three Channels at the Junction of the San Joaquin River Mainstem and the Head of Old River

Notes: There are three DSM2 channel reaches at the junction (three panels). Within each panel there are three scenarios: low inflow/low export, high inflow/low export, and high inflow /high export.

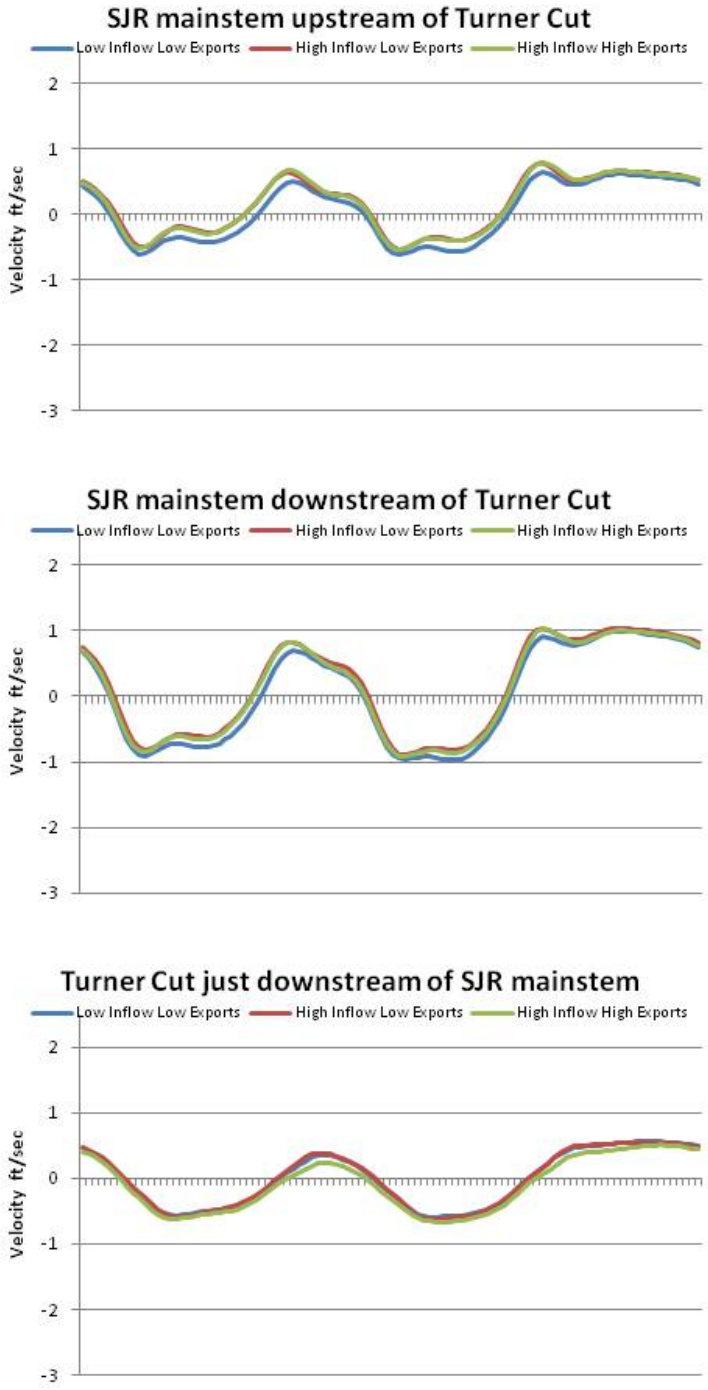

Figure B.5-19. DMS2 Modeled Instantaneous 15-minute Velocity Versus Time Over a Complete Tidal Cycle (~25 Hours) in Three Channels at the Junction of the San Joaquin River Mainstem and Turner Cut

Notes: There are three DSM2 channel reaches at the junction (three panels). Within each panel there are three scenarios: low inflow/low export, high inflow/low export, and high inflow/high export.

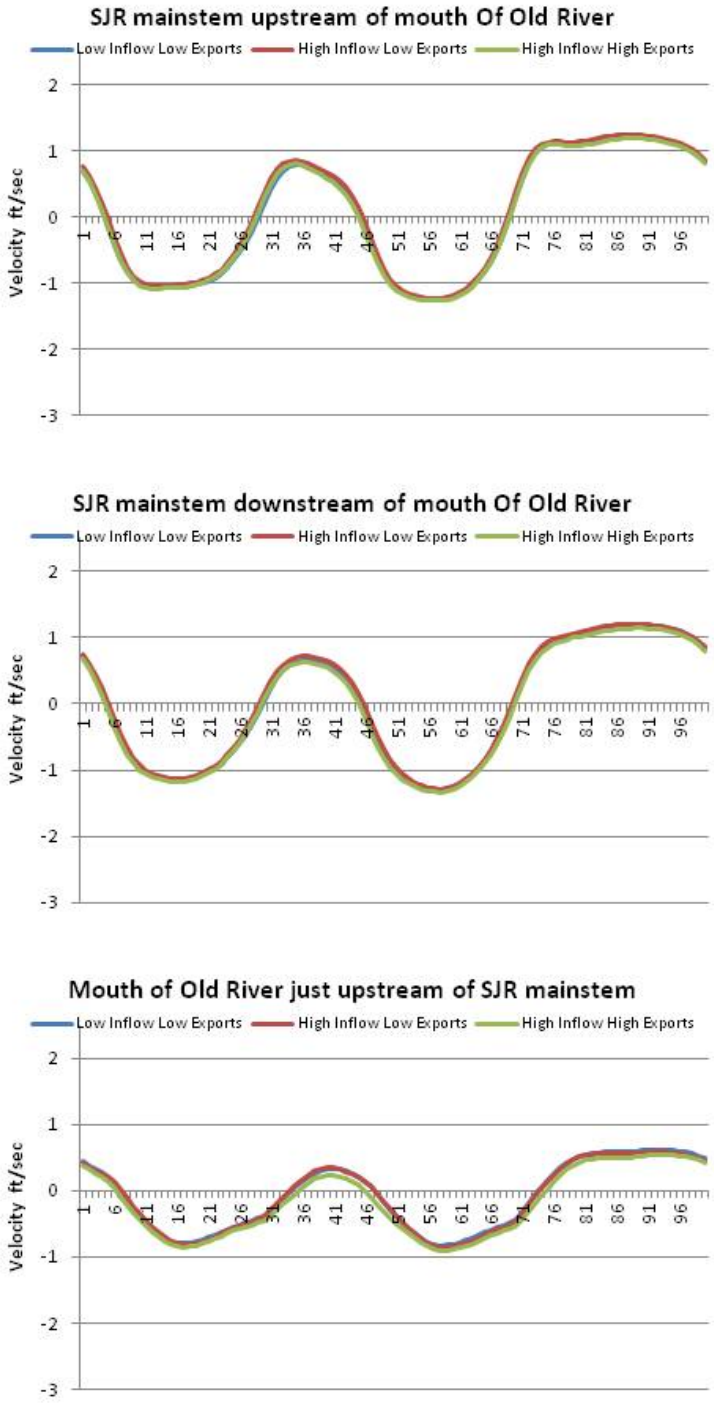

Figure B.5-20. DMS2 Modeled Instantaneous 15-minute Velocity Versus Time Over a Complete Tidal Cycle (~25 Hours) in Three Channels at the Junction of the San Joaquin River Mainstem and the Mouth of Old River

Notes: There are three DSM2 channel reaches at the junction (three panels). Within each panel there are three scenarios: low inflow/low export, high inflow/low export, and high inflow/high export.

- Old River had a positive change in instantaneous velocity, in the context of tides, due to Delta inflows that was similar to the San Joaquin River, but greater than Middle River (
- Figure B.5-14 through Figure B.5-17; Table B.5-3). As an example of the positive effect of inflow in upper Old River, near the head, the difference in instantaneous minimum velocity due to a change in Delta inflow from 12,000 to 38,000 cfs (low export, no HORB) was +1.44 ft/sec. For comparison, in Middle River at the head, the difference in minimum velocity was +0.64 ft/sec (Figure B.5-17; Table B.5-3).
- From upstream to downstream, in the Old River route, the positive change in instantaneous minimum velocity due to increasing Delta inflow was greatest downstream of the head of Old River (+1.44 ft/sec), then dissipated to less than +0.2 ft/sec downstream of Grant Line Canal (Figure B.5-15 and Figure B.5-17).

B.5.4.3 Middle River

Relative to the three routes, Middle River had the least change in minimum and maximum velocities due to inflows, and an intermediate change in minimum and maximum velocities due to exports (Figure B.5-14 through Figure B.5-17; Table B.5-3).

- Increasing exports from 2,000 to 10,000 cfs (high inflow, no HORB) resulted in a decrease in instantaneous minimum velocity at the head of Middle River (-0.27 ft/sec), which dissipated to upstream of Victoria Canal (+0.09 ft/sec), then decreased again at Victoria Canal (-0.52 ft/sec), and dissipated to less than -0.1 ft/sec at Connection Slough (Figure B.5-15 and Figure B.5-17).
- Increasing Delta inflow from 12,000 cfs to 38,000 cfs (low export, no HORB) increased instantaneous minimum velocity at the head of Middle River (+0.64 ft/sec), then dissipated to less than 0.1 ft/sec at Tracy Boulevard (Figure B.5-15 and Figure B.5-17).

B.5.4.4 Conclusions

Modeled exports had the greatest negative effect on instantaneous minimum and maximum velocity in Old River; immediately downstream of the export facilities and gradually dissipating towards the mouth:

- Exports had a positive effect upstream of the exports and a negative effect downstream.
- Modeled exports had the least effect on instantaneous maximum and minimum velocity in the San Joaquin River mainstem, and an intermediate effect on Middle River.
- Modeled Delta inflow had the greatest effect on instantaneous minimum and maximum velocities in Old River between the head of Old River and Grant Line Canal, and in the San Joaquin River mainstem between the head of Old River and Rough and Ready Island.
- The effect of modeled Delta inflow at the head of Old River had a greater positive effect on instantaneous minimum and maximum velocity than the negative effect of exports at the export facilities.
- Modeled Delta inflow had the least effect on Middle River. In Middle River, the greatest effect of Delta inflow was between the head of Middle River and Tracy Boulevard.

B.5.4.5 Gaps in Information

The same gaps described in Section B.5.3.6 are applicable here:

- The flow and velocity of water in Clifton Court channel are not measured directly—they are estimated.
- Delta Consumptive Use, diversions on to and returns from the Delta islands, is not estimated adequately. Delta Consumptive Use becomes extremely important at low net Delta outflows. There are ongoing efforts to improve the estimations.
- Channel bathymetry data in the South Delta are inadequate. Channel configuration has a major effect on the influence of inflow and exports on the magnitude, direction, and proportion of flow entering downstream channels through the Interior, Central, and South Delta.

B.6 REFERENCES

Bombardelli, F.A., S. Reddy, and J.R. Kohne. 2011. *Comparing Delta Flow and Transport Models: Theoretical and Numerical Basis*. Prepared for the California Water Resources Control Board, 89 p.

Brater, E.F., H.W. King, J.E. Lindell, and C.Y. Wei. 1996. *Handbook of Hydraulics. McGraw Hill*.

Brunell, M., G.M. Litton, C. Jordan, ICF International. 2010. *Effects of the Head of Old River Barrier on flow and water quality in the San Joaquin River and Stockton deep water ship channel.* Prepared for California Department of Water Resources. March 2010.

Casulli, V. and G.S. Stelling. 2010. *Semi-implicit subgrid modelling of three-dimensional free-surface flows. International Journal for Numerical Methods in Fluids*. DOI:10.1002/fld.2361.

Cavallo, B., P. Gaskill, and J. Melgo. 2013. *Investigating the influence of tides, inflows, and exports on sub-daily flow in the Sacramento-San Joaquin Delta*. Available from: http://www.fishsciences.net/reports/2013/Cavallo_et_al_Delta_Flow_Report.pdf.

Clark, K., M. Bowen, R. Mayfield, K. Zehfuss, J. Taplin, and C. Hanson. 2009. *Quantification of Pre-Screen Loss of Juvenile Steelhead in Clifton Court Forebay*. State of California, California Natural Resources Agency, Department of Water Resources. March 2009.

DeGeorge, J. 2013. An Overview of Delta Hydrodynamics and Transport. Presentation for Workshop on the State of the Science on Fish Predation on Salmonids in the

Bay-Delta, July 22, 2013. For the California Water Resources Control Board and Department of Wildlife and Fish.

Delaney, D., P. Bergman, B. Cavallo, and J. Malgo. 2014. *Stipulation Study: Steelhead Movement and Survival in the South Delta with Adaptive Management of Old and Middle River Flows*. State of California, California Natural Resources Agency, Department of Water Resources. February 2014.

Dinehart, R.L. and J.R. Burau. 2005a. Averaged indicators of secondary flow in repeated acoustic Doppler current profiler crossing of bends. *Water Resources Research* 41:1-18.

Dinehart, R.L. and J.R. Burau. 2005b. Repeated survey by acoustic Doppler current profiler for flow and sediment dynamics in a tidal river. *Journal of Hydrology* 314(1-4):1-21.

DWR (California Department of Water Resources). 2011a. *South Delta Temporary Barriers Project: 2008 South Delta Temporary Barriers Monitoring Report*. July 2011.

DWR. 2011b. *South Delta Temporary Barriers Project: 2009 South Delta Temporary Barriers Monitoring Report*. July 2011.

DWR. 2012. *2011 Georgiana Slough Non-Physical Barrier Performance Evaluation Project Report*. Prepared for DWR by AECOMM. September 5, 2012. Available from: http://baydeltaoffice.water.ca.gov/sdb/GS/docs/GSNPB_2011_Final_Report+Append_090512.pdf.

DWR. 2013. *Methodology for flow and salinity estimates in the Sacramento-San Joaquin Delta and Suisun Marsh*. 35th Annual Progress Report to the State Water Resources Control Board.

DWR. 2014a. *Dayflow An Estimate of Daily Average Delta Outflow*. Available from: http://www.water.ca.gov/dayflow/.

DWR. 2014b. *California Data Exchange Center*. Available from: https://cdec.water.ca.gov/.

Gross, E.S., J.R. Koseff, and S.G. Monismith. 1999. Evaluation of advective transport schemes for simulation of salinity in a shallow estuary. *Journal of Hydraulic Engineering* 125(1):32-46.

Kimmerer, W.J. and M.L. Nobriga. 2008. *Investigating Particle Transport and Fate in the Sacramento-San Joaquin Delta Using a Particle Tracking Model*. San Francisco Estuary and Watershed Science.

MacWilliams, M.L., F.G. Salcedo, and E.S. Gross. 2008. *POD 3-D Particle Tracking Modeling Study San Francisco Bay-Delta UnTRIM Model Calibration Report*. Prepared for California Department of Water Resources. December 19, 2008.

Moffat & Nichol Engineers. 2003. *Hydrodynamic Modeling Tools and Techniques South Bay Salt Pond Restoration Project*. October 2003.

Monismith, S.G., W. Kimmerer, J.R. Burau, and M.T. Stacey. 2002. Structure and flow-induced variability of the subtidal salinity field in northern San Francisco Bay. *Journal of Physical Oceanography* 32(11):3003-3019.

Paulsen, S. and W.L. Chiang. 2008. *Effect of increased flow in the San Joaquin River on stage, velocity and water fate, water years 1964 and 1988*. Prepared by Flow Science for San Joaquin River Group Authority. November 24, 2008.

RMA. 2015. *Overview of Hydrodynamic Models*. Prepared by RMA for Collaborative Adaptive Management Team, Salmon Scoping Team. July 2015.

Umlauf, L. and H. Burchard. 2003. A generic length-scale equation for geophysical turbulence models. *Journal of Marine Research* 61:235-265.

USGS (U.S. Geological Survey). 2000. *Delta Subsidence in California. The sinking heart of the State*. Available from: https://pubs.usgs.gov/fs/2000/fs00500/pdf/fs00500.pdf

USGS. 2014. USGS surface water flow and velocity monitoring sites in the Delta are available at: https://waterdata.usgs.gov/nwis/current?huc_cd=18040003&index_pmcode_STATION_NM=1&index_pmcode_00065=3&index_pmcode_00060=4&index_pmcode_00062=5&index_pmcode_72020=6&sort_key=site_no&group_key=county_cd&sitefile_output_format=html_table&index_pmcode_DATETIME=2

Wang B., S.N. Giddings, O.B. Fringer, E.S. Gross, D.A. Fong, and S.G. Monismith. 2011. Modeling and Understanding Turbulent Mixing in a Macrotidal Salt Wedge Estuary. *Journal of Geophysical Research* 116, 23p.

Willmott, A. J. 1981. The spin down of a stratified ocean. *Deep Sea Research Part A.: Oceanography Research Papers* 28(3):239-250.